Ricardo Marçalo da Silva Marques

Mestre em Biotecnologia

Assessment of the metabolism and N_2O producing capacity of Biological Nutrient Removal Systems

Dissertação para obtenção do Grau de Doutor em

Química Sustentável

Orientador: Adrian Michael Oehmen, Professor Auxiliar Convidado, Faculdade de Ciências e Tecnologia, Universidade Nova de Lisboa

Co-orientadores: Maria d'Ascensão Miranda Reis, Professora Catedrática, Faculdade de Ciências e Tecnologia, Universidade Nova de Lisboa

Gilda de Sousa Carvalho, Investigadora Principal, Faculdade de Ciências e Tecnologia, Universidade Nova de Lisboa

Júri:

Presidente: Prof. Doutor José Paulo Barbosa Mota

Arguentes: Doutora Paula Maria Lima Castro

Doutor António Manuel Pedro Martins

Vogais: Prof. Doutor Adrian Michael Oehmen

Doutora Nídia Dana Mariano Lourenço de Almeida

Doutora Joana Sofia Cassidy

FACULDADE DE CIÊNCIAS E TECNOLOGIA
UNIVERSIDADE NOVA DE LISBOA

Abril, 2016

Assessment of the metabolism and N_2O producing capacity of Biological Nutrient Removal Systems

Acknowledgements

I would like to express deep gratitude to Professor Adrian Oehmen for the opportunity to perform this work and for his constant support during all these years, his guidance and encouragement to pursuit the goals defined during this work and his friendship and friendly guidance always applied in every situation.

To Professor Maria Ascensão Reis and Doctor Gilda Carvalho for their continuous encouragement, support and guidance throughout my work mainly in finding solutions and new perspectives to approach the problems that I had during my work. And for the scientific discussions and brainstorming and friendship in all the moments.

To all the colleagues in the Bioeng and LMP group, to whom I had the opportunity to work with, collaborate and share joyful moments during all these years I have been part of it. Special thanks to Mónica, Jorge and Virgínia for all the collaboration in the lab and help solving the issues that were needed to overcome during this work. To the people in office 602 for the friendship and companion during this time.

To Doctor Maite Pinjuan for the possibility to work in the Technologies and evaluation Catalan Institute for Water Research, Girona, Spain. For integrating me in the group, encouragement, enthusiasm and guidance expressed during the 9 months' collaboration. For all the people I had the opportunity to work with and meet in ICRA, and specially to Anna, Adri and Corrado and all the people and friends I met during my time in Girona.

To Doctor Mikkel Holmen Andersen and Doctor Lars Hauer Larsen for the joint research Industry project with the Danish company "Unisense" during this work and helpful comments during this collaboration.

To Professor Per Nielsen and Doctor Hien Nguyen for the collaboration developed between our group and the Environmental Engineering group, at the Aalborg University, Denmark.

I would also like to acknowledge the financial support for this thesis, in the form of my PhD grant (SFRH/BD/74515/2010), awarded from the Fundação para a Ciência e Tecnologia.

A special word goes to my girlfriend, parents, brother and friends for the unconditional support during this last month's where most of my time was committed to this work.

ABSTRACT

Phosphorus (P) and Nitrogen (N) promote eutrophication and their release to the environment can be minimized by efficient wastewater treatment plants (WWTPs). This thesis focuses on two important aspects associated with biological nutrient removal (BNR) from WWTPs, 1) assessing greenhouse gas emissions directly produced during biological treatment and 2) understanding the metabolism associated with a group of polyphosphate accumulating organisms (PAOs) that are highly abundant in WWTPs.

N removal is achieved by nitrification and denitrification, where nitrous oxide (N_2O) can be produced as a direct (denitrification) or indirect (nitrification) intermediate of the process. N_2O is potent greenhouse gas (GHG) with a radiative force that is 300-fold stronger than carbon dioxide (CO_2), and can contribute to over 80% of the total greenhouse gases emitted from WWTPs in some cases. In this work, lab and full-scale sensors for N_2O were tested and validated for online gas measurements. The sensors displayed a linear response with different concentration ranges and an exponential correlation between temperature and sensor signal was adequately predicted with few experimental measurements needed. The N_2O emission dynamics from lab-scale and full-scale sequencing batch reactors (SBR) systems were accurately described by these sensors, supporting their application for assessing gaseous N_2O emissions. This sensor methodology overcomes some limitations of conventional methods that include a wider quantification range, increasing the accuracy of assessing N_2O gas emissions. Liquid-phase N_2O measurements and mass transfer models were also used to predict online the gaseous N_2O emissions.

Tetrasphaera are a highly abundant group of organisms in full-scale BNR systems, and their metabolism and contribution towards P and N removal was also addressed in this work. A culture enrichment was obtained with *Tetrasphaera* as the predominant PAO group in addition to the more widely studied *Candidatus* Accumulibacter, achieving high anaerobic amino acids consumption and P-removal. *Tetrasphaera* performed the majority of the P removal in this culture and the energy generated by fermentation led to anaerobic P uptake. Batch tests demonstrated that *Tetrasphaera* had a preference towards the uptake of certain amino acids. *Tetrasphaera* and *Candidatus* Accumulibacter were found to contribute to P uptake through different ecological niches. The denitrifying capacity of a *Tetrasphaera* enriched culture was also assessed in a BNR system through an anaerobic/anoxic/aerobic cycle operation fed with amino acids. *Tetrasphaera* was the main group responsible for denitrification, however only little anoxic P uptake was

observed. The culture revealed a preference for nitrate (NO_3^-) and nitrite (NO_2^-) reduction as opposed to N_2O reduction, and electron competition occurred when two or more electron acceptors were present simultaneously. The increased understanding of the ecological niche of *Tetrasphaera*-related PAOs has the potential to improve the efficiency of P and N removal in EBPR WWTPs, and understand their contribution towards the production of N_2O emissions as well as their versatility for dealing with wastewaters with different compositions of organic carbon.

KEYWORDS: Microsensors, Nitrous oxide (N_2O), Biological nutrient removal (BNR), Polyphosphate Accumulating Organisms, *Tetrasphaera*-related organisms, Denitrification.

RESUMO

A contaminação por fósforo (P) e azoto (N) origina problemas ambientais, nomeadamente a eutrofização. A libertação destes nutrientes para o meio ambiente pode ser minimizada através de uma eficiente remoção em estações de tratamento de águas residuais (ETARs). O objetivo desta tese consiste no estudo de dois aspetos importantes associados à remoção biológica de nutrientes (BNR) em ETARs: 1) a avaliação das emissões de gases com efeito de estufa produzidos diretamente durante o tratamento biológico e 2) a compreensão do metabolismo associado a um grupo de organismos acumuladores de fosfatos (PAO), muito abundantes em ETARs.

A remoção biológica de N ocorre através de processos designados por nitrificação e desnitrificação, sendo o óxido nitroso (N_2O) um intermediário produzido de forma direta (desnitrificação) ou indireta (nitrificação). O N_2O é um gás de efeito estufa (GHG) com uma carga radiativa 300 vezes mais forte do que o dióxido de carbono (CO_2), e podendo contribuir, em alguns casos, para mais de 80% do total de GHG emitidos por uma ETAR. Neste trabalho foram testados e validados sensores gasosos de N_2O à escala laboratorial e real. Os sensores demonstraram uma resposta linear para diferentes gamas de concentração, e foi possível simular com sucesso a correlação exponencial observada entre a temperatura e sinal do sensor com base num número reduzido de medições experimentais. As emissões de N_2O obtidas em reactores à escala laboratorial e real foram descritas com precisão por estes sensores, validando a sua aplicação para monitorizar emissões gasosas de N_2O. Os sensores apresentam vantagens em relação a métodos convencionais permitindo a medição de N_2O em gamas de concentração mais altas e com maior precisão. Medições de N_2O na fase líquida usando modelos de transferência de massa permitiram ainda prever emissões gasosas em tempo real.

Tetrasphaera é um grupo de microrganismos muito abundante em sistemas BNR à escala real e o seu metabolismo e contribuição para a remoção de P e N nunca foram estudados. Neste trabalho foi obtida uma cultura mista enriquecida em *Tetrasphaera,* como grupo dominante e uma menor fração do grupo PAO mais estudado, *Candidatus* Accumulibacter. Os resultados obtidos mostraram uma eficiente remoção anaeróbia de aminoácidos e aeróbia de fósforo. Nesta cultura, a remoção de fósforo foi maioritariamente levada a cabo por *Tetrasphaera*. Ensaios realizados em descontínuo demonstraram que este grupo de PAOs tem preferência por alguns aminoácidos em detrimento de outros. *Tetrasphaera* e *Candidatus* Accumulibacter contribuem através de diferentes nichos ecológicos para a remoção de fósforo. A capacidade de desnitrificação

da cultura enriquecida em *Tetrasphaera* foi avaliada num sistema BNR operado em ciclos sequenciais anaeróbio/anóxico/aeróbio e alimentado com aminoácidos. Membros do género *Tetrasphaera,* que dominavam a comunidade, foram os principais responsáveis pela desnitrificação, no entanto a remoção anóxica de fósforo foi mais baixa do que normalmente observado por *Candidatus* Accumulibacter. A cultura demonstrou uma maior preferência pela redução de nitrato e nitrito em comparação com o N_2O, ocorrendo competição quando dois ou mais aceitadores de eletrões estavam presentes simultaneamente. Este estudo permitiu compreender melhor o papel das PAOs *Tetrasphaera* na remoção biológica de P e N em ETARs, elucidar a sua contribuição para as emissões de N_2O, e entender a sua versatilidade na utilização de diferentes composições de carbono orgânico.

PALAVRAS-CHAVE: Micro sensores, óxido nitroso (N_2O), remoção biológica de nutrientes, organismos acumuladores de fósforo, organismos *Tetrasphaera*-related, desnitrificação.

TABLE OF CONTENTS

LIST OF FIGURES

LIST OF TABLES

NOTATIONS AND ABBREVIATIONS

*pha*B	Acetoacetyl-CoA reductase gene
*pha*A	Acetyl-CoA acetyltransferase gene
ATP	Adenosine triphosphate molecule
adk	Adenylate kinase
ald	Alanine dehydrogenase
adh	Alcohol dehydrogenase
aldA	Aldehyde dehydrogenase
NH_4^+	Ammonium
AOB	Ammonium oxidizing bacteria
BNR	Biological nutrient removal
CO_2	Carbon dioxide
Cas aa	Casein hydrolysate
COD	Chemical oxygen demand
N_2	Di-nitrogen
DPAOs	Denitrifying PAOs
DO	Dissolved oxygen
EBPR	Enhanced biological phosphorus removal
FISH	Fluorescence in situ hybridisation
FNA	Free nitrous acid
GAO	Glycogen accumulating organisms
GC	Gas chromatography
GC-ECD	GC–electron capture detector
GC-MS	GC–mass spectrometry
GHG	Greenhouse gas
NH_2OH	Hydroxylamine
Pst	High affinity phosphate specific transporter
HRT	Hydraulic retention time
Pit	Low affinity phosphate transporter
MAR-FISH	Microautoradiography-FISH
NADH	Nicotinamide adenine dinucleotide
NO_3^-	Nitrate
nar	Nitrate reductase
NO_2^-	Nitrite
nir	Nitrite reductase

NO	Nitric oxide
nor	Nitric reductase
N	Nitrogen
NOx	Nitrogen oxide species
N_2O	Nitrous oxide
nos	Nitrous oxide reductase
PO_4^{-3}-P	Orthophosphate
P	Phosphorus
PAO	Polyphosphate accumulating organisms
PHA	Polyhydroxyalkanoates
*pha*C	PHA synthase gene
PH_2MB	Polyhydroxy-2-methylbutyrate
PH_2MV	Polyhydroxy-2-methylvalerate
PHB	Polyhydroxybutyrate
PHV	Polyhydroxyvalerate
Poly-P	Polyphosphate
pap	Polyphosphate AMP phosphotransferase
ppk	Polyphosphate kinase
ppk1	Polyphosphate kinase 1
ppk2	Polyphosphate kinase 2
R^2	Coefficient of determination
SBR	Sequencing batch reactor
SRT	Solid retention time
SEIFC	Surface emission isolation flux chamber
TCA	Tricarboxylic acid
TOC	Total organic carbon
TSS	Total suspended solids
UQ/UQH_2	Ubiquinone/ubiquinol pool
USEPA	United States environmental protection agency
VFA	Volatile fatty acids
VSS	Volatile suspended solids
WWTPs	Wastewater treatment plants

SPECIFIC TERMS IN CHAPTERS 3 AND 4

A_{Tank}	Aeration field size
A_{hood}	Area of the tank covered by the hood
C_{N2O}, air	Average concentration of N_2O in the atmosphere of the northern hemisphere
$S_{N2O\ Liquid\ sensor}$	Concentration of dissolved N_2O measured by the N_2O liquid microsensor, after temperature compensation
C_{N2O}	Concentration of N_2O
$S_{N2O\ Gas\ sensor}$	Concentration of N_2O in the gas measured by the N_2O gas sensor, after temperature compensation
$S_{N2O}T_{proc}$	Concentration of N_2O in the liquid measured by the N_2O liquid microsensor without temperature compensation
$S_{N2O}T_{Comp}$	Concentration of N_2O in the liquid measured by the N_2O liquid microsensor, after temperature compensation
D_L	Depth of lab stripping column
D_R	Depth over the diffuser of the reactor
Gas emitted (aerated)	Emissions of N_2O during the aerated phases
Gas emitted (non-aerated)	Emissions of N_2O during the non-aerated phases
$-\Delta_{soln}H$	Enthalpy of the solution
a_1	Fitting parameters
b_1	Fitting parameters
Q_{in}	Flow at which the sample conditioning system pumps gas into the analyser
R	Gas constant
$Q_{gas(aerated)}$	Gas flow coming out of the reactor during aerated zones
$H_{N2O,}T_{process}$	Henry`s constant at the process temperature
K_H	Henry's constant at process temperature
K_H^{θ}	Henry's constant at standard temperature
S	Microsensor signal
mV	millivolt
D_{FN2O}	Molecular diffusivity of N_2O in water
D_{FO2}	Molecular diffusivity of oxygen in water
C	N_2O concentration
N_2O gas emitted (aerated)	N_2O gas emitted during aerated operational times
N_2O gas emitted(non-aerated)	N_2O gas emitted during non-aerated operational times
K_La_{N2O} (20°C)	N_2O mass transfer coefficient at a temperature of 20°C
$K_LaN_2O_{Tprocess}$	N_2O mass transfer coefficient at the process temperature
$K_LaN_2O_{Tprocess}$ (non-aerated)	N_2O mass transfer coefficient during non-aerated phases

Z	N_2O microsensor signal at the zero current
K_La_{O2} (20°C)	Oxygen mass transfer coefficient at the temperature of 20°C
DO_{sat}	Oxygen saturation concentration in water at 20°C
$OTR_{Liq.-Gas}$	Oxygen transfer rate
OUR	Oxygen uptake rate
F	Reduction in transfer rate caused by fouling in the air diffusers
α	Reduction in transfer rate caused by impurities in WWTP
β	Reduction in transfer rate caused by salinity
Θ	Standard factor
T^{θ}	Standard temperature
V_g	Superficial gas velocity of the reactor
T	Temperature
$T_{calibration}$	Temperature of the water when the calibration was performed
$T_{process}$	Temperature of water during the monitoring process
Δt	Time interval by which the off-gas concentration was recorded

SPECIFIC TERMS IN CHAPTERS 5 AND 6

ε	Aerobic phosphate transport coefficient (PAO only)
$Glycogen_{FORMATION}$	ATP consumed per C-mmol of aspartate consumed
$Maitenance_{ANO2}$	ATP consumed per C-mmol of glycogen consumed
$Glycogen_{Consumption}$	ATP generated per C-mmol of glycogen consumed
P_{UPTAKE}	ATP mmol consumed per P-mmol uptake
$Aspartate_{AC}$	ATP mmol generated per aspartate C-mmol fermented to acetate
$Glucose_{AC}$	ATP mmol generated per glucose C-mmol fermented to Acetate
$Glutamate_{AC}$	ATP mmol generated per glutamate C-mmol fermented to Acetate
$Glycine_{AC}$	ATP mmol generated per glycine C-mmol fermented to acetate
K_1	ATP needed for biomass synthesis from Acetyl-CoA*

K_2	ATP needed for biomass synthesis from Propionyl-CoA*
δ (Y_{NADH_ATP})	ATP produced per NADH oxidized (Aerobic P/O ratio)
rNar,e	Electron consumption rates for Nar
rNir,e	Electron consumption rates for Nir
rNor,e	Electron consumption rates for Nor
rNos,e	Electron consumption rates for Nos
rNO	Maximum consumption rates of N_2O
rN_2O	Maximum consumption rates of NO
rNO_2^-	Maximum consumption rates of NO_2^-
rNO_3^-,	Maximum consumption rates of NO_3^-
λ	Percentage of Acetyl-CoA* in PHA
β	Percentage of Propionyl-CoA* in PHA
c	PH2MV fraction in PHA
a	PHB fraction in PHA
b	PHV fraction in PHA
Y_{PHA_PP}	Yield of poly-P formation to PHA used

MOTIVATION AND THESIS OUTLINE

1.1 MOTIVATION AND OBJECTIVES

Increasing levels of Phosphorus and Nitrogen are being released into the environment, affecting water bodies and promoting eutrophication. Wastewater treatment plants (WWTPs) are an instrument to minimise the release of these two key elements. Biological nutrient removal (BNR) processes has been used from many years as a reliable method to reduce organic carbon, P and N before releasing it into the environment. Removal of N is achieved by Nitrification and Denitrification. Nitrous oxide (N_2O) is an intermediate of the process than can accumulate and end up being released in the dissolved or gaseous form. N_2O is potent greenhouse gas (GHG) with 300-fold stronger radiative force than carbon dioxide (CO_2) and has been found to contribute over 80% of the total greenhouse gases emitted from WWTPs. It is important to minimise N_2O production and understand its release into the environment. N_2O gas emissions can be analysed with off-line methodologies, although these can lead to an over or under estimation of N_2O emissions due to their high variability over time. Current online methodologies, based on online analysers, require gas sample preconditioning and minimum gas flowrates, leading to increased uncertainty at low N_2O concentrations. Surpassing the limitations inherent to these methodologies to measure N_2O gaseous concentrations would be advantageous for modelling and optimization proposes. The integration of N_2O liquid and gas measurements would allow validation mass transfer relationships used to describe gaseous N_2O emissions using liquid data measurements. This approach would enable the estimation of liquid and gas N_2O fluxes with one measurement in order to study N_2O production and consumption mechanisms.

P removal is typically achieved by polyphosphate accumulating organism (PAOs). These organisms are selected by anaerobic and aerobic sequential operational conditions in a process known as enhanced biological phosphorus removal (EBPR). Typically, these organisms uptake organic acids anaerobically and use internal carbon metabolites to P removal in aerobic and/or anoxic conditions. *Tetrasphaera*-related organisms are putative PAOs and uptake amino acids, while little is known about their P-uptake ability and metabolism that differentiate them from other PAO organisms. The metabolism of organisms present in WWTPs has been frequently studied using enriched cultures of microorganisms, so far only for *Accumulibacter* and not *Tetrasphaera*. The enrichment of a culture mainly constituted by *Tetrasphaera* would allow the identification of specific characteristics that distinguish them from

Accumulibacter. In full-scale EBPR plants, P-removal is usually combined with N-removal. *Tetrasphaera* have been reported to have the potential to remove nitrogen oxide (NOx) species while no report has shown their capability to perform full denitrification. Consumption of electron donors, as internal metabolites, has been associated as a key factor triggering N_2O production and emissions. Acclimatization of a *Tetrasphaera* culture to perform N and P removal would allow us to understand the contribution of this organism to denitrification in full-scale EBPR plants. Wastewater is usually composed of up to 30% of proteins and amino acids, and the potential of this carbon source to be used in P and/or N removal should be assessed to improve the removal of these two key elements in EBPR WWTPs.

This thesis includes the following main goals in its scope:

- To study the performance and validate a new sensor for online N_2O gas measurements and assess its feasibility for application in lab-scale systems with different emission ranges.
- To assess the applicability of N_2O gas-phase electrodes to quantify the emissions from a full-scale WWTP. Integration of liquid and gas-phase sensor measurements to compare different methodologies to estimate N_2O gas emissions from dissolved N_2O measurements.
- To operate bioreactor in order to enrich *Tetrasphaera*-related organisms from EBPR sludge, aiming at investigating their mechanism for achieving P-uptake with amino acids. Also to establish their metabolic transformations, assess storage products and their ability to metabolise different carbon sources.
- To operate a *Tetrasphaera*-EBPR culture under anaerobic-anoxic-aerobic conditions to evaluate and characterise their denitrifying capabilities, contribution towards anoxic P uptake and tendency to produce N_2O as a function of the nitrogen oxide metabolised.

1.2 THESIS OUTLINE

The content of this thesis is divided in seven chapters, describing the work performed during this PhD project:

Chapter 1 includes the Motivation and Objectives along with this Thesis outline.

Chapter 2 comprises a bibliographic review regarding P and N removal applying Biological Nutrient Removal processes. This review focusses on Nitrification and Denitrification processes in BNR, the main factors involved in the production, accumulation and emission of N_2O, a GHG, in lab-scale and full-scale WWTPs, and the methodologies used for quantifying N_2O emissions in WWTPs. The EBPR process, the organisms involved in EBPR, denitrifying EBPR and factors triggering N_2O production by organisms present in EBPR systems are also contained within this review.

Chapter 3 comprises the validation of a new online methodology using Clark-type nitrous oxide (N_2O) microelectrodes to measure N_2O emissions from lab-scale wastewater systems. The microelectrodes were tested and validated for online gas measurements and assessed with respect to the key factors affecting their performance. The N_2O emission dynamics were validated in two lab-scale SBRs performing N removal with different emission ranges.

This work was published in an international peer reviewed scientific journal article: Marques, R., Oehmen, A., Pijuan, M., 2014. Novel Microelectrode-Based Online System for Monitoring N_2O Gas Emissions during Wastewater Treatment. Environ. Sci. Technol. 48, 12816–12823 (DOI information: 10.1021/es504061h).

Chapter 4 comprises the validation of an online methodology using a Clark-type nitrous oxide (N_2O) sensor to measure N_2O emissions from full-scale systems. The N_2O gas sensor was tested and validated for online gas measurements, and assessed with respect to key parameters affecting their performance. The N_2O emission dynamics were validated in a full-scale SBR Wastewater Treatment Plant. Integration of liquid and gas-phase N_2O measurements to assess mass transfer models described

in literature to predict N_2O emission based on liquid N_2O measurements was performed.

This work was accepted for publication in an international peer reviewed scientific journal at the date of the thesis delivery: Marques, R., Rodriguez-Caballero, A., Oehmen, A., Pijuan, M., 2016. Assessment of online monitoring strategies for measuring N_2O emissions from full-scale wastewater treatment systems, Water Research (in press, DOI information: 10.1016/j.watres.2016.04.052).

Chapter 5 comprises the enrichment of two abundant polyphosphate accumulating organisms, *Tetrasphaera* and *Accumulibacter*, to evaluate metabolic behaviour and ecological niche of each culture. Microautoradiography and fluorescence *in situ* hybridisation as well as energetic balances were used in order to differentiate the niche of *Tetrasphaera* and *Accumulibacter* in the enriched cultures through a series of anaerobic-aerobic batch tests fed with either an amino acid, VFA or glucose. Anaerobic fermentation of amino acids was found to lead to P uptake instead of P release. Chemical analytical methodologies were applied to identify the internal metabolites stored by *Tetrasphaera* as carbon sources that can be used for aerobic P uptake.

Portions of this work will be submitted to international peer reviewed scientific journals, including: Marques, R., Santos, J., Nguyen, H., Carvalho, V., Carvalho, G., Freitas, E., Noronha, J. P., Nielsen, P. H., Reis, M. A. M., Oehmen, A., 2016 (in preparation). Metabolism and ecological niche of *Tetrasphaera* and *Accumulibacter* in enhanced biological phosphorus removal.

Chapter 6 comprises the acclimatization of the enriched culture obtained in Chapter 5 to anaerobic-anoxic-aerobic conditions to evaluate *Tetrasphaera*'s denitrifying capabilities. The performance of this culture was compared to *Accumulibacter* and GAO cultures operated under similar conditions. Energetic balances were used in order to evaluate the effectiveness of *Tetrasphaera* for denitrifying P removal. Different nitrogen oxide sources, individually or in combinations, were added in anoxic batch tests to assess the culture's denitrifying capacities. Reduction rates and electron consumption rates were calculated to assess the rate limiting steps and electron competition in the culture.

This work will be submitted to an international peer reviewed scientific journal: Marques, R., Ribera-Guardia, A., Santos, J., Carvalho, G., Reis, M. A. M., Pijuan, M., Oehmen, A., 2016 (in preparation). Denitrifying capabilities of *Tetrasphaera* and their contribution towards nitrous oxide production in enhanced biological phosphorus removal processes

Chapter 7 includes a summary of the main findings obtained in this work along with some questions that emerged from the present work that should be addressed in the future.

Other relevant publications not included in this thesis:

Rodriguez-Caballero, A., Aymerich, I., Marques, R., Poch, M., Pijuan, M., 2015. Minimizing N_2O emissions and carbon footprint on a full-scale activated sludge sequencing batch reactor. Water Res. 71, 1–10.

Ribera-Guardia, A., Marques, R., Arangio, C., Carvalheira, M., Oehmen, A., Pijuan, M., 2016. Distinctive denitrifying capabilities lead to differences in N2O production by denitrifying polyphosphate accumulating organisms and denitrifying glycogen accumulating organisms. Bioresource Technology (in press,2016).

2

STATE OF THE ART

Phosphorus (P) and Nitrogen (N) are two key elements essential to life, with the undesirable effect of promoting eutrophication of waterbodies, when released in excess (Tchobanoglous et al., 2003). This problem is mainly caused by growth of algae and other photosynthetic microorganisms such as toxic cyanobacteria (blue-green algae) in natural clean water. Eutrophication can lead to dissolved oxygen (DO) depletion causing decrease of aquatic wildlife, especially fish, and water contamination by reducing the drinking water quality. Free ammonia is toxic to the aquatic environment and especially to fish. With a lower effect on promoting eutrophication as compared with P, N can also be released into the environment in its gaseous form, where stable atmospheric gas phases associated within its natural cycle (Ip et al., 2001; Tchobanoglous et al., 2003). Of the gaseous nitrogenous species, nitrous oxide (N_2O) is known as a potent greenhouse gas with 300-fold stronger radiative force than carbon dioxide and is the primary ozone-depleting substance of the 21st century (IPCC, 2013; Portmann et al., 2012; Ravishankara et al., 2009). Thus, the releases of N sources can contribute to atmospheric contamination and to global warming.

Efficient operation of wastewater treatment plants (WWTPs) can decrease the load of these elements, preventing growth of algae and other photosynthetic microorganisms such as toxic cyanobacteria (blue-green algae) in natural clean water (Tchobanoglous et al., 2003). Overpopulated cities will increase pressure over WWTPs by increasing load of carbon and nutrients in the influent of these systems. Global warming will affect global availability of clean water bodies by increasing evaporation rates, promoting early snow melt and extreme precipitation events, affecting more the availability of drinking water. These two issues will promote new challenges to wastewater technology to minimise the contamination of clean water bodies. Wastewater treatment is a technology based on microbial degradation of wastewater that has been used over the past 100 years. The process was being continuously modified and evolved from its initial goal to remove colloidal, suspended and floatable material, the biodegradation of organics and the elimination of pathogenic organisms (Figure 2.1, a) (Tchobanoglous et al., 2003; Water Environment Federation, 2007), to a more complex system where key elements such as N and P were removed to avoid eutrophication of waterbodies.

2.1 BIOLOGICAL NUTRIENT REMOVAL:

Biological nitrogen removal process aims at converting influent nitrogen sources into gaseous di-nitrogen (N_2). Biological nitrogen removal is typically divided into three main steps (Figure 2.1, b): mineralization (conversion of complex organic nitrogen into ammonium (NH_4^+)); nitrification (biological oxidation of NH_4^+ to NO_3^-) and denitrification (biochemical reduction of NO_3^- to gaseous N_2). The addition of an anaerobic zone, prior to the anoxic zone allows conditions for the selection of organisms able to perform P removal (Figure 2.1, c) (Barnard, 1975; Grady et al., 2011; Wiesmann et al., 2006). When biological phosphorus removal is combined with nitrification and denitrification, the process is known as Biological Nutrient Removal.

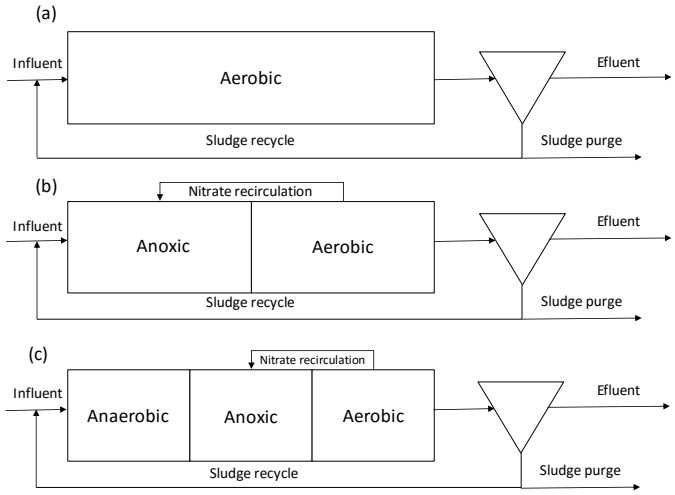

Figure 2.1 – Examples of WWTP configurations: a) the Conventional Activated Sludge process; b) Biological Nitrogen Removal process; c) Enhanced Biological Phosphorus Removal.

Nitrification is the biological oxidation of ammonium to nitrate performed by autotrophic microorganisms. It consists of two coupled reactions, (1) a first oxidation step of NH_4^+ to the intermediate hydroxylamine (NH_2OH) followed by NO_2^-, called nitritation, (2) and NO_2^- oxidation to NO_3^- called nitratation. Two different nitrifying bacteria are involved in this process, Ammonium Oxidizing Bacteria (AOB) perform the nitritation while Nitrite Oxidizing Bacteria (NOB) are responsible for nitratation (Desloover et al., 2012; Wiesmann et al., 2006) (Figure 2.2). Denitrification is the biochemical reduction of NO_3^- to gaseous N_2, as an end product, being removed from the WWTP. Complete denitrification involves four consecutive reduction steps, starting with NO_3^-, leading to the sequential production of NO_2^-, NO, and N_2O as three obligatory intermediates, before producing N_2 (Desloover et al., 2012; Wiesmann et al.,

2006) (Figure 2.2). The denitrification reduction process is mediated by four different denitrification reductases, NO_3^- reductase (Nar), NO_2^- reductase (Nir), NO reductase (Nor) and N_2O reductase (Nos) (Zumft, 1997). Denitrification is performed by ordinary heterotrophic organisms, under anoxic conditions by reducing NO_3^- or NO_2^- (electron acceptors) coupled with oxidation of organic matter (electron donors) to CO_2 and water (H_2O). N_2O is an intermediate of this process and several factors have been identified to promote the accumulation of this intermediate (Kampschreur et al., 2009).

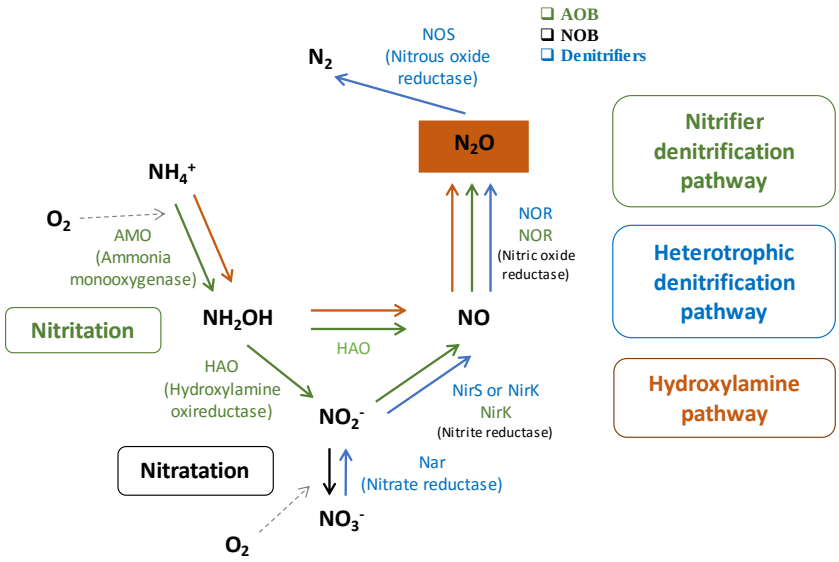

Figure 2.2 – Representation of N_2O production and consumption pathways during BNR (adapted from Desloover et al., (2012)).

2.2 FACTORS PROMOTING N_2O PRODUCTION

2.2.1 Nitrification

Both bacterial groups associated with nitrification have different involvements and influence on N_2O production. While NOB do not contribute significantly to N_2O production, AOB activity has been suggested as the predominant source of N_2O in nitrification (Kampschreur et al., 2009; Kim et al., 2010; Wunderlin et al., 2012). An important contributing factor is the incapacity of AOB to perform N_2O reduction, due to the lack of N_2O reductase in the two most abundant AOBs, *Nitrosospira* and *Nitrosomonas* (Nielsen et al., 2010; Norton et al., 2008; Stein et al., 2007). Observations made by Law et al., (2012), concluded that N_2O was the final product of the Nitrifier denitrification pathway (Figure 2.2), supporting this idea. This pathway,

which leads to N_2O production and emission, is influenced by several operational conditions. One of the factors promoting N_2O production by this pathway is the oxygen level (Tallec et al., 2006). Limiting DO levels in aerobic zones has been associated with an increase in N_2O production by AOBs (Chuang et al., 2007; Goreau et al., 1980). Meanwhile, high aeration levels have been associated with an increase in N_2O production by partial or full nitritation systems (Brotto et al., 2015; Kampschreur et al., 2009). With high DO concentrations, the hydroxylamine pathway (Figure 2.2) contribution to N_2O production has been observed to be of increased importance (Law et al., 2013; Ni and Yuan, 2015). In the hydroxylamine pathway, N_2O can be formed as a by-product during NH_2OH oxidation (biological and/or chemical) to NOH, followed by NO_2^- (Law et al., 2012). In a recent work, Ni et al., (2014) created metabolic models to describe the N_2O production by the hydroxylamine and nitrifier denitrification pathways. Transient conditions, which involves rapid changes in the process conditions, changes in DO concentration, NH_4^+ shock loads, NO_2^- levels can also trigger production of N_2O by AOBs (Ahn et al., 2010; Kampschreur et al., 2009; Tallec et al., 2006; Yu et al., 2010). Recovery from anoxic conditions to aerobic conditions was observed to shift the low specific metabolic activity to high metabolic activity in AOBs, also triggering N_2O production (Ahn et al., 2010; Yu et al., 2010). NO_2^- accumulation has been shown to be an important factor leading to increased N_2O production in lab-scale and full-scale systems (Foley et al., 2010; Kampschreur et al., 2009; Law et al., 2012). However, very high NO_2^- concentration (> 50 mgN/L) can inhibit the nitrifier denitrification pathway, leading to less N_2O production (Law et al., 2013). Other factors can promote N_2O production indirectly by leading to NO_2^- accumulation, favouring the activity of AOBs over NOBs. These factors include high temperature, short sludge retention times (SRT), high salinity, presence of sulphides, heavy metals and toxic compounds (Kampschreur et al., 2009). While nitrification has been more frequently associated with the N_2O production as compared with denitrification, some studies suggested that denitrification can play a significant role in N_2O production in WWTPs.

2.2.2 Denitrification

N_2O is an intermediate of the denitrification process, and several factors have been identified to promote the accumulation of this intermediate. As also observed for nitrifiers, DO and NO_2^- accumulation can trigger N_2O production by denitrifiers. The presence of oxygen in anoxic zones has been proven to promote N_2O production due to the sensitivity of N_2O reductase to oxygen, which is more affected by oxygen when shifting from anoxic to aerobic conditions (Kampschreur et al., 2009; Law et al., 2012;

Otte et al., 1996; Tallec et al., 2008). Also, NO_2^- accumulation has an impact on the NO and N_2O reduction, leading to N_2O accumulation (Schulthess et al., 1995). Low COD/N ratios, often resulting from a lack of organic matter, can also contribute to N_2O production (Kishida et al., 2004; Schulthess and Gujer, 1996). When subjected to low COD/N ratios, denitrification enzymes compete for electron donors, where NO and N_2O reductases have lower affinity for electrons as compared with NO_3^- and NO_2^- reductases (Law et al., 2012). N_2O accumulation was also observed under non-limiting chemical oxygen demand (COD) levels when testing denitrifying cultures with different carbon sources (Pan et al., 2013; Ribera-Guardia et al., 2014).

2.2.3 N_2O Mitigation strategies

Some of the main factors contributing to N_2O production can be mitigated by applying certain strategies: accumulation of NO_2^- can be avoided by promoting full nitrification (Ahn et al., 2010; Rodriguez-Caballero and Pijuan, 2013); low DO can be avoided by maintaining high aeration in aerobic zones (Rodriguez-caballero et al., 2014); accumulation of ammonia and NO_2^- can be minimised by applying intermittent aeration strategy (alternating short aerobic with short anoxic phases in Sequencing batch Reactor (SBR) systems) (Rodriguez-Caballero et al., 2015).

2.3 N_2O EMISSIONS FROM LAB-SCALE AND FULL-SCALE SYSTEMS

WWTPs have been shown to release significant amounts of N_2O and contribute to anthropogenic emissions, where it is produced during nitrification and denitrification (Ahn et al., 2010; Foley et al., 2010; Kampschreur et al., 2009). The N_2O that is produced and accumulated in the liquid phase can be transferred to the gas phase when N_2O is over-saturated, or stripped by aeration that facilitates the transfer of dissolved N_2O to the gas-phase. In this way, both in lab-scale reactors and WWTPs, emissions are typically higher in aeration zones/phases as compared with anaerobic or anoxic zones/phases. This causes time and spatial variation of N_2O emissions. Along with this variation, reports suggested a wide range of variation in lab and full-scale systems. Lab-studies reported different emission factors along different configurations of reactors and processes studied. Lab scale N_2O emissions have been found to vary between 0-95% of the N load in systems such as: denitrifying activated sludge (Hanaki et al., (1992); nitrifying activated sludge (Zheng et al., (1994); oxic–anoxic SBR

activated sludge (Benthum et al., 1998); anaerobic–anoxic SBR activated sludge Zeng et al., (2003b) and oxic–anoxic SBR activated sludge (Lemaire et al., 2006). In full-scale systems a smaller but still very significant variability was observed (0-14.6% of the N-load) within most of the different WWTPs studied: 25 activated sludge plants Wicht and Beier (1995); 12 different configurations of WWTPs Ahn et al., (2010); full-scale nitrifying activated sludge systems Aboobakar et al., (2013); Ye et al., (2014) Rodriguez-Caballero et al., (2015). An emission factor as low as 0.5% of total nitrogen removed as N_2O can lead to emissions comparable to the indirect CO_2 emissions related with energy consumption in conventional biological nutrient removal WWTPs (de Haas and Hartley 2004), while in some cases N_2O emissions have been found to contribute over 80% to the total greenhouse gases emitted from WWTPs (Daelman et al., 2013a; Daelman et al., 2013b). This implies that it is very important to correctly measure the emissions using online monitoring methodologies. N_2O analysers should have high versatility to measure very high and very low emission peaks/concentrations emitted from these systems.

2.4 MONITORING METHODOLOGIES

Due to its impact on N_2O emissions, substantial efforts have been performed to identify where the majority of the emissions occur, as well as their dynamics, using on-line monitoring methodologies for quantification. Initially monitoring campaigns were performed off-line with grab-sampling methods and the concentration was quantified using gas chromatography with an electron capture detector (GC-ECD) (Jenni et al., 2012; Yu et al., 2010). This methodology can lead to an over or under estimation of N_2O emissions due to their high variability over time. Currently, the majority of monitoring campaigns are performed using online methodologies based on N_2O commercial analysers using Fourier transform infrared spectroscopy and gas filter correlation (Jenni et al., 2012; Joss et al., 2009). To collect the gas, the floating hood methodology is applied. This methodology was adapted by Chandran (2011, 2009) to measure N_2O emissions from a BNR plant based on a method used to measure volatile organic compounds (VOCs) from WWTPs (Tata et al., 2003) and the methodology was certified by the United States environmental protection agency (USEPA). It is based on a surface emission isolation flux chamber (SEIFC) and a gas flow of helium as tracer method to determinate the emission N_2O flux. The flux can be then calculated by the difference of the concentrations obtained by the dilution of the

helium gas tracer. This methodology can be applied to aerated and non-aerated zones of the WWTP.

Due to its complexity, alternative methodologies have been applied for calculating the gas flow rate. This is obtained by measuring the air flow in the blower air piping and dividing it by the area of the grid of the diffuser, or alternatively, obtaining the gas flow out of the hood by installing a gas flow meter. In non-aerated zones, the emission gas flux can be obtained with the sweep gas method. With a hood vent port open, atmospheric air will be pulled into the hood at a known gas flow defined by the online gas analyser. The emission of gas flow from the tank can then be calculated by performing a mass balance between the concentration of oxygen inside the hood and the atmospheric oxygen concentration measured. This methodology has been applied to successfully measure the emission of plants with different configurations (Rodriguez-Caballero et al., 2015; Rodriguez-caballero et al., 2014).

Using the protocol developed by (Chandran, 2011, 2009) as a guide, several researchers performed with success adaptations to this methodology to measure emissions from WWTPs based on the following protocol (Aboobakar et al., 2013; Ahn et al., 2010; Desloover et al., 2012; Rodriguez-Caballero et al., 2015; Rodriguez-Caballero et al., 2014): (a) apply a floating hood to collect N_2O gas emissions; (b) quantify the N_2O gas concentration with an online gas analyser; (c) determine the flux of emissions. Pan et al. (2016) proposed a methodology based on a multiple gas hood system connected to an online gas analyser to simultaneously analyse the emissions from various locations, accounting for spatial variability.

To carry the gas from the gas hood to the online gas analyser, air tight PTFE tubing is often used. Typically, these conventional analysers require preconditioning of the gas sample (removing humidity and particles) and a minimum gas flow (0.5 − 1 L/min depending on the analyser). This last step dilutes the concentration of N_2O, increasing uncertainty in the low N_2O concentration range. These constraints indicate that new online measuring technologies should be developed and validated to better characterize and mitigate the N_2O emissions from WWTPs.

2.5 ENHANCED BIOLOGICAL PHOSPHORUS REMOVAL

The enhanced biological phosphorus removal (EBPR) process is an efficient, relatively inexpensive and environmentally sustainable option for phosphorus (P)

removal in wastewater treatment plants (WWTP) (Oehmen et al., 2007a). The process consists in enrichment of organisms able to accumulate, in excess, intracellular polyphosphate (poly-P) when subjected to recirculation through anaerobic followed by aerobic and/or anoxic conditions. P is removed from the system by wastage of sludge with a high poly-P content. In full-scale EBPR plants, P-removal is usually combined with N-removal. The process can be achieved in a SBR operated in a single tank with sequential anaerobic and anoxic and/or aerobic phases, followed by settling and decanting to remove the treated water, or in a continuous operation mode, with the wastewater subjected to sequential anaerobic and anoxic and/or aerobic tanks.

The EBPR system has some advantages as compared with typical activated sludge systems (Mullan et al., 2002; Oehmen et al., 2007a): achieves higher P removal (>90%) as compared with conventional activated sludge (20-40%); reduces 20% the sludge production as compared with chemical precipitation.; promotes energy savings (25%) due to less cost associated with sludge treatment; and reduces the use of chemical precipitants (calcium, aluminium and iron slats) to remove phosphorus (Yeoman et al., 1988).

2.6 MAIN ORGANISMS INVOLVED IN EBPR SYSTEMS

2.6.1 *Accumulibacter*

"*Candidatus* Accumulibacter phosphatis" (referred to as *Accumulibacter* hereafter) is the most important Gram-negative identified PAO present in most full-scale EBPR plants. It belongs to the family *Rhodocyclaceae* of subclass 2 of the *Betaproteobacteria*. These bacteria demonstrate a typical PAO phenotype, performing anaerobic/aerobic cycling of poly-P and polyhydroxyalkanoates (PHA) (Crocetti et al., 2000; Garcia Martin et al., 2006; Hesselmann et al., 2000). *Accumulibacter* is present in relatively high abundance in different WWTP configurations (1–22% of all Bacteria) (Crocetti et al., 2000; Kong et al., 2007, 2005, 2004; A. A. B. Lanham et al., 2013; Nguyen et al., 2011; Saunders et al., 2003). Despite many attempts, *Accumulibacter* has not yet been isolated and cultivated in pure culture. To study their metabolism, enriched PAO cultures were cultivated in lab-scale. Highly enriched *Accumulibacter* cultures in lab-scale EBPR systems were reported in several studies (Crocetti et al., 2000; Hesselmann et al., 2000; Liu et al., 2001). In more recent studies, using new techniques involving functional genes expression, the gene encoding the

polyphosphate kinase (*ppk*) was used as phylogenetic marker. It was observed that *Accumulibacter* are divided in two major groups (Type I and II), each comprised of several subgroups (clades) (He et al., 2007; Mcmahon et al., 2002; Peterson et al., 2008). These two Types of *Accumulibacter* have in some cases been found to display different morphologies, cocci-bacilli and cocci, respectively for Type I and II (Carvalho et al., 2007; Flowers et al., 2009).

As one of the main organisms involved in EBPR systems, metabolic pathways of *Accumulibacter* PAO in anaerobic and anoxic/aerobic conditions are intensively described. These PAOs are able to store large amounts of poly-P aerobically after taking up organic substrates anaerobically, unlike ordinary heterotrophic organisms. *Accumulibacter* PAOs take up volatile fatty acids (VFAs) (e.g., acetate and propionate) anaerobically and store them as PHAs. This conversion is mainly obtained with energy from hydrolysis of intracellular poly-P, release of P from the cell and the reducing power obtained from glycolysis of intracellular glycogen (Mino et al., 1987) or the tricarboxylic acid (TCA) cycle (Comeau et al., 1986; Wentzel et al., 1986). More recent findings have indicated that both pathways are active in lab-scale cultures (Hesselmann et al., 2000; Louie et al., 2000; Pereira et al., 1996) and in full-scale plants (A. A. B. Lanham et al., 2013; Zhou et al., 2009). In the subsequent aerobic or anoxic phase, *Accumulibacter* PAOs degrade PHA as energy source for P uptake and poly-P production, glycogen regeneration, biomass growth and cell maintenance (Figure 2.3, Table 2.1).

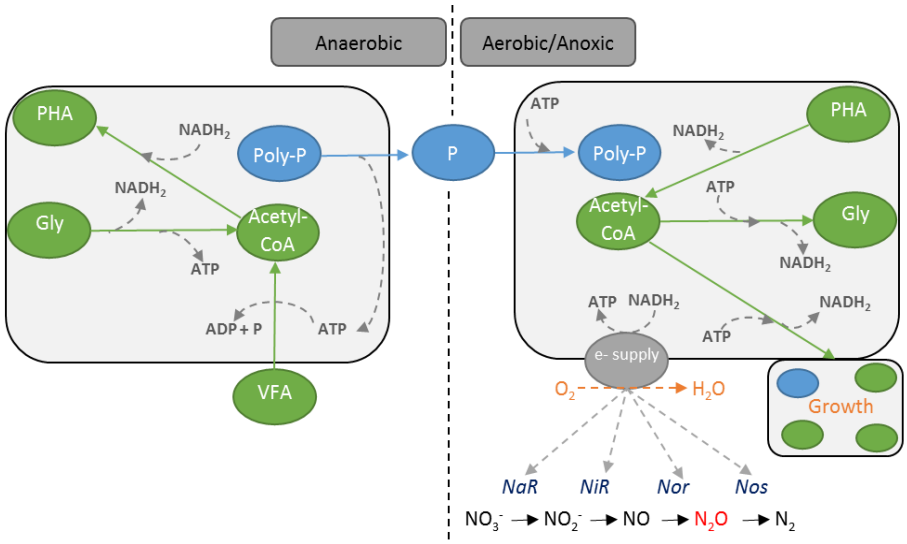

Figure 2.3 – Simplified schematic representation of *Accumulibacter* PAO metabolism in anaerobic and anoxic/aerobic conditions.

Accumulibacter PAOs have the capacity to perform P-uptake in aerobic and anoxic conditions. Simultaneous P and N removal can have the added advantage of savings in plant operational costs. Less COD is required for P and N removal and consequently lower sludge production is obtained. P removal under anoxic conditions promotes savings in aeration by the use of nitrogen instead of oxygen as electron acceptor, leading to a decrease in energy costs (Kuba et al., 1996; Oehmen et al., 2007a). Enriched cultures of denitrifying *Accumulibacter* PAOs revealed different affinities for NO_3^- and difference in their capacity to perform partial or complete denitrification (Ahn et al., 2002; Tsuneda et al., 2006; Zeng et al., 2003a; Zilles et al., 2002). This led to the hypothesis that the presence of two groups of PAOs with different capacities to reduce nitrogen oxide (NOx) species exists. In later studies, it was associated to denitrifying PAOs (DPAOs) with *Accumulibacter* Type I able to reduce NO_3^- to N_2, while *Accumulibacter* Type II unable to reduce NO_3^- but could reduce NO_2^- to N_2 (Carvalho et al., 2007; Flowers et al., 2009; Adrian Oehmen et al., 2010).

Table 2.1 – Ecophysiology of PAOs and GAOs in EBPR plants adapted from (Nielsen et al., (2010).

	Accumulibacter	*Tetrasphaera*	*Competibacter*	*Defluvicoccus*
EBPR (% bacteria)	1-22%	1-30%	0-12%	0-9%
Morphotypes	cocci-bacilli and cocci	short rods, branched rods, small cocci, cocci in tetrads, filaments, and thin filaments	cocci and rod	tetrad and filamentous
electron acceptors	O_2, NO_3^-, NO_2^-	O_2, NO_3^-, NO_2^-	O_2, NO_3^-, NO_2^-	O_2, NO_3^-
Carbon uptake	acetate, propionate, pyruvate	acetate, propionate, glucose, amino acids	acetate, propionate, pyruvate	acetate, propionate, pyruvate
Ferment	-	+	-	-
Poly-P storage	+	+	-	-
Storage C compound produced anaerobically	PHA	Glycogen, amino acids	PHA	PHA
References	(Crocetti et al., 2000; Flowers et al., 2010, 2008; Kong et al., 2005, 2004)	(Kong et al., 2008, 2007, 2005; Kristiansen et al., 2013; Nguyen et al., 2015, 2011)	(Crocetti R. et al., 2002; Kong et al., 2006, 2002; Saunders et al., 2003)	(Burow et al., 2007; Wang et al., 2008; Wong and Liu, 2007)

2.6.2 Glycogen accumulating organism

Another group is present in EBPR systems that compete for the same organic carbon sources as the aforementioned PAOs, and are known as glycogen accumulating organisms (GAOs). There are two main groups of bacteria that exhibit the GAO phenotype and have been identified in full and lab-scale EBPR systems,

"*Candidatus* Competibacter phosphatis" (henceforth referred to as *Competibacter*) (Crocetti R. et al., 2002; Kong et al., 2006) within the *Gammaproteobacteria* phylum and Alphaproteobacterial *Defluviicoccus vanus*-related organisms (Meyer et al., 2006; Wong et al., 2004).

Seven subgroups of *Competibacter* were identified (GB 1 to 7), exhibiting mainly cocci or rod morphologies. These bacteria can be highly enriched in lab-scale cultures fed with acetate (Crocetti R. et al., 2002; Kong et al., 2002) or present in significant numbers in full-scale plants (Crocetti R. et al., 2002; Kong et al., 2006, 2002; Wong et al., 2005). The other GAOs group identified in some EBPR plants, *Defluviicoccus vanus*, is composed of four distinct subgroups. *Defluviicoccus vanus* were generally observed to be present in full-scale EBPR plants in lower abundance as compared with *Competibacter* (Burow et al., 2007; Oehmen et al., 2007a; Wong and Liu, 2007; Wong et al., 2004). Clusters I and II are more highly studied (Meyer et al., 2006; Wong et al., 2004) as compared with cluster III (McIlroy et al., 2010; Nittami et al., 2009) and IV (McIlroy and Seviour, 2009). These bacteria display tetrad and filamentous morphologies (Burow et al., 2007; McIlroy et al., 2010; Nittami et al., 2009).

GAOs are able to survive and grow under alternating anaerobic and anoxic/aerobic conditions with similar metabolic processes as PAOs, without contributing to P removal (Oehmen et al., 2007a; Seviour et al., 2003). Anaerobically the consumed carbon (e.g. acetate, propionate) is used for synthesis of PHA with the energy generated by glycogen utilization. In the following aerobic or anoxic phase, they use the intracellular stored PHA for glycogen production, cell maintenance and growth (Nielsen et al., 2010; Oehmen et al., 2007a; Seviour et al., 2003) (Figure 2.4, Table 2.1). Different denitrifying capabilities have been reported for the different GAO groups and sub-groups. *Competibacter* GAOs can be grouped according to their denitrifying capabilities within the 7 subgroups identified: complete denitrification (subgroups 6), NO_3^- reduction (subgroup 1,4 and 5), unable to denitrify (subgroup 3 and 7) (Kong et al., 2006). The *Defluviicocus* GAOs can also be grouped according with their denitrifying capabilities, cluster I can reduce NO_3^- but not NO_2^-, while cluster II was unable to denitrify (Burow et al., 2007; Wang et al., 2008).

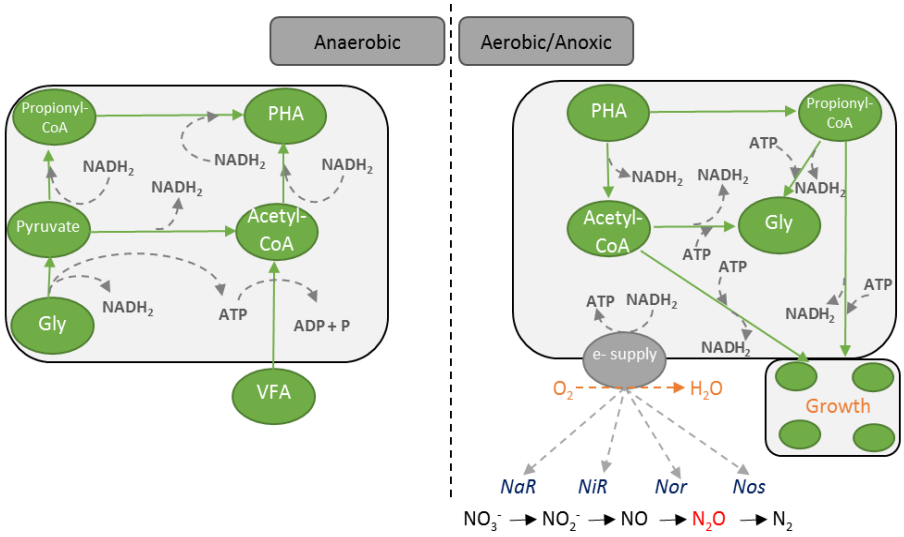

Figure 2.4 – Simplified schematic representation of GAO metabolism in anaerobic and anoxic/aerobic conditions.

2.6.3 *Tetrasphaera*-related organism

Besides *Accumulibacter*, another group of bacteria in full-scale EBPR systems is present *Tetrasphaera*, reaching even higher abundance than *Accumulibacter*, up to 30% of the total biomass (Kong et al., 2005; A. A. B. Lanham et al., 2013; Mielczarek et al., 2013; Nguyen et al., 2011). However, this Gram-positive organism doesn't share all of the typical PAO characteristics known from *Accumulibacter*. These organisms can take up P aerobically and store it intracellularly as poly-P, while assimilating different organic substrates (such as glucose and amino acids) under anaerobic conditions, as assessed through microautoradiography combined with fluorescence *in situ* hybridisation (MAR-FISH) of full-scale EBPR sludge (Kong et al., 2005; Nguyen et al., 2011). It has been shown that *Tetrasphaera*-related PAOs cannot store PHAs, although some can take up acetate. Also they can synthesize glycogen, ferment glucose and can express extracellular surface-associated amylases for degradation of starch (Kong et al., 2008; Kristiansen et al., 2013; Nguyen et al., 2011; Xia et al., 2008).

Using phylogenetic analysis of cloned sequences, Nguyen et al., (2011) observed that *Tetrasphaera* are grouped into three separate clades belonging to the family *Intrasporangiaceae* in the *Actinobacteria*. These three clades exhibit six different morphotypes (short rods, branched rods, small cocci, cocci in tetrads, filaments, and thin filaments) (Figure 2.5, Table 2.1). A few isolates were cultured from activated sludge, and include T. *australiensis*, T. *japonica* (Maszenan et al., 2000), *Tetrasphaera*

elongata (strain LP2) (Hanada et al., 2002), T. *elongata* (strain ASP12) (Onda and Takii, 2002), and the filamentous T. *jenkinsii*, T. *vanveenii*, and T. *veronensis* (McKenzie et al., 2006). By using cloned sequences, the isolated species were related with the different clades. Clade 1 includes clones related to sequences of *T. elongata* and *T. duodecadis*, and clade 2 contains four isolated species: *T. jenkinsii*, *T. australiensis*, *T.veronensis* and the filamentous "*Candidatus Nostocoida limicola*", while clade 3 contains only sequences from uncultured clones (Nguyen et al., 2011).

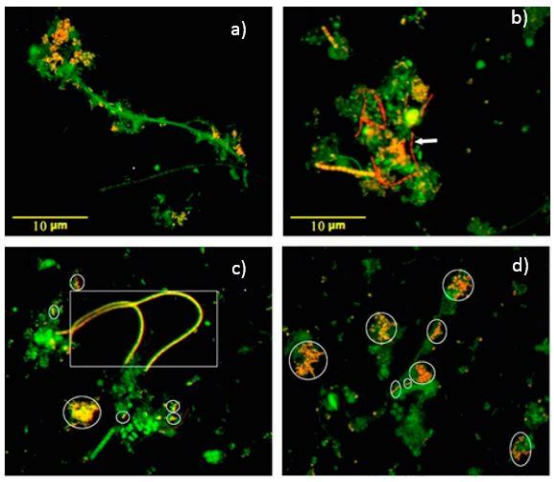

Figure 2.5 – FISH images of *Tetrasphaera* in activated sludge, Tet3-654 (a), Tet2-892 (b), Tet2-174 (b), Tet3-654 (d). In yellow are shown *Tetrasphaera* while other bacteria are in green (Nguyen et al., 2011).

Nguyen et al (2011) developed five sets of FISH probes to detect *Tetrasphaera*, where most of the probe-defined *Tetrasphaera* were shown to be putative PAO. Tests with MAR-FISH and DAPI identified that four of the five probe-defined populations were able to perform P-uptake and store poly-P after anaerobic carbon uptake. Only the population targeted with probe Tet3-19 and some thin filaments hybridizing probe Tet2-174 were unable to perform P-uptake with any of the carbon sources (Nguyen et al., 2011) (Figure 2.5). Nguyen et al., (2011) also observed that P uptake depended on the type of organic substrate and that only certain morphotypes could take up P. Glucose and casamino acids were taken up by all clades, while acetate and glutamic acid were taken up by clades 2 and 3. The uptake pattern of different carbon sources (acetate, glucose, casamino acids and glutamic acid) in anaerobic and aerobic conditions were similar for Tet2-892, Tet2-174 and Tet3-654. Glucose and glutamic acid were taken up by Tet3-19 in anaerobic and aerobic conditions, but without P uptake. The physiology of these organisms are more complex than that of *Accumulibacter*, and they are not

able to store PHA. *Tetrasphaera*'s fermentation capacity was also demonstrated: they were not able to uptake acetate after 3h of continuous feeding, meaning that the storage capacity of the intracellular metabolite was reached and no growth was observed; however, after 9h of continuous feeding, all *Tetrasphaera* were able to uptake glucose, suggesting that fermentation took place (Nguyen et al., 2011).

Kristiansen et al., (2013) performed genome sequencing of four *Tetrasphaera* isolates (T. *australiensis*, T. *japonica*, T. *elongata*, and T. *jenkinsii*) in order to investigate their metabolic pathways. *Accumulibacter* and *Tetrasphaera* share some metabolic pathways such as the TCA cycle, glycolysis, gluconeogenesis, and polyphosphate metabolism. However, they differ in other important aspects, especially the ability to ferment, only found in *Tetrasphaera* (Kristiansen et al., 2013).

Regarding the poly-P metabolic machinery *Tetrasphaera* share much of it with *Accumulibatcer* as expressed by the similarity of the genes involved (polyphosphate kinase 1 (*ppk1*), polyphosphate kinase 2 (*ppk2*), exopolyphosphatase (*ppx*), polyphosphate AMP phosphotransferase (*pap*), adenylate kinase (*adk*), a membrane bound proton-pumping pyrophosphatase, high affinity phosphate specific transporter (Pst), and a low affinity phosphate transporter (Pit)). This suggests a similar process between both bacteria in the intracellular poly-P degradation and P release to generate energy for substrate uptake and conversion to intracellular metabolites (Kristiansen et al., 2013). As for carbon source uptake, *Tetrasphaera* can take up a variety of carbon sources (propionate, acetate, glucose, amino acids, glutamate, and aspartate). Genes encoding for assimilating acetate, glucose, glutamate and aspartate are present and confirm the versatility of this organism (Kristiansen et al., 2013). These results confirmed observations made by previous studies (Kong et al., 2008, 2007, 2005; Nguyen et al., 2011). The genes encoding for enzymes involved in the glycolysis, gluconeogenesis, glycogen synthesis, glycogenolysis and TCA cycle are present in the genome of all *Tetrasphaera* studied by Kristiansen et al (2013). Glycogen shunt genes were not found in the *Tetrasphaera* genome, which might explain the low growth observed when acetate was fed as sole carbon source (Kristiansen et al., 2013). As mentioned before, ecophysiology studies performed *in situ*, reveal PHA was not the intracellular storage compound for *Tetrasphaera* in the anaerobic phase (Kong et al., 2008, 2007, 2005; Nguyen et al., 2011). This was further confirmed in three genome sequences obtained for T. *australiensis*, T. *elongata*, and T. *jenkinsii*. In all three, the genes essential for PHA synthesis were not detected (PHA synthesis gene (*pha*C)). These three isolates, had genes encoding for acetyl-CoA acetyltransferase (*pha*A) and

acetoacetyl-CoA reductase (*pha*B). However, only in T. *japonica* all three genes involved in the PHA synthesis were found (*pha*A, *pha*B and *pha*C) (Kristiansen et al., 2013). One of the main differences between *Accumulibacter* and *Tetrasphaera* is the capacity of the latter to perform fermentation (Nguyen et al., 2011; Xia et al., 2008). Genes encoding for aldehyde dehydrogenase (*aldA*), alcohol dehydrogenase (*adh*) and alanine dehydrogenase (*ald*), which are involved in glucose fermentation, were found in all *Tetrasphaera* isolates. Kristiansen et al., (2013) suggested that ethanol and alanine might be end products of glucose fermentation. The reversibility of lactate dehydrogenase suggests T. *elongate* has the potential to produce lactate as end product of glucose fermentation. Acetate and succinate might be also end products of glucose fermentation in all isolates. The ability of *Tetrasphaera* to generate energy from fermentation might provide a different niche as compared with *Accumulibacter*.

A metabolic model based on glucose metabolism for members of the genus *Tetrasphaera* involved in EBPR systems was proposed by Kristiansen et al., (2013). They suggested that under anaerobic conditions the *Tetrasphaera* take up glucose and ferment this to acetate, succinate and other components. Furthermore, glycogen is produced as a storage polymer and the energy required for these anabolic reactions is obtained from fermentation and poly-P degradation. Aerobically, the stored glycogen is degraded to provide carbon and energy for growth, P uptake and poly-P formation. *Tetrasphaera* metabolism seems more complex and diverse than *Accumulibacter*, where development of new biochemical reaction-based models to describe the ecophysiology of this organism should be pursued to better describe and understand their role in EBPR systems (Figure 2.6, Table 2.1).

The metagenomic results of Kristiansen et al (2013) also led to the observation that all four existing *Tetrasphaera* isolates (T. *australiensis*, T. *elongate*, T. *jenkinsii* and T. *japonica*) have the genomic capabilities to code for enzymes able to reduce NO_3^- to nitric oxide (NO). The *nir*K gene was found in all 4 genomes of the isolates. While only in two of them (T. *australiensis,* T. *japonica*), the genes necessary for the NO reductase, large subunit (NorB) and NO reductase (NorZ) synthesis were found, required to reduce NO to N_2O. While N_2O reductase (nosZ) haven't been found in any of the 4 genomes of the isolates (Kristiansen et al., 2013). The reduction of N_2O by *Tetrasphaera* has not been demonstrated in any of the studies so far.

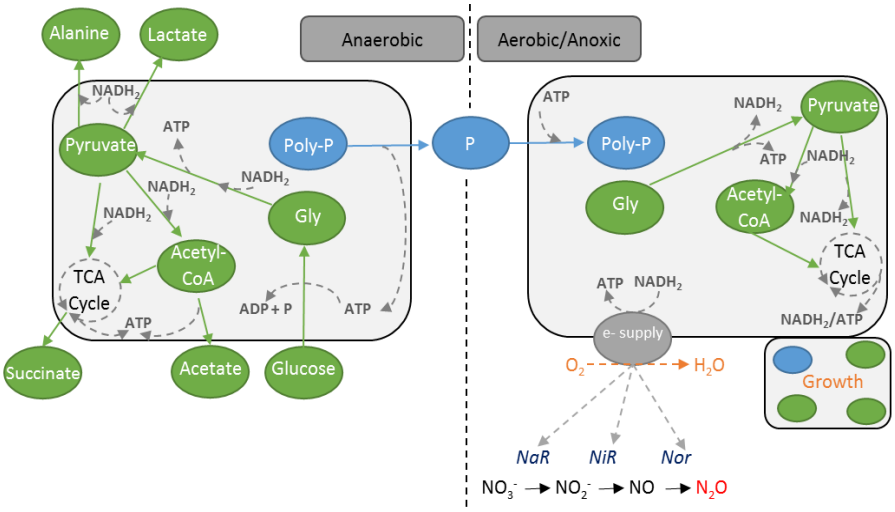

Figure 2.6 – Simplified schematic representation of *Tetrasphaera* metabolism in anaerobic and anoxic/aerobic conditions, adapted from Kristiansen et al., (2013).

Nguyen et al., (2015) has observed consumption of labelled glycine linked with P release in tests performed with activated sludge and with a T. *elongate* isolate. Consumption of glycine was also accompanied with accumulation of intracellular glycine and small amounts of glutamine, serine and alanine. This intracellular glycine reached 9-15% of the total carbon consumption, while glutamine, serine and alanine were lower than 1%. A large fraction of the carbon consumed (35-60%) was excreted to bulk media as fermentation products, such as, acetate, succinate and alanine. Interestingly, the non-labelled intracellular glutamate concentration increased during the anaerobic phase, with cells using other carbon sources that were not identified. The uptake of glycine stopped when intracellular pools of poly-P were exhausted in both tests, suggesting glycine uptake was controlled by the amount of intracellular poly-P available. In the subsequent aerobic phase, the stored glycine was consumed along with the other internal metabolites. The oxidation of internal metabolites was linked with P uptake.

2.7 N_2O ACCUMULATION IN EBPR SYSTEMS

The denitrifying capacities of denitrifying PAOs (*Accumulibacter*) and GAOs (*Competibacter* and *Defluviicoccus*) has been often demonstrated (Burow et al., 2007; Flowers et al., 2009; Kong et al., 2006; Wang et al., 2008). Some reports have been made to the emissions of N_2O in those systems, reaching up to 90% of the N load: Continuous anaerobic–anoxic SBR activated (Zeng et al., 2003c), Continuous oxic–

anoxic SBR activated sludge (Lemaire et al., 2006). However, the factors leading to N_2O accumulation have not been clearly identified. Consumption of internal carbon sources, electron competition and NO_2^- accumulation have been suggested as important factors. In EBPR systems where internal carbon sources (PHAs) are utilised during denitrification as electron donor, electron competition may also impact on N_2O accumulation (Kampschreur et al., 2009), although this has yet to be conclusively demonstrated. Although not conclusively demonstrated, some factors have been associated with the production and accumulation of N_2O. NO_2^- accumulation was also observed in some of these studies, where the acidified form of NO_2^- (free nitrous acid - FNA) was found to be the main factor leading to N_2O production, making it difficult to assess the influence of PHA as carbon source towards N_2O production independently of FNA accumulation (Zhou et al., 2008). Zhou et al., (2012) also suggested that PHA consumption for denitrification is a potentially rate-limiting step for N_2O reduction.

Metabolomics studies performed with pure culture organisms suggest N_2O as an end-product of denitrification of *Tetrasphaera*. The contribution of this abundant organism group present in EBPR systems to N_2O accumulation and emission should be considered. Contrarily to *Accumulibacter*, the intracellular storage compound of *Tetrasphaera* PAOs has not been entirely revealed, with glycogen, amino acids or macromolecules being observed as storage compounds (Kristiansen et al., 2013; Nguyen et al., 2015). The consumption of these carbon sources can lead to different affinities to NOx species as compared with *Accumulibacter*. The role of *Tetrasphaera* under anoxic conditions should be investigated to understand their contribution to N_2O accumulation in EBPR systems.

2.8 THESIS RATIONALE

N_2O is a potent GHG with 300-fold stronger radiative stronger than CO_2 and have been found to contribute over 80% of the total greenhouse gases emitted from WWTPs. Currently an effort has been performed to assess the N_2O emissions of different lab and full-scale systems to contribute to a final goal of increasingly understanding the main factors affecting N_2O production and consumption pathways. Some factors have been already identified (e.g. NO_2^- accumulation, low DO, low COD/N, transitions from anoxic to aerobic phases, low temperature, short SRT, high ammonia concentration) while others have not yet been recognized. N_2O gas emissions can be analysed with off-line methodologies, however it can lead to an over

or under estimation of N_2O emissions due to their high variability over time. Current methodologies use online analysers with added advantages compared with off-line methods, however, these analysers require preconditioning of the gas sample (removing humidity and particles) and a minimum gas flow (0.5 − 1 L/min depending on the analyser). These limitations suggest the possibility of developing and validation of new online measuring technologies to improve the characterization of N_2O emissions. Mass transfer relationships can be an adequate approach to estimate the N_2O emissions using liquid data measurements. The integration of N_2O liquid and gas measurements can be used as a validation of these relationships, simplifying the methodology to estimate N_2O emissions. This method integration would enable estimation of liquid and gas N_2O fluxes with one measurement system in order to study N_2O production and consumption mechanisms.

Tetrasphaera are a high abundant organism in full-scale BNR systems, and their metabolism and contribution towards P and N removal and the impact on N_2O should be studied. Ecophysiology studies in EBPR plants and lab-scale with some isolates and full-scale sludge allowed increased understanding of the capacity of *Tetrasphaera* to perform P-uptake and consume carbon. These results were further validated with genome sequences of four *Tetrasphaera* isolates which allowed to establish a metabolic model (Kristiansen et al., 2013). Since *Tetrasphaera* is a rather broad group of organisms, which possesses metabolic differences on a species level, the metabolism of these isolates might not be fully representative of the high diversity of probe-identified organisms found in full-scale EBPR plants. The metabolism of *Accumulibacter* has been frequently studied using enriched cultures of microorganisms, although thus far, no enriched cultures of *Tetrasphaera*-related PAOs have been obtained. Little is known about the P removal efficiency of *Tetrasphaera*-related PAOs in EBPR systems, as compared to *Accumulibacter*, which is a key point when investigating the importance of *Tetrasphaera* for EBPRs. Much remains to be learned regarding their metabolic behaviour, as it is difficult to distinguish their activity from *Accumulibacter*'s, particularly in full-scale systems where they are present in comparatively lower abundance. Furthermore, the potential synergy that may exist between *Tetrasphaera* and Accumulibacter has never been studied before. A better understanding of the ecophysiology of *Tetrasphaera* is needed to understand their function, and improve our understanding of the EBPR process and our ability to optimise it. Metabolomics studies suggested *Tetrasphaera* have the genomic capabilities to encode enzymes able to reduce NO_3^- to NO. No other information was

yet obtained regarding the capacity of *Tetrashaera* to perform denitrification. Also, the capacity of *Tetrapshaera* to couple denitrification with P uptake has never been established, nor the kinetics of denitrification in the presence of different NOx. Contrarily to *Accumulibacter*, *Tetrasphaera* do not synthesise PHAs, and they seem to use amino acids and/or glycogen as internal storage products. *Tetrasphaera* intracellular storage compound has not been entirely revealed, amino acids and glucose can be stored, and further research is necessary. The consumption of these internal products might lead to a different behaviour in the formation/consumption of N_2O as compared with *Accumulibacter*. As one of the most abundant organism group present in EBPR systems, *Tetrasphaera*, should be characterised toward their contribution to N_2O production and emissions in EBPR systems.

REFERENCES

Aboobakar, A., Cartmell, E., Stephenson, T., Jones, M., Vale, P., Dotro, G., 2013. Nitrous oxide emissions and dissolved oxygen profiling in a full-scale nitrifying activated sludge treatment plant. Water Res. 47, 524–34.

Ahn, J., Daidou, T., Tsuneda, S., Hirata, A., 2002. Characterization of denitrifying phosphate-accumulating organisms cultivated under different electron acceptor conditions using polymerase chain reaction-denaturing gradient gel electrophoresis assay. Water Res. 36, 403–412.

Ahn, J.H., Kim, S., Park, H., Rahm, B., Pagilla, K., Chandran, K., 2010. N2O emissions from activated sludge processes, 2008-2009: results of a national monitoring survey in the United States. Environ. Sci. Technol. 44, 4505–4511.

Barnard, J.L., 1975. Biological nutrient removal without the addition of chemicals. Water Res. 9, 485–490.

Benthum, W.A.J. van, Garrido, J.M., Mathijssen, J.P.M., Sunde, J., Loosdrecht, M.C.M. van, Heijnen, J.J., 1998. Nitrogen removal in intermittently aerated biofilm airlift reactor. J. Environ. Eng. 124, 239–248.

Brotto, A.C., Kligerman, D.C., Andrade, S.A., Ribeiro, R.P., Oliveira, J.L.M., Chandran, K., de Mello, W.Z., 2015. Factors controlling nitrous oxide emissions from a full-scale activated sludge system in the tropics. Environ. Sci. Pollut. Res. 22, 11840–11849.

Burow, L.C., Kong, Y., Nielsen, J.L., Blackall, L.L., Nielsen, P.H., 2007. Abundance and ecophysiology of Defluviicoccus spp., glycogen-accumulating organisms in full-scale wastewater treatment processes. Microbiology 153, 178–185.

Carvalho, G., Lemos, P.C., Oehmen, A., Reis, M. a M., 2007. Denitrifying phosphorus removal: linking the process performance with the microbial community structure. Water Res. 41, 4383–96.

Chandran, K., 2009. Characterization of nitrogen greenhouse gas emissions from wastewater treatment BNR operations, in: Field Protocol with Quality Assurance Plan (U4R07). Water Environment Research Foundation.

Chandran, K., 2011. Protocol for the measurement of nitrous oxide fluxes from biological wastewater treatment plants., 1st ed, Methods in enzymology. Elsevier Inc.

Chuang, H.P., Ohashi, A., Imachi, H., Tandukar, M., Harada, H., 2007. Effective partial nitrification to nitrite by down-flow hanging sponge reactor under limited oxygen condition. Water Res. 41, 295–302.

Comeau, Y., Hall, K., Hancock, R., Oldham, W., 1986. Biochemical model for enhanced biological phosphorus removal. Water Res. 20, 1511–1521.

Crocetti R., G., Banfield F., J.F., Keller, J., Bond, P.L., Blackall, L.L., 2002. Glycogen-accumulating organisms in laboratory-scale and full-scale wastewater treatment processes. Microbiology 148, 3353–3364.

Crocetti, G.R., Hugenholtz, P., Bond, P.L., Schuler, a, Keller, J., Jenkins, D., Blackall, L.L., 2000. Identification of polyphosphate-accumulating organisms and design of 16S rRNA-directed probes for their detection and quantitation. Appl. Environ. Microbiol. 66, 1175–82.

Daelman, M.R.J., De Baets, B., van Loosdrecht, M.C.M., Volcke, E.I.P., 2013. Influence of sampling strategies on the estimated nitrous oxide emission from wastewater treatment plants. Water Res. 47, 3120–3130.

Daelman, M.R.J., van Voorthuizen, E.M., van Dongen, L.G.J.M., Volcke, E.I.P., van Loosdrecht, M.C.M., 2013. Methane and nitrous oxide emissions from municipal wastewater treatment - results from a long-term study. Water Sci. Technol. 67, 2350–5.

De Haas, D., Hartley, K., 2004. Greenhouse gas emission from BNR plants-do we have the right focus? In: Paper Presented at the Proceedings of EPA Workshop: Sewage Management, Risk Assessment & Triple Bottom Line. Cairns, Australia, 5-7 April 2004

Desloover, J., Vlaeminck, S.E., Clauwaert, P., Verstraete, W., Boon, N., 2012. Strategies to mitigate N2O emissions from biological nitrogen removal systems. Curr. Opin. Biotechnol. 23, 474–82.

Flowers, J.J., He, S., Carvalho, G., Peterson, S.B., Lopez, C., Yilmaz, S., Zilles, J.L., Morgenroth, E., Lemos, P.C., M, M. a, Crespo, M.T.B., Noguera, D.R., Mcmahon, K.D., 2008. Ecological Differentiation of Accumulibacter in EBPR Reactors. Environment 2008, 31–42.

Flowers, J.J., He, S., Yilmaz, S., Noguera, D.R., McMahon, K.D., 2009. Denitrification capabilities of two biological phosphorus removal sludges dominated by different “Candidatus Accumulibacter” clades. Environ. Microbiol. Rep. 1, 583–588.

Flowers, J.J., He, S., Yilmaz, S., Noguera, D.R., McMahon, K.D., 2010. Denitrification capabilities of two biological phosphorus removal sludges dominated by different “Candidatus Accumulibacter” clades. Environ. Microbiol. Rep. 1, 583–588.

Foley, J., de Haas, D., Yuan, Z., Lant, P., 2010. Nitrous oxide generation in full-scale biological nutrient removal wastewater treatment plants. Water Res. 44, 831–44.

Garcia Martin, H., Ivanova, N., Kunin, V., Warnecke, F., Barry, K.W., McHardy, A.C., Yeates, C., He, S., Salamov, A.A., Szeto, E., Dalin, E., Putnam, N.H., Shapiro, H.J., Pangilinan, J.L., Rigoutsos, I., Kyrpides, N.C., Blackall, L.L., McMahon, K.D., Hugenholtz, P., 2006. Metagenomic analysis of two enhanced biological phosphorus removal (EBPR) sludge communities. Nat Biotechnol 24, 1263–1269.

Goreau, T.J., Kaplan, W.A., Wofsy, S.C., Mcelroy, M.B., Valois, F.W., Watson, S.W., 1980. Production of nitrite and nitrous oxide by nitrifying bacteria at reduced concentrations of oxygen. Appl. Environ. Microbiol. 40, 526–532.

Grady, C., Daigger, G., Love, N., Filipe, C., 2011. Biological Wastewater Treatment, CRC Press. ed. IWA Publishing, London, New York.

Hanada, S., Liu, W., Shintani, T., Kamagata, Y., 2002. polyphosphate-accumulating bacterium isolated from activated sludge 883–887.

Hanaki, K., Z. Hong, T. Matsuo, 1992. Production of Nitrous-Oxide Gas During Nitrification of Waste-Water. Water Sci. Technol. 26, 1027–1036.

He, S., Gall, D.L., McMahon, K.D., 2007. “Candidatus accumulibacter” population structure in enhanced biological phosphorus removal sludges as revealed by polyphosphate kinase genes. Appl. Environ. Microbiol. 73, 5865–5874.

Hesselmann, R.P.X., Rummell, R. Von, Resnick, S.M., Hany, R., Zehnder, A.J.B., 2000. Anaerobic Metabolism of Bacteria Performing Biological Phosphate Removal. Water Res. 34, 3487–3494.

Ip, Y.K., Chew, S.F., Randall, D.J., 2001. Ammonia toxicity, tolerance, and excretion. Fish Physiol. 20, 109–148.

IPCC, Stocker, T.F., Qin, D., Plattner, G.-K., Tignor, M.M.B., Allen, S.K., Boschung, J., Nauels, A., Xia, Y., Bex, V., Midgley, P.M., 2013. Climate Change 2013 - The Physical Science Basis, Intergovernmental Panel on Climate Change.

Jenni, S., Mohn, J., Emmenegger, L., Udert, K.M., 2012. Temperature dependence and interferences of NO and N_2O microelectrodes used in wastewater treatment. Environ. Sci. Technol. 46, 2257–66.

Joss, A., Salzgeber, D., Eugster, J., König, R., Rottermann, K., Burger, S., Fabijan, P., Leumann, S., Mohn, J., Siegrist, H., 2009. Full-scale nitrogen removal from digester liquid with partial nitritation and anammox in one SBR. Environ. Sci. Technol. 43, 5301–6.

Kampschreur, M.J., Temmink, H., Kleerebezem, R., Jetten, M.S.M., van Loosdrecht, M.C.M., 2009. Nitrous oxide emission during wastewater treatment. Water Res. 43, 4093–103.

Kim, S.-W., Miyahara, M., Fushinobu, S., Wakagi, T., Shoun, H., 2010. Nitrous oxide emission from nitrifying activated sludge dependent on denitrification by ammonia-oxidizing bacteria. Bioresour. Technol. 101, 3958–63.

Kishida, N., Kim, J.H., Kimochi, Y., Nishimura, O., Sasaki, H., Sudo, R., 2004. Effect of C/N ratio on nitrous oxide emission from swine wastewater treatment process. Water Sci Technol 49, 359–365.

Kong, Y., Nielsen, J.L., Nielsen, P.H., Icrobiol, A.P.P.L.E.N.M., 2004. Microautoradiographic Study of Rhodocyclus -Related Polyphosphate- Accumulating Bacteria in Full-Scale Enhanced Biological Phosphorus Removal Plants. Appl. Environ. Microbiol. 70, 5383–5390.

Kong, Y., Nielsen, J.L.J.J.L., Nielsen, P.H.P.P.H., 2005. Identity and Ecophysiology of Uncultured Actinobacterial Polyphosphate-Accumulating Organisms in Full-Scale Enhanced Biological Phosphorus Removal Plants. Appl. Environ. Microbiol. 71, 4076–4085.

Kong, Y., Ong, S.L., Ng, W.J., Liu, W.T., 2002. Diversity and distribution of a deeply branched novel proteobacterial group found in anaerobic-aerobic activated sludge processes. Environ. Microbiol. 4, 753–757.

Kong, Y., Xia, Y., Nielsen, J.L., Nielsen, P.H., 2006. Ecophysiology of a group of uncultured Gammaproteobacterial glycogen-accumulating organisms in full-scale enhanced biological phosphorus removal wastewater treatment plants. Environ. Microbiol. 8, 479–489.

Kong, Y., Xia, Y., Nielsen, J.L., Nielsen, P.H., 2007. Structure and function of the microbial community in a full-scale enhanced biological phosphorus removal plant. Microbiology 153, 4061–4073.

Kong, Y., Xia, Y., Nielsen, P.H., 2008. Activity and identity of fermenting microorganisms in full-scale biological nutrient removing wastewater treatment plants. Environ. Microbiol. 10, 2008–19.

Kristiansen, R., Nguyen, H.T.T., Saunders, A.M., Nielsen, J.L., Wimmer, R., Le, V.Q., Mcilroy, S.J., Petrovski, S., Seviour, R.J., Calteau, A., Nielsen, K.L., Nielsen, P.H.H., Thi, H., Nguyen, T., Saunders, A.M., Lund Nielsen, J., Wimmer, R., Le, V.Q., Mcilroy, S.J., Petrovski, S., Seviour, R.J., Calteau, A., Lehmann Nielsen, K., Nielsen,

P.H.H., 2013. A metabolic model for members of the genus Tetrasphaera involved in enhanced biological phosphorus removal. Iternational Soc. Microb. Ecol. 7, 543–554.

Kuba, T., Murnleitner, E., Loosdrecht, M.C.M. Van, Heijnen, J.J., 1996. A Metabolic Model for Biological Phosphorus Removal by Denitrifying Organisms. Biotechnol. Bioeng. 52, 685–695.

Lanham, A.A.B., Oehmen, A.A., Saunders, A.M.A., Carvalho, G., Nielsen, P.H., Reis, M. a M., 2013. Metabolic versatility in full-scale wastewater treatment plants performing enhanced biological phosphorus removal. Water Res. 47, 7032–41.

Law, Y., Lant, P., Yuan, Z., 2013. The confounding effect of nitrite on N2O production by an enriched ammonia-oxidizing culture. Environ. Sci. Technol. 47, 7186–7194.

Law, Y., Ye, L., Pan, Y., Yuan, Z., 2012. Nitrous oxide emissions from wastewater treatment processes. Philos. Trans. R. Soc. B Biol. Sci. 367, 1265–1277.

Lemaire, R., Meyer, R., Taske, A., Crocetti, G.R., Keller, J., Yuan, Z., 2006. Identifying causes for N2O accumulation in a lab-scale sequencing batch reactor performing simultaneous nitrification, denitrification and phosphorus removal. J. Biotechnol. 122, 62–72.

Liu, W.-T., Nielsen, A.T., Wu, J.H., Tsai, C.S., Matsuo, Y., Molin, S., 2001. In situ identification of polyphosphate- and polyhydroxyalkanoate-accumulating traits for microbial populations in a biological phosphorus removal process. Environ. Microbiol. 3, 110–122.

Louie, T.M., Mah, T.J., Oldham, W., Ramey, W.D., 2000. Use of metabolic inhibitors and gas chromatography/mass spectrometry to study poly-β-hydroxyalkanoates metabolism involving cryptic nutrients in enhanced biological phosphorus removal systems. Water Res. 34, 1507–1514.

Maszenan, a M., Seviour, R.J., Patel, B.K., Schumann, P., Burghardt, J., Tokiwa, Y., Stratton, H.M., 2000. Three isolates of novel polyphosphate-accumulating gram-positive cocci, obtained from activated sludge, belong to a new genus, Tetrasphaera gen. nov., and description of two new species, Tetrasphaera japonica sp. nov. and Tetrasphaera australiensis sp. no. Int. J. Syst. Evol. Microbiol. 50 Pt 2, 593–603.

McIlroy, S., Seviour, R.J., 2009. Elucidating further phylogenetic diversity among the Defluviicoccus-related glycogen-accumulating organisms in activated sludge. Environ. Microbiol. Rep. 1, 563–568.

McIlroy, S.J., Nittami, T., Seviour, E.M., Seviour, R.J., 2010. Filamentous members of cluster III Defluviicoccus have the in situ phenotype expected of a glycogen-accumulating organism in activated sludge. FEMS Microbiol. Ecol. 74, 248–256.

McKenzie, C.M., Seviour, E.M., Schumann, P., Maszenan, a M., Liu, J.-R., Webb, R.I., Monis, P., Saint, C.P., Steiner, U., Seviour, R.J., 2006. Isolates of “Candidatus Nostocoida limicola” Blackall et al. 2000 should be described as three novel species of the genus Tetrasphaera, as Tetrasphaera jenkinsii sp. nov., Tetrasphaera vanveenii sp. nov. and Tetrasphaera veronensis sp. nov. Int. J. Syst. Evol. Microbiol. 56, 2279–90.

Mcmahon, K.D., Dojka, M. a, Pace, N.R., Jenkins, D., Keasling, J.D., 2002. Polyphosphate Kinase from Activated Sludge Performing Enhanced Biological

Phosphorus Removal Polyphosphate Kinase from Activated Sludge Performing Enhanced Biological Phosphorus Removal †. Appl. Environ. Microbiol. 68, 4971–4978.

Meyer, R.L., Saunders, A.M., Blackall, L.L., 2006. Putative glycogen-accumulating organisms belonging to the Alphaproteobacteria identified through rRNA-based stable isotope probing. Microbiology 152, 419–429.

Mielczarek, A.T., Nguyen, H.T.T., Nielsen, J.L., Nielsen, P.H., 2013. Population dynamics of bacteria involved in enhanced biological phosphorus removal in Danish wastewater treatment plants. Water Res. 47, 1529–1544.

Mino, T., Arun, V., Tsuzuki, Y., Matsuo, T., 1987. Effect of phosphorus accumulation on acetate metabolism in the biological phosphorus removal process. Adv. Water Pollut. Control 27–38.

Mullan, a, Quinn, J.P., McGrath, J.W., 2002. Phosphate Removal from Wastewaters: A Novel Approach. Eng. Life Sci. 2, 63–66.

Nguyen, H.T.T., Kristiansen, R., Vestergaard, M., Wimmer, R., Nielsen, P.H., 2015. Intracellular Accumulation of Glycine in Polyphosphate-Accumulating Organisms in Activated Sludge, a Novel Storage Mechanism under Dynamic Anaerobic-Aerobic Conditions. Appl. Environ. Microbiol. 81, 4809–18.

Nguyen, H.T.T., Le, V.Q., Hansen, A.A., Nielsen, J.L., Nielsen, P.H.H., 2011. High diversity and abundance of putative polyphosphate-accumulating Tetrasphaera-related bacteria in activated sludge systems. FEMS Microbiol. Ecol. 76, 256–67.

Ni, B., Peng, L., Law, Y., Guo, J., Yuan, Z., 2014. Modeling of Nitrous Oxide Production by Autotrophic Ammonia- Oxidizing Bacteria with Multiple Production Pathways.

Ni, B.J., Yuan, Z., 2015. Recent advances in mathematical modeling of nitrous oxides emissions from wastewater treatment processes. Water Res. 87, 336–346.

Nielsen, P.H.H., Mielczarek, A.T., Kragelund, C., Nielsen, J.L., Saunders, A.M., Kong, Y., Hansen, A.A., Vollertsen, J., 2010. A conceptual ecosystem model of microbial communities in enhanced biological phosphorus removal plants. Water Res. 44, 5070–5088.

Nittami, T., McIlroy, S., Seviour, E.M., Schroeder, S., Seviour, R.J., 2009. Candidatus Monilibacter spp., common bulking filaments in activated sludge, are members of Cluster III Defluviicoccus. Syst. Appl. Microbiol. 32, 480–489.

Norton, J.M., Klotz, M.G., Stein, L.Y., Arp, D.J., Bottomley, P.J., Chain, P.S.G., Hauser, L.J., Land, M.L., Larimer, F.W., Shin, M.W., Starkenburg, S.R., 2008. Complete genome sequence of Nitrosospira multiformis, an ammonia-oxidizing bacterium from the soil environment. Appl. Environ. Microbiol. 74, 3559–3572.

Oehmen, A., Carvalho, G., Freitas, F., Reis, M.A.M., 2010. Assessing the abundance and activity of denitrifying polyphosphate accumulating organisms through molecular and chemical techniques. Water Sci. Technol. 61, 2061–2068.

Oehmen, A., Lemos, P.C., Carvalho, G., Yuan, Z., Keller, J.J., Blackall, L.L., Reis, M. a M., 2007. Advances in enhanced biological phosphorus removal: From micro to macro scale. Water Res. 41, 2271–2300.

Onda, S., Takii, S., 2002. Isolation and characterization of a Gram-positive polyphosphate-accumulating bacterium. J. Gen. Appl. Microbiol. 48, 125–33.

Otte, S., Grobben, N.G., Robertson, L. a, Jetten, M.S., Kuenen, J.G., 1996. Nitrous oxide production by Alcaligenes faecalis under transient and dynamic aerobic and anaerobic conditions. Appl Env. Microbiol 62, 2421–2426.

Pan, Y., Ni, B.J., Bond, P.L., Ye, L., Yuan, Z., 2013. Electron competition among nitrogen oxides reduction during methanol-utilizing denitrification in wastewater treatment. Water Res. 47, 3273–3281.

Pereira, H., Lemos, P.C.P.C.P.C., Reis, M.A.M.A.M., Crespo, J.P.S.G., Carrondo, M.J.T., Santos, H., Cresp, J.P.S.G., Carrondo, M.J.T., Santos, H., 1996. Model for carbon metabolism in biological phosphorus removal processes based on in vivo13C-NMR labelling experiments. Water Res. 30, 2128–2138.

Peterson, S.B., Warnecke, F., Madejska, J., McMahon, K.D., Hugenholtz, P., 2008. Environmental distribution and population biology of Candidatus Accumulibacter, a primary agent of biological phosphorus removal. Environ. Microbiol. 10, 2692–2703.

Portmann, R.W., Daniel, J.S., Ravishankara, a. R., 2012. Stratospheric ozone depletion due to nitrous oxide: influences of other gases. Philos. Trans. R. Soc. B Biol. Sci. 367, 1256–1264.

Ravishankara, A.R., Daniel, J.S., Portmann, R.W., 2009. Nitrous oxide (N2O): the dominant ozone-depleting substance emitted in the 21st century. Science (80-.). 326, 123–5.

Ribera-Guardia, A., Kassotaki, E., Gutierrez, O., Pijuan, M., 2014. Effect of carbon source and competition for electrons on nitrous oxide reduction in a mixed denitrifying microbial community. Process Biochem. 49, 2228–2234.

Rodriguez-Caballero, a., Aymerich, I., Marques, R., Poch, M., Pijuan, M., 2015. Minimizing N2O emissions and carbon footprint on a full-scale activated sludge sequencing batch reactor. Water Res. 71, 1–10.

Rodriguez-caballero, A., Aymerich, I., Poch, M., Pijuan, M., 2014. Evaluation of process conditions triggering emissions of green-house gases from a biological wastewater treatment system. Sci. Total Environ. 493, 384–391.

Rodriguez-Caballero, A., Pijuan, M., 2013. N2O and NO emissions from a partial nitrification sequencing batch reactor: exploring dynamics, sources and minimization mechanisms. Water Res. 47, 3131–40.

Saunders, A.M., Oehmen, A., Blackall, L.L., Yuan, Z., Keller, J., 2003. The effect of GAOs (glycogen accumulating organisms) on anaerobic carbon requirements in full-scale Australian EBPR (enhanced biological phosphorus removal) plants. Water Sci. Technol. 47, 37–43.

Schulthess, R. V, Kuhni, M., Gujer, W., 1995. Release of nitric and nitours oxides from denitrifying activated sludge. Wat. Res. 29, 215–226.

Schulthess, R., Gujer, W., 1996. Release of nitrous oxide (N 2 O) from denitrifying activated sludge: Verification and application of a mathematical model. Water Res. 30, 521–530.

Seviour, R.J., Mino, T., Onuki, M., 2003. The microbiology of biological phosphorus removal in activated sludge systems. FEMS Microbiol. Rev. 27, 99–127.

Stein, L.Y., Arp, D.J., Berube, P.M., Chain, P.S.G., Hauser, L., Jetten, M.S.M., Klotz, M.G., Larimer, F.W., Norton, J.M., Op Den Camp, H.J.M., Shin, M., Wei, X., 2007. Whole-genome analysis of the ammonia-oxidizing bacterium, Nitrosomonas eutropha C91: Implications for niche adaptation. Environ. Microbiol. 9, 2993–3007.

Tallec, G., Garnier, J., Billen, G., Gousailles, M., 2006. Nitrous oxide emissions from secondary activated sludge in nitrifying conditions of urban wastewater treatment plants: effect of oxygenation level. Water Res. 40, 2972–80.

Tallec, G., Garnier, J., Billen, G., Gousailles, M., 2008. Nitrous oxide emissions from denitrifying activated sludge of urban wastewater treatment plants, under anoxia and low oxygenation. Bioresour. Technol. 99, 2200–9.

Tata, P., Witherspoon, J., Lue-Hing, C., 2003. VOC Emissions from Wastewater Treatment Plants: Characterization, Control and Compliance. Lewis Publishers.

Tchobanoglous, G., Burton, F.L., Stensel, H.D., 2003. Wastewater engineering: Treatment and Reuse, 4th ed, McGraw-Hill Education. New York.

Tsuneda, S., Ohno, T., Soejima, K., Hirata, A., 2006. Simultaneous nitrogen and phosphorus removal using denitrifying phosphate-accumulating organisms in a sequencing batch reactor. Biochem. Eng. J. 27, 191–196.

Wang, X., Zeng, R.J., Dai, Y., Peng, Y., Yuan, Z., 2008. The denitrification capability of cluster 1 Defluviicoccus vanus-related glycogen-accumulating organisms. Biotechnol. Bioeng. 99, 1329–1336.

Water Environment Federation, 2007. Operation of Municipal Wastewater Treatment Plants, Sixth Edit. ed, WEF Press. WEF Press : New York, Chicago, San Francisco, Lisbon, London, Madrid, Mexico City, Milan, New Delhi, San Juan, Seoul, Singapore, Sydney, Toronto.

Wentzel, M.C., Lotter, L.H., Loewenthal, R.E., Marais, G., 1986. Metabolic behaviour of Acinetobacter spp. in enhanced biological phosphorus removal - a biochemical model. Water SA 12, 209–224.

Wiesmann, U., Choi, I.S., Dombrowski, E.-M., 2006. Fundamentals of Biological Wastewater Treatment, 1 edition. ed, Wiley-VCH Verlag GmbH & Co. KGaA. Weinheim, Germany.

Wong, M.T., Liu, W.T., 2007. Ecophysiology of Defluviicoccus-related tetrad-forming organisms in an anaerobic-aerobic activated sludge process. Environ. Microbiol. 9, 1485–1496.

Wong, M.-T., Mino, T., Seviour, R.J., Onuki, M., Liu, W.-T., 2005. In situ identification and characterization of the microbial community structure of full-scale enhanced biological phosphorous removal plants in Japan. Water Res. 39, 2901–14.

Wong, M.T., Tan, F.M., Ng, W.J., Liu, W.T., 2004. Identification and occurrence of tetrad-forming Alphaproteobacteria in anaerobic-aerobic activated sludge processes. Microbiology 150, 3741–3748.

Wunderlin, P., Mohn, J., Joss, A., Emmenegger, L., Siegrist, H., 2012. Mechanisms of N2O production in biological wastewater treatment under nitrifying and denitrifying conditions. Water Res. 46, 1027–37.

Xia, Y., Kong, Y., Thomsen, T.R., Halkjaer Nielsen, P., 2008. Identification and Ecophysiological Characterization of Epiphytic Protein-Hydrolyzing Saprospiraceae (“Candidatus Epiflobacter” spp.) in Activated Sludge. Appl. Environ. Microbiol. 74, 2229–2238.

Ye, L., Ni, B.J., Law, Y., Byers, C., Yuan, Z., 2014. A novel methodology to quantify nitrous oxide emissions from full-scale wastewater treatment systems with surface aerators. Water Res. 48, 257–268.

Yeoman, S., Stephenson, T., Lester, J.N., Perry, R., 1988. The removal of phosphorus during wastewater treatment: A review. Environ. Pollut. 49, 183–233.

Yu, R., Kampschreur, M.J., Van Loosdrecht, M.C.M., Chandran, K., 2010. Mechanisms and specific directionality of autotrophic nitrous oxide and nitric oxide generation during transient anoxia. Environ. Sci. Technol. 44, 1313–1319.

Zeng, R.J., Lemaire, R., Yuan, Z., Keller, J.J., 2003a. Simultaneous nitrification, denitrification, and phosphorus removal in a lab-scale sequencing batch reactor. Biotechnol. Bioeng. 84, 170–178.

Zeng, R.J., Yuan, Z., Keller, J.J., 2003b. Enrichment of denitrifying glycogen-accumulating organisms in anaerobic/anoxic activated sludge system. Biotechnol. Bioeng. 81, 397–404.

Zheng, H., Hanaki, K., Matsuo, T., 1994. Production of nitrous oxide gas during nitrification of wastewater. Water Sci. Technol. 30, 133–141.

Zhou, Y., Lim, M., Harjono, S., Ng, W.J., 2012. Nitrous oxide emission by denitrifying phosphorus removal culture using polyhydroxyalkanoates as carbon source. J. Environ. Sci. 24, 1616–1623.

Zhou, Y., Pijuan, M., Zeng, R.J., Yuan, Z., 2008. Free nitrous acid inhibition on nitrous oxide reduction by a denitrifying-enhanced biological phosphorus removal sludge. Environ. Sci. Technol. 42, 8260–8265.

Zhou, Y., Pijuan, M., Zeng, R.J., Yuan, Z., 2009. Involvement of the TCA cycle in the anaerobic metabolism of polyphosphate accumulating organisms (PAOs). Water Res. 43, 1330–40.

Zilles, J.L., Peccia, J., Kim, M., Hung, C., Noguera, D.R., 2002. Involvement of Rhodocyclus -Related Organisms in Phosphorus Removal in Full-Scale Wastewater Treatment Plants Involvement of Rhodocyclus -Related Organisms in Phosphorus Removal in Full-Scale Wastewater Treatment Plants. Appl. Environ. Microbiol. 68, 2763–2769.

Zumft, W.G., 1997. Cell biology and molecular basis of denitrification. Microbiol. Mol. Biol. Rev. 61, 533–616.

3

A NOVEL MICROELECTRODE-BASED ONLINE SYSTEM FOR MONITORING N_2O GAS EMISSIONS DURING WASTEWATER TREATMENT

SUMMARY: Clark-type N_2O microelectrodes are commonly used for measuring dissolved N_2O levels, but have not previously been tested for gas-phase applications, where the N_2O emitted from wastewater systems can be directly quantified. In this study, N_2O microelectrodes were tested and validated for online gas measurements, and assessed with respect to their temperature, gas flow, composition dependence, gas pressure and humidity. An exponential correlation between temperature and sensor signal was found, whereas gas flow, composition, pressure and humidity did not have any influence on the signal. Two of the sensors were tested at different N_2O concentration ranges (0-422.3, 0-50, 0-10 and 0-2 ppmv N_2O) and exhibited a linear response over each range. The N_2O emission dynamics from two laboratory scale sequencing batch reactors performing ammonia or nitrite oxidation were also monitored using one of the microsensors and results were compared with two other analytical methods. Results show that N_2O emissions were accurately described with these microelectrodes and support their application for assessing gaseous N_2O emissions from wastewater treatment systems. Advantages of the sensors as compared to conventional measurement techniques include a wider quantification range of N_2O fluxes, and only one measurement system can assess both liquid and gas-phase N_2O dynamics.

PUBLISHED AS: Marques, R., Oehmen, A., Pijuan, M., 2014. Novel Microelectrode-Based Online System for Monitoring N_2O Gas Emissions during Wastewater Treatment. Environ. Sci. Technol. 48, 12816–12823.

3.1 INTRODUCTION

There is a growing concern regarding the production of nitrous oxide (N_2O) from nitrogen removing WWTP (Foley et al., 2010; Kampschreur et al., 2009). N_2O can be produced during nitrification and denitrification, and is an important greenhouse gas contributor, that is about 300 times stronger than CO_2, and also causes ozone-depletion in the stratosphere (Foley et al., 2010; Kampschreur et al., 2009; Wunderlin et al., 2012). N_2O emissions have been shown to have a significant impact on the greenhouse gas budget from WWTP (Aboobakar et al., 2013; Desloover et al., 2012; Wunderlin et al., 2012). Current efforts are focused on identifying where the majority of these emissions occur, as well as their dynamics, in order to develop effective mitigation strategies. Developing new methodologies for the online measurement of this gas contributes towards quantifying its real production.

N_2O can be analysed off-line via gas chromatography with an electron capture detector (GC-ECD) (Jenni et al., 2012; Yu et al., 2010). However, the use of grab samples for off-line analysis can lead to an over or under estimation of N_2O emissions due to their high variability over time. Currently, the majority of the studies use commercial online N_2O gas analysers based on Fourier transform infrared spectroscopy and gas filter correlation (Jenni et al., 2012; Joss et al., 2009). However, these analysers require preconditioning of the gas sample (removing humidity and particles) and a minimum gas flow (0.5-1 L/min depending on the analyser). This last step dilutes the concentration of N_2O, increasing uncertainty in the low N_2O concentration range. To overcome this limitation, a Clark-type N_2O microelectrode (UNISENSE A/S) was adapted to measure N_2O in the gas phase. These electrodes have been extensively used to measure online dissolved N_2O of many different WWTP and other aquatic environments (Andersen et al., 2001; Fux et al., 2006; Marlies J. Kampschreur et al., 2008; Meyer et al., 2008; Revsbech et al., 1988; Schreiber et al., 2008), but the testing of these sensors for the application of measuring N_2O gaseous emissions has not been previously reported.

The N_2O sensor is connected to a high-sensitivity picoamperemeter and the cathode is polarized against the internal reference (Unisense, 2014). Driven by the external partial pressure, N_2O penetrates through the sensor membrane at the tip (silicone membrane) and is reduced at the metal cathode surface (Jenni et al., 2012; Unisense, 2014). The picoamperemeter converts the resulting current to a signal (Jenni et al., 2012; Unisense, 2014). One of the characteristics of this type of sensor is

its signal dependency on temperature changes. Recently, an exponential temperature dependency was described for the N_2O liquid microsensors, based on an adapted Arrhenius equation (Jenni et al., 2012). Using two calibration curves at two different temperatures in the liquid phase, equation 3.1 was able to predict the concentration at different temperatures (Jenni et al., 2012):

$$C_{N_2O}(T,S) = \frac{S - a_1 e^{b_1 T}}{a_2 e^{b_2 T}} \quad (3.1)$$

where a_1 and b_1 are fitting parameters, T is the temperature in the liquid and S is the signal of the sensor. Chemical and physical processes such as solubility, diffusion in water and in the silicone membrane and reduction or oxidation at the electrode are responsible for the temperature dependence of these sensors (Gundersen et al., 1998; Jenni et al., 2012). However, measuring N_2O in the gas phase changes the response of the sensor with respect to temperature variations and therefore this relationship requires investigation for the N_2O gas phase microsensors.

In this study, the performance of N_2O gas microsensors was tested and compared with online commercial N_2O analysers and off-line analysers. The effect of temperature, gas flow, gas type, humidity in the gas mixture and pressure increases were tested to validate the reliability of the sensor under a range of conditions relevant to environmental applications. Different N_2O concentration ranges were also evaluated to assess the linearity of the sensors and to determine their detection limit. Finally, one of these sensors was used to monitor gaseous N_2O emissions from two nitrifying laboratory scale reactors and the results were compared with a conventional infrared online gas analyser and with off-line analysis via GC-ECD. The goal was to test and validate a new sensor for online N_2O gas measurements and assess its feasibility for application in wastewater treatment systems. Such a device would facilitate on-line monitoring of N_2O, since both the liquid- and gas-phase dynamics could be simultaneously monitored using only one experimental setup, and could be useful for the modelling and optimisation of WWTPs.

3.2 MATERIALS AND METHODS

Six Clark-Type N_2O gas microsensors were used for this study (Unisense A/S, Denmark) (Appendix A1, Figure A1), with all sensors containing an internal reference and a guard cathode. Prior to experimentation, all N_2O microsensors were connected to a highly sensitive picoamperemeter (Unisense Multimeter version 2.01, Unisense A/S, Denmark) and polarised overnight following manufacturer instructions. A commercial N_2O online gas analyser (VA-3000, Horiba, Japan) and a gas chromatograph coupled to an electron capture detector (Thermo Fisher Scientific, Trace GC Ultra, USA) with a column (TracePLOT TG-BOND Q, 30 m x 0.32 mm x 10 um), were used to validate the N_2O concentration in the tests described below. The N_2O concentration ranges for the calibration curves were chosen according to the literature. A high range covering N_2O concentrations up to 422.3 ppmv of N_2O was chosen based on reports by Kampschreur et al. (2008) in nitritation processes, with N_2O concentrations in the off gas reaching 400 ppmv. Furthermore, Ahn et al., (2010) reported in different stages of BNR processes N_2O concentrations in the off gas reaching levels up to 350 ppmv. A medium concentration range (up to 50 ppmv of N_2O) was reported by Ahn et al., (2010) in plug flow and four-stage Bardenpho processes. A low concentration range (up to 10 ppmv of N_2O) was reported by Ahn et al., (2010) in oxidation ditch, Modified Ludzack Ettinger (MLE) and separation stage BNR processes. Moreover, to test the limits of the sensors a very low range (0-2 ppmv) was also tested. To reach the selected N_2O concentration ranges, three different commercial N_2O gas mixtures were used in this experiment with the following N_2O concentrations, 422.3, 104.3 and 83.7 ppmv (Linde, Germany). Mass flow controllers (Applikon Biotechnolgy, Netherlands) were also used to achieve other desired N_2O concentrations using nitrogen or air as dilution gases. A 330 mL calibration chamber (CAL300, Unisense, Denmark) and a 1 L reactor (Applikon Biotechnolgy, Netherlands) were used as the vessels to perform the sensor tests. The calibration chamber or the reactor was immersed in a water bath to control the temperature at the desired set-point. Temperature was measured with a temperature probe connected to an ez-control box (Applikon Biotechnolgy, Netherlands). The vessel was connected via gas tubing to a commercial N_2O analyser (Appendix A1, Figure A2 and A3). Gas tight valves were used to seal the chamber after the volume of gas was fluxed to reach the desired N_2O concentration.

3.2.1 Experimental Procedure

Several sets of tests were conducted to assess the influence of different parameters on the sensor signal, to assess its linear response to different N_2O concentrations and to validate its ability to accurately measure the N_2O emission dynamics of two lab-scale wastewater treatment reactors.

Linearity of the sensor response: Four different N_2O concentration ranges were tested in two of the sensors (High range: 0-422.3 ppmv N_2O; Medium range: 0-50 ppmv N_2O; Low range: 0-10 ppmv N_2O, Very low range 0-2 ppmv) using air and nitrogen as dilution gases. The temperature of the gas mixture was controlled at 25 °C. The signal was recorded during 10 min after the temperature stabilised. The concentration of the gas flow was validated by a commercial gas online analyser and by GC-ECD.

Repetitive and random peak tests: The N_2O concentration was changed between 0 and 10.4 ppmv during 5 consecutive tests, to check the variability of the sensors after being subjected to N_2O concentration peaks. Nitrogen was used as dilution gas, temperature was controlled at 25 °C and the signal was recorded during 10 min after the temperature stabilised. The sensors were also subjected to tests with random N_2O concentration peaks under similar operating conditions.

Effect of type of gas and flow tests: These tests were carried out with air and nitrogen, respectively, where the gas flow was controlled by mass flow controllers at a range of 0.2 to 4 L/min. The temperature was maintained at 25 °C. After the signal was stable, it was measured during 10 min.

Response time: The time required to reach 90% of the sensor signal at a desired concentration (30 ppmv N_2O) was tested using two of the sensors. The temperature in these tests was maintained at 25ºC. For each sensor three repeated tests were conducted.

Sensor drift over time: The drift in the signal of four sensors was measured during 5h in a N_2O-free environment at a controlled temperature of 25 °C.

Temperature dependency tests: The signal of the microelectrodes consists of a zero current (i.e. the current in an N_2O free environment), which increases as a function of the N_2O concentration (Jenni et al., 2012). Calibration curves were performed using four sensors within the range of 12.3 - 32.6 °C. The signal was recorded during 10 min after the temperature stabilised. To describe the influence of

temperature on the sensor signal, an exponential function (equation 3.2) was found to describe the relationship between temperature and the N_2O microsensor signal at the zero current (i.e. the current in a N_2O free environment) (Jenni et al., 2012):

$$Z(T) = a_1 e^{b_1 T} \tag{3.2}$$

where a_1 and b_1 are the fitting parameters. To predict and describe the signal of a sensor at different concentrations and temperatures, equation 3.3 was applied (Jenni et al., 2012):

$$S_{N_2O}(T,C) = a_1.e^{b_1 T} + a_2.C.e^{b_2 T} \tag{3.3}$$

where T is the temperature in the liquid and C the concentration measured by the sensor, a_i and b_i are the fitting parameters.

Effect of humidity on sensor signal: A nitrogen stream with 50 ppmv of N_2O was passed via a water vessel. The gas coming out from the water vessel either directly entered a reactor (in tests with humidity) or was passed through a gas condenser before entering the reactor (in tests without humidity), where four N_2O gas microsensors were placed. The reactor temperature was controlled at 25 ºC, and after 5 min, the sensor signal was recorded for 2 min.

Effect of small pressure changes on sensor signal: A nitrogen stream with 50 ppmv of N_2O was fluxed in the 1000 mL vessel with four sensors. After 5 min, the gas inflow and outflow valves were closed and 3 injections of the same gas mixture were added to the system (25, 25 and 5 mL, respectively) with an interval of 60s between them. The signal was recorded to monitor the influence of small variations of pressure on the sensors' signal. Temperature was controlled at 25 °C.

SBR monitoring tests: N_2O emission dynamics were monitored online in two laboratory scale SBRs using one sensor and a commercial N_2O gas analyser. One SBR was enriched with AOB and the other was enriched with NOB. More details about the operation of these reactors can be found in Rodriguez-Caballero and Pijuan, (2013). Grab samples were also taken during the cycles for N_2O analysis via GC-ECD. At the time of the monitoring, the two SBRs were operated at a controlled temperature of 25 ºC.

3.3 RESULTS AND DISCUSSION

3.3.1 Linearity of the Sensor

Two sensors (Sensor 1 and Sensor 2) were tested at a range of N_2O concentrations from 0-50 ppmv, with either air or nitrogen as dilution gas. Both sensors showed a linear response to this concentration range (i.e. y=ax). Using air or nitrogen as dilution gas did not affect the linear response of the sensor, with an $r^2 \geq 0.999$ in each case (Appendix A2, Figure A4).

The two sensors were also tested up to a range of 422.3 ppmv of N_2O, where the N_2O concentration was compared with that given by a commercial online gas analyser, where the upper range of the online gas analyser used was 500 ppmv. Off-line samples were also analysed using GC-ECD to validate the results obtained. The linear regression between the results of the sensors and the online analyser and between the sensors and the GC-ECD measurements had very high coefficients of determination, 0.999 and 0.982, respectively (Figure 3.1). No saturation of the signal was observed up to the maximum concentration tested, which validates the use of these sensors for high N_2O concentration ranges. These results indicate a high corroboration between these three methods for measuring N_2O over a wide concentration range.

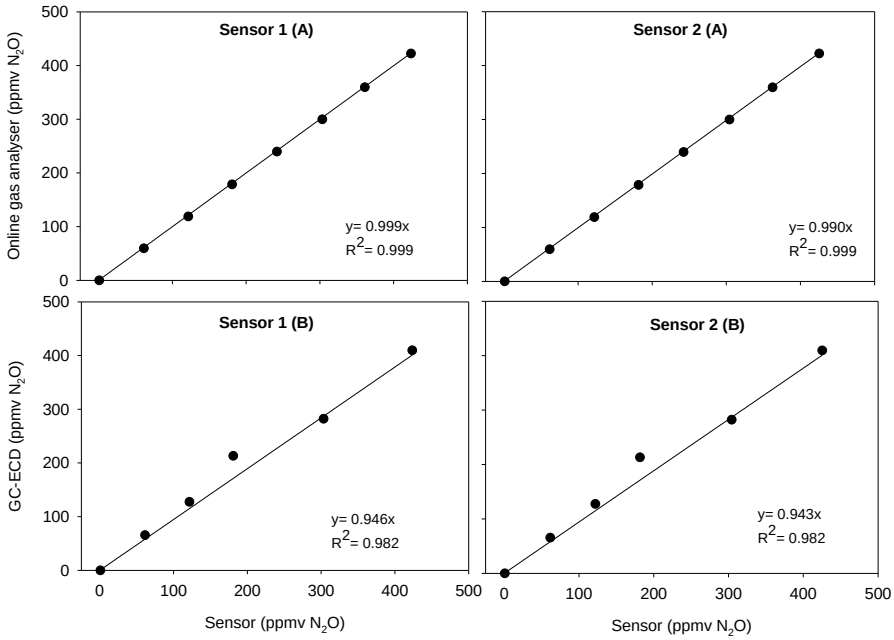

Figure 3.1 – High-range concentration measured by the commercial gas analyser vs sensors (1 and 2, A) and GC-ECD vs Sensors (1 and 2, B) at controlled temperature (25 °C) and with nitrogen as dilution gas.

A low N_2O concentration range was also tested with one sensor (Sensor 1) and validated with the online gas analyser and with GC-ECD. Very high linear regression coefficients were again obtained when comparing the commercial analyser results with the sensor, and also for the case of GC-ECD versus the sensor, 0.999 and 0.995 (Figure 3.2, A and B), respectively. This result validates the use of the sensor for low N_2O concentration ranges.

Furthermore, Sensor 1 was also tested at a very low range of 0 to 2 ppmv of N_2O. The sensor was shown to have a linear relationship, with the coefficient of determination being 0.984 (Appendix A2, Table A1). The lowest concentration tested was 0.2 ppmv of N_2O, which was discernible by the sensor and was within the linear range. This validates the use of the sensor at very low concentrations and could be an advantage to characterise systems with low N_2O production. Overall, the sensors were shown to respond linearly over a very wide concentration range of N_2O, increasing the versatility of this method to analyse gas streams or gas mixtures with different concentrations of N_2O.

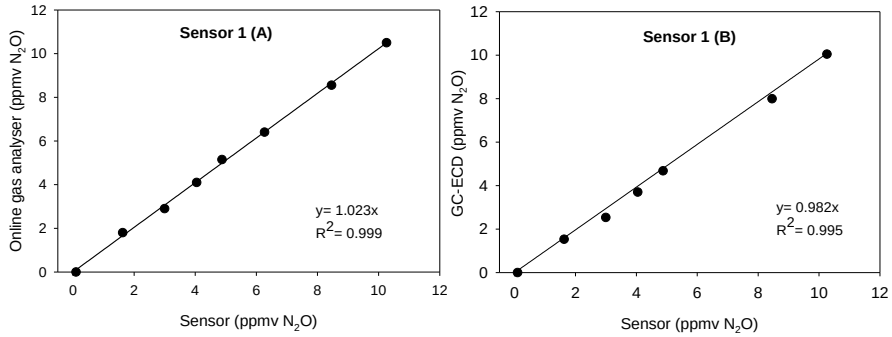

Figure 3.2 – Low-range concentration measured by the online gas analyser (A) and GC-ECD (B) vs Sensor 1 with N_2 as dilution gas at a controlled temperature (25 °C).

3.3.2 Repetitive and random peak tests

Two sensors (Sensor 1 and Sensor 2) were subjected to a repetitive N_2O concentration peak test in order to investigate the repeatability of the sensors under fluctuating N_2O levels. The average signal at 0.0 ppmv N_2O was 9.57±0.10 and 12.79±0.11 mV for Sensor 1 and Sensor 2, respectively, and 32.89±0.04 and 35.48±0.04 mV, respectively at a concentration of 10.4 ppmv of N_2O with N_2 as the dilution gas. This low variability shows that peaks of N_2O can be repeatably detected with accuracy and signal saturation does not occur.

A similar test with random concentrations in the range 0 to 50 ppmv of N_2O was also performed. The results were used to perform a calibration curve of the signal with the concentration, where Sensor 1 and Sensor 2 each had coefficients of determination of 0.999 (Appendix A3, Figure A5). This result shows the accuracy of the sensor in response to changes in the concentration of the N_2O peak.

3.3.3 Effect of the type of gas and flowrate on sensor signal

The effect of using air or nitrogen as dilution gases on the microsensor signal was evaluated since these gases are commonly used in nitrification and denitrification studies. Two of the sensors (Sensor 1 and Sensor 2) were used for this test and results demonstrated that the sensor signal was not affected by the use of air or nitrogen (Appendix A4, Table A2, A). The average signal was 11.21±0.23 and 33.50±0.25 mV for Sensor 1 and Sensor 2 respectively, when exposed to nitrogen gas. A similar profile was obtained with the same conditions using air with an average signal of 12.08±0.08 and 34.56±0.38 mV for Sensor 1 and Sensor 2, respectively. The small difference observed within the same sensor when exposed to air or nitrogen is due to the fact that a small concentration of N_2O (0.3 ppmv) was detected in the compressed air used for this test. Thus, using air or nitrogen as dilution gas did not affect the response of the sensor. This could be an advantage when performing studies involving sequential cycles with different gases for e.g. aerobic/anoxic/anaerobic phases, without influencing the target signal. Also, changes in the gas flow in the range of 0.2-4 L/min did not affect the zero current of the sensors (Appendix A4, Table A2, B)

3.3.4 Response time

The response time of the N_2O sensor was determined as the time needed to reach 90 % of the new equilibrium signal starting from an N_2O-free gas mixture. The sensor used for this test (Sensor 1) had an average response time of 15.4±1.8s to reach a signal equivalent to 30 ppmv of N_2O (Appendix A5, Table A3). This value was smaller to that obtained in the liquid phase by Jenni et al., (2012), 84±28s, and also smaller than the value the obtained by Andersen et al., (2001), which was 40s on average. This is an advantage when analysing fast changing continuous gas flows containing N_2O. The reason for the faster response time was likely due to the modifications in the gas sensor design as compared to the liquid sensor. The sensor

was slightly changed to optimize the high sensitivity needed in the gas phase. The sensor orifice was larger and the membrane length shorter as compared to the liquid sensor. Furthermore, the diffusive boundary layer that builds up in the front of the sensor in water is eliminated in the gas phase. These factors likely contribute to the faster response time.

3.3.5 Signal drift over time

Four sensors (Sensor 1, Sensor 2, Sensor 3 and Sensor 4) were evaluated for signal drift during 5 hours in the absence of N_2O. The signal drift for all 4 sensors was very low (Sensor 1 =0.001 mV/h, Sensor 2 = 0.020 mV/h, Sensor 3 = -0.046 mV/h and Sensor 4 = 0.021 mV/h), indicating that they are suitable for long-term experiments with negligible influence on the target signal. Nevertheless, routine recalibration is recommended when measurements are performed for several days.

3.3.6 Temperature dependency

The temperature dependency of the sensors was tested for the zero current and for selected N_2O concentrations (Figure 3.3). Four sensors were used in this study (Sensor 1, Sensor 2, Sensor 3 and Sensor 4). For all four sensors, the influence of temperature was well described and the coefficient of determination had a value of ≥0.83 and an average of 0.96±0.03 (Figure 3.3). Sensors 1 and 4 had a lower dependence on temperature as compared with Sensors 2 and 3. Sensors 2 and 3 had an increase in the signal of 7.10±0.77 mV and 6.89±0.54 mV from 12.3 ^oC to 32.6 ^oC, respectively, as compared to only 3.27±0.44 mV and 4.09±0.91 mV for Sensors 1 and 4. Thus, it is important to characterize the temperature influence on each individual sensor. Furthermore, after calibrating a sensor at 25 °C and measuring 25 ppmv of N_2O at 12.3 and 32.6 °C, the sensors will indicate concentrations of 20.83±1.24 and 31.29±2.64 ppmv of N_2O, respectively. These measurements underestimate by an average of 16.7 % and overestimate by 25.1 % the real N_2O concentration. It is clear that neglecting the temperature effect will lead to measurement errors in N_2O concentrations.

The relationship described in equation 3.1 was able to predict the N_2O concentration in the gas phase as a function of temperature. To predict the sensor signal using equation 3.1 and in order to simplify the process, the estimations were

performed using calibration curves with only 3 different concentrations (0, 25.5 and 50.1 ppmv of N_2O) at 2 different temperatures (12.3 and 32.6 °C) (Figure 3.4). The coefficient of determination values obtained in this case between the measured and the predicted levels was > 0.997 for all four sensors (Appendix A5, Figure A8). The maximum difference between the measured and the predicted sensor signal values was 1.03 %. Therefore, the temperature influence on all sensors was effectively predicted using only 6 points of experimental data (Figure 3.4).

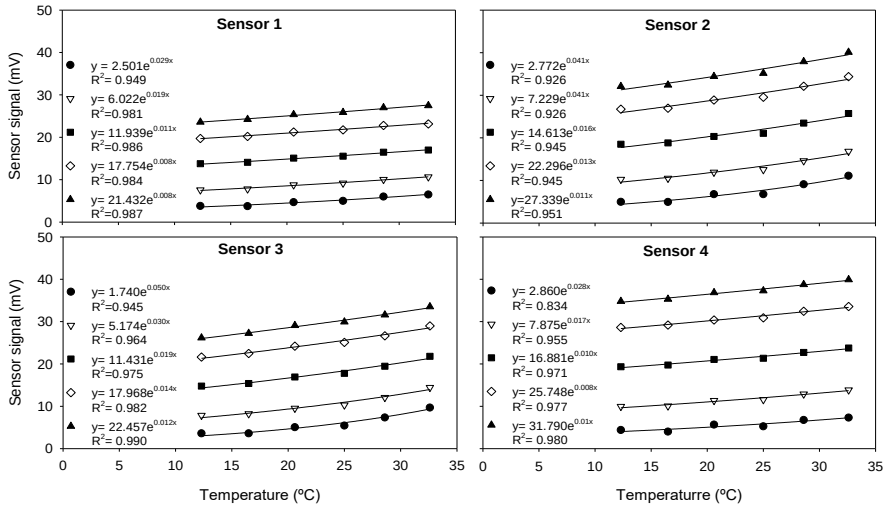

Figure 3.3 – Exponential variation of sensor signal with five different N_2O gas mixtures (● 0 ppmv, ▽ 10.2 ppmv, ■ 25.5 ppmv, ◊ 40.3 ppmv, ▲ 50.1 ppmv) as a function of temperature at a range of 10 to 35 °C, for the four sensors.

Estimations were also performed using all measured points obtained from the experiment present in Figure 3.3 (Appendix A5, Figure A6). Coefficients of determination between the measured and the predicted concentrations were ≥ 0.99 for all four sensors (Appendix A5, Figure A7). The maximum difference between the measured and the predicted sensor signal for the four sensors was only 0.78 %. The increase of the measured points used for the second estimation did not have a significant impact on the quality of the predictions, while requiring a much greater amount of time needed to perform the calibration curves. The first approach, using only 6 data points, allowed a significant decrease in the time needed to calibrate and use the sensor. While defined and controlled temperature conditions can be feasibly maintained in the laboratory, when temperature variations are unavoidable (e.g. full-scale WWTP), the correction of the sensor signal should be performed to obtain valid results.

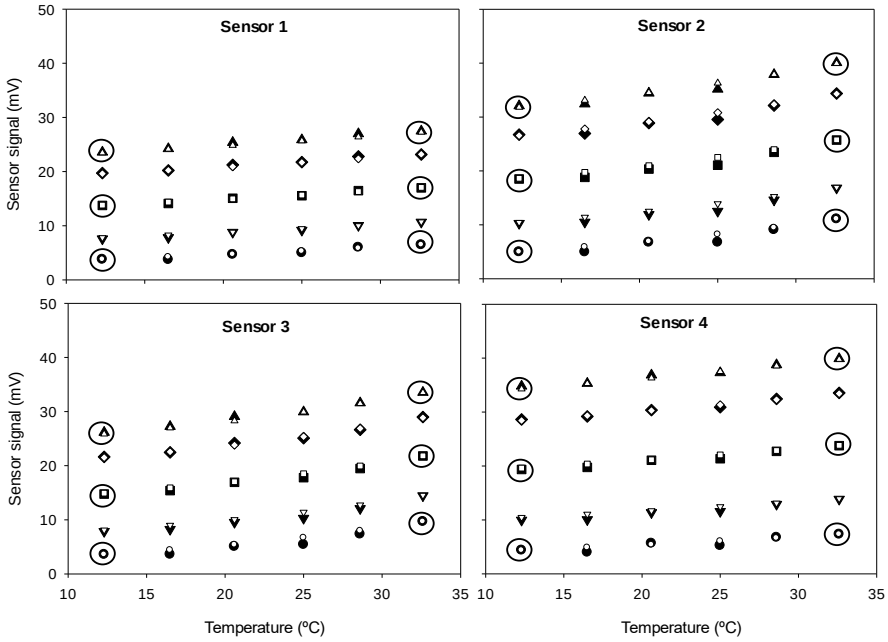

Figure 3.4 – Measured (black symbols) and predicted (white symbols) signal values for concentrations of 0 (● ○), 10.2 (▼ ▽), 25.5 (■□), 40.3 (♦ ◊) and 50.1 (▲ Δ) ppmv of N_2O for the four sensors. Prediction equations for each sensor were 1) $S_{N_2O}(T,C) = 2.736e^{0.027T}+0.380.C.e^{0.003T}$, 2) $S_{N_2O}(T,C) = 3.067e^{0.039T}+0.512.C.e^{0.004T}$, 3) $S_{N_2O}(T,C) = 1.967e^{0.049T}+0.426.C.e^{0.003T}$, 4) $S_{N_2O}(T,C) = 3.213e^{0.025T}+0.568.C.e^{0.004T}$. The large circles show the selected values used for calibration.

3.3.7 Effect of Humidity

The effect of humidity on the sensor signal was tested with four sensors (Sensor 1, Sensor 2, Sensor 3 and Sensor 4). Figure 3.5A presents the average sensor signals and standard deviations for each of the sensors. The difference obtained between the humid and dry gas stream mixtures was ≤0.63 % for all four sensors (Figure 3.5A). This low difference between the two streams indicates that moisture in the gas stream has no significant influence on the sensor signal. This constitutes an advantage of the microsensor methodology as compared with most online commercial analysers, which require preconditioning of the gas samples (to remove humidity or particles) coming from WWTP.

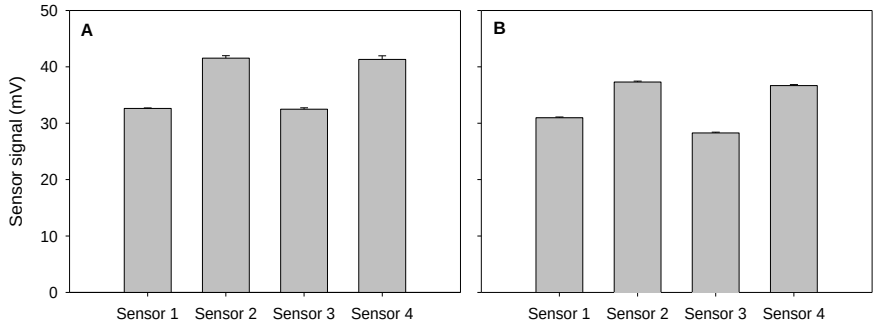

Figure 3.5 – Influence of the dry and humid gas streams (A) and of pressure increases (B) on sensor measurements using a gas mixture with 50 ppmv of N_2O.

3.3.8 Effect of small pressure changes

The influence of pressure fluctuations on the N_2O sensors was also tested. Figure 3.5B presents the average sensor signal and standard deviations for each of the sensors. The average difference obtained between the initial signal (at atmospheric pressure) and the final signal obtained after an 11 % increase in pressure was ≤0.20 % for each of the four microsensors (Figure 3.5B). This demonstrates that low pressure increases to the system have no significant influence on the sensor signal. This could be an advantage when using the microsensors to study the gas-phase dynamics in a closed vessel.

3.3.9 SBR monitoring

One of the sensors was used to monitor the N_2O emission dynamics in lab-scale SBRs. Figure 3.6 shows the results obtained with the sensor, a commercial N_2O gas analyser and GC-ECD. The sensor was able to describe correctly the emissions from the SBR-AOB (Figure 3.6B), agreeing well with the results obtained by the online gas analyser. In this reactor, a high peak of N_2O was detected during the first minutes of aeration when the feed entered the system due to its formation during the settling phase (Rodriguez-Caballero and Pijuan, 2013). After these first minutes, N_2O decreased again to very low levels (between 2-4 ppmv). The grab samples for offline analyses for the GC-ECD also confirm the trend of N_2O emission by SBR-AOB as recorded by the sensor and the online gas analyser.

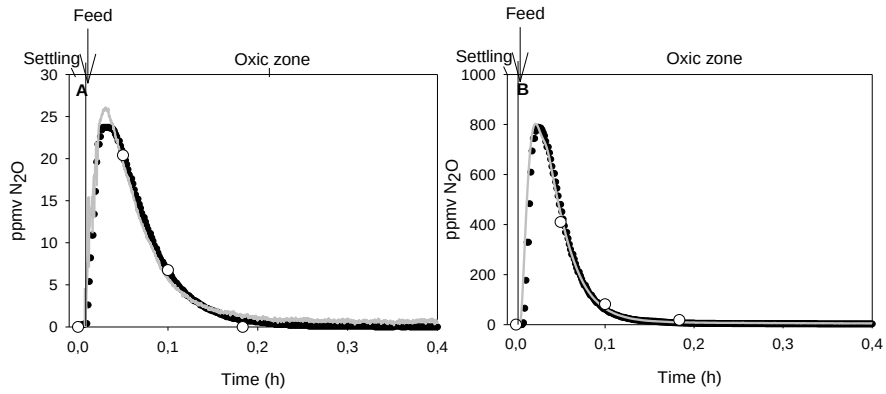

Figure 3.6 – N_2O emissions over time of the cycles of two SBRs with temperature control (25 ºC): NOB (a) and AOB (b), as measured with the N_2O sensor (grey line), Commercial analyser (black line) and GC (white circles).

The emission from the SBR-NOB (Figure 3.6A) was also correctly described by the sensor, agreeing with the results obtained by the online gas analyser, with a minor difference observed at the maximum peak obtained. A peak value of 23.70 ppmv of N_2O was obtained with the online gas analyser while the sensor measured a peak value of 26.08 ppmv of N_2O. The production of this N_2O is also attributed to the settling phase, being stripped as soon as aeration started. Due to the operational conditions of this reactor (i.e. with no nitrite accumulation) and the different microbial community present (NOB enrichment), the N_2O peak emission was lower. The grab samples for offline analyses for the GC-ECD also confirm the trend of SBR-NOB emissions recorded by the sensor and the online gas analyser. With these results, the sensor was able to accurately follow the N_2O emission dynamics at both high and low concentration ranges. When comparing total emissions for both N_2O emission profiles measured during the SBR cycles by the sensor and the commercial analyser, the AOB had a total average emission of 16.45±0.91 mg N as N_2O, and the NOB a total average emission 0.74±0.08 mg N as N_2O. This low difference between both analytical methodologies validates the N_2O miscrosensor as a reliable method to measure gaseous N_2O emissions from wastewater systems. The sensor was able to detect low concentrations down to 0.2 ppmv of N_2O and high concentrations up to 500 ppmv without any saturation of the sensor signal.

3.4 CONCLUSIONS

This study demonstrates that the adapted Clark-type gas N_2O microsensors can be used as a reliable alternative to standard methods for online detection of N_2O in the

gas phase. There are a number of advantages with utilising these microsensors as compared to conventional systems. The sensors require lower gas flows as compared to online commercial analysers, thus, the detection of low-range N_2O emissions from gas streams can be better characterized. This study shows that gas flow, composition, humidity and pressure does not influence the sensor signal. Furthermore, the sensors display high linearity at both low and high ranges of N_2O concentrations, increasing the range of detection as compared to commercial online analysers, and they also exhibit a fast response time. The use of Clark-type microsensors to measure N_2O emissions in gas streams adds the advantage of forming an integrated measuring device that can simultaneously assess the liquid- and gas-phase N_2O production fluxes, eliminating the need of two separate systems to measure the N_2O dynamics in both phases. It should be noted that these microsensors require re-calibration over the sensor lifetime, and the temperature influence on the sensor signal must be adequately predicted, as shown in this study. The N_2O measurements conducted with a microsensor in two lab-scale SBRs were shown to be highly reliable over a wide concentration range, which was corroborated with other analytical methods. The applicability of the microsensors to perform N_2O measurements in full-scale WWTPs should be tested in the future to further validate the applicability of this system.

Acknowledgements

This study was funded by the Spanish Government (MINECO) (CTM 2011-27163), the European Commission (FP7-PEOPLE-2011-CIG 303946) and the Portuguese Fundação para a Ciência e Tecnologia (PTDC/AAC-AMB/12058/2010, PEST-C/EQB/LA0006/2013, PhD grant SFRH/BD/74515/2010). Spanish and Portuguese Governments are acknowledged for Acciones Integradas (PRI-AIBPT-2011-1232) and Luso-Espanhola action E-61/12. The European Commission is also acknowledged through COST action ES1202 (Water 2020). M. Pijuan acknowledges the Ramon y Cajal Research fellowship (RYC-2009-04959). We thank Unisense for providing the sensors and helpful comments. Mr. Adrian Rodriguez-Caballero is also acknowledged for helping with the SBR N_2O monitoring.

REFERENCES

Aboobakar, A., Cartmell, E., Stephenson, T., Jones, M., Vale, P., Dotro, G., 2013. Nitrous oxide emissions and dissolved oxygen profiling in a full-scale nitrifying activated sludge treatment plant. Water Res. 47, 524–34.

Ahn, J.H., Kim, S., Park, H., Rahm, B., Pagilla, K., Chandran, K., 2010. N2O emissions from activated sludge processes, 2008-2009: results of a national monitoring survey in the United States. Environ. Sci. Technol. 44, 4505–4511.

Andersen, K., Kjær, T., Revsbech, N., 2001. An oxygen insensitive microsensor for nitrous oxide. Sensors Actuators B Chem. 81, 42–48.

Desloover, J., Vlaeminck, S.E., Clauwaert, P., Verstraete, W., Boon, N., 2012. Strategies to mitigate N2O emissions from biological nitrogen removal systems. Curr. Opin. Biotechnol. 23, 474–82.

Foley, J., de Haas, D., Yuan, Z., Lant, P., 2010. Nitrous oxide generation in full-scale biological nutrient removal wastewater treatment plants. Water Res. 44, 831–44.

Fux, C., Velten, S., Carozzi, V., Solley, D., Keller, J., 2006. Efficient and stable nitritation and denitritation of ammonium-rich sludge dewatering liquor using an SBR with continuous loading. Water Res. 40, 2765–75.

Gundersen, J., Ramsing, N., Glud, R., 1998. Predicting the signal of O2 microsensors from physical dimensions, temperature, salinity, and O2 concentration. Limnol. Oceanogr. 43, 1932–1937.

Jenni, S., Mohn, J., Emmenegger, L., Udert, K.M., 2012. Temperature dependence and interferences of NO and N_2O microelectrodes used in wastewater treatment. Environ. Sci. Technol. 46, 2257–66.

Joss, A., Salzgeber, D., Eugster, J., König, R., Rottermann, K., Burger, S., Fabijan, P., Leumann, S., Mohn, J., Siegrist, H., 2009. Full-scale nitrogen removal from digester liquid with partial nitritation and anammox in one SBR. Environ. Sci. Technol. 43, 5301–6.

Kampschreur, M.J., Tan, N.C.G., Kleerebezem, R., Picioreanu, C., Jetten, M.S.M., Loosdrecht, M.C.M. Van, Van Loosdrecht, M.C.M., 2008. Effect of Dynamic Process Conditions on Nitrogen Oxides Emission from a Nitrifying Culture. Environ. Sci. Technol. 42, 429–435.

Kampschreur, M.J., Temmink, H., Kleerebezem, R., Jetten, M.S.M., van Loosdrecht, M.C.M., 2009. Nitrous oxide emission during wastewater treatment. Water Res. 43, 4093–103.

Kampschreur, M.J., van der Star, W.R.L., Wielders, H. a, Mulder, J.W., Jetten, M.S.M., van Loosdrecht, M.C.M., 2008. Dynamics of nitric oxide and nitrous oxide emission during full-scale reject water treatment. Water Res. 42, 812–26.

Meyer, R.L., Allen, D.E., Schmidt, S., 2008. Nitrification and denitrification as sources of sediment nitrous oxide production: A microsensor approach. Mar. Chem. 110, 68–76.

Revsbech, N.P., Nielsen, L.P., Christensen, P.B., Sørensen, J., 1988. Combined oxygen and nitrous oxide microsensor for denitrification studies. Appl. Environ. Microbiol. 54, 2245–9.

Rodriguez-Caballero, A., Pijuan, M., 2013. N2O and NO emissions from a partial nitrification sequencing batch reactor: exploring dynamics, sources and minimization mechanisms. Water Res. 47, 3131–40.

Schreiber, F., Polerecky, L., de Beer, D., 2008. Nitric oxide microsensor for high spatial resolution measurements in biofilms and sediments. Anal. Chem. 80, 1152–8.

Unisense, 2014. Nitrous Oxide Sensor User Manual. Unisense, Aarhus.

Wunderlin, P., Mohn, J., Joss, A., Emmenegger, L., Siegrist, H., 2012. Mechanisms of N2O production in biological wastewater treatment under nitrifying and denitrifying conditions. Water Res. 46, 1027–37.

Yu, R., Kampschreur, M.J., Van Loosdrecht, M.C.M., Chandran, K., 2010. Mechanisms and specific directionality of autotrophic nitrous oxide and nitric oxide generation during transient anoxia. Environ. Sci. Technol. 44, 1313–1319.

4

ASSESSMENT OF ONLINE MONITORING STRATEGIES FOR MEASURING N_2O EMISSIONS FROM FULL-SCALE WASTEWATER TREATMENT SYSTEMS

SUMMARY: Clark-Type nitrous oxide (N_2O) sensors are routinely used to measure dissolved N_2O concentrations in wastewater treatment plants (WWTPs), but have never before been applied to assess gas-phase N_2O emissions in full-scale WWTPs. In this study, a full-scale N_2O gas sensor was tested and validated for online gas measurements, and assessed with respect to its linearity, temperature dependence, signal saturation and drift prior to full-scale application. The sensor was linear at the concentrations tested (0 − 422.3, 0 – 50 and 0 − 10 ppmv N_2O) and had a linear response up to 2750 ppmv N_2O. An exponential correlation between temperature and sensor signal was described and predicted using a double exponential equation while the drift did not have a significant influence on the signal. The N_2O gas sensor was used for online N_2O monitoring in a full-scale SBR treating domestic wastewater and results were compared with those obtained by a commercial online gas analyser. Emissions were successfully described by the sensor, being even more accurate than the values given by the commercial analyser at N_2O concentrations above 500 ppmv. Data from this gas N_2O sensor was also used to validate two models to predict N_2O emissions from dissolved N_2O measurements, one based on oxygen transfer rate and the other based on superficial velocity of the gas bubble. Using the first model, predictions for N_2O emissions agreed by 98.7% with the measured by the gas sensor, while 87.0% similarity was obtained with the second model. This is the first study showing a reliable estimation of gas emissions based on dissolved N_2O online data in a full-scale wastewater treatment facility.

PUBLISHED AS: Marques, R., Rodriguez-Caballero, A., Oehmen, A., Pijuan, M., 2016. Assessment of online monitoring strategies for measuring N_2O emissions from full-scale wastewater treatment systems, Water Research (in press, DOI information: 10.1016/j.watres.2016.04.052).

4.1 INTRODUCTION

N_2O is an important greenhouse gas with an approximate global warming potential 300-fold stronger than carbon dioxide (IPCC, 2013). WWTPs have been shown to release significant amounts of N_2O and contribute to anthropogenic emissions, where it is produced during nitrification and denitrification (Ahn et al., 2010; Foley et al., 2010; Kampschreur et al., 2009). An emission factor as low as 0.5% of total nitrogen removed as N_2O can lead to emissions comparable to the indirect CO_2 emissions related with energy consumption in conventional biological nutrient removal WWTPs (de Haas and Hartley 2004), while in some cases N_2O emissions have been found to contribute over 80% of the total greenhouse gases emitted from WWTPs (Daelman et al., 2013a; Daelman et al., 2013b). Ahn et al., 2010 reported emission factors in the range of 0.01-1.8% and other studies have shown similar or even higher emission factors (Aboobakar et al., 2013; Daelman et al., 2015; Kampschreur et al., 2009; Rodriguez-Caballero et al., 2015; Ye et al., 2014). This high variability of emissions and the importance that N_2O has on the greenhouse gas budget of WWTPs highlights the need for assessing N_2O on an individual WWTP basis to be able to implement effective mitigation strategies suitable for each facility.

N_2O emissions from fully covered WWTPs can be determined with measurements of outlet N_2O gas concentrations and the total gas flow rate. However, most WWTPs are open-surface sludge systems, which are typically assessed using the floating chamber methodology, where the N_2O flux is captured (Law et al., 2012; Ye et al., 2014). The N_2O gas measurements can then be analysed off-line via e.g. GC by the use of grab samples or preferably via online commercial N_2O gas analysers, which can capture the variability of the emissions over time. However, these analysers require preconditioning of the gas sample (removing humidity and particles) and a minimum gas flow (0.5-1L/min depending on the analyser). This last step dilutes the concentration of N_2O, increasing uncertainty at the low N_2O concentration range (Chapter 3). To overcome this limitation, a Clark-type N_2O microelectrode (Unisense Environment A/S) was adapted to measure N_2O in the gas phase, and was recently shown to be able to describe well the gas-phase N_2O emissions from lab-scale bioreactors (Chapter 3). However, these sensors have not previously been applied to full-scale WWTPs, where the highly dynamic conditions inherent to WWTPs could have an important impact. Full-scale application is of high importance to validate the

applicability of this novel methodology, in order to compare its effectiveness with conventional infrared online gas analysers.

Furthermore, the quantification of N_2O emissions based on liquid-phase N_2O measurements coupled with liquid-gas mass transfer estimations constitutes an alternative methodology for the assessment of N_2O emission factors in WWTPs. The N_2O that is produced and accumulated in the liquid phase can be transferred to the gas phase when N_2O is over-saturated, or stripped by aeration that facilitates the transfer of dissolved N_2O. The rate of the emissions in aerated and non-aerated zones can be estimated using volumetric mass transfer coefficients (K_La), liquid phase N_2O concentrations and the interphase transport between liquid and gas phases, relationships described by e.g. Schulthess and Gujer (1996) and Foley et al., (2010). Another alternative method to measure the dissolved N_2O concentration in the liquid phase was developed by Mampaey et al. (2015), based on gas-phase measurements and mass transfer correlations. However, the use of liquid N_2O microsensors for continuous estimation of gas-phase N_2O emissions has not previously been reported, to the best of our knowledge, and could simplify the methodological procedure for assessing N_2O emissions.

In this study, the N_2O emissions of a full-scale WWTP treating domestic wastewater were measured via gas-phase microelectrodes and a conventional infrared online gas analyser, in order to assess the advantages/disadvantages with each monitoring approach. The impact of temperature as well as the sensor range and stability were firstly assessed for this purpose. Further, dissolved N_2O dynamics were also monitored with N_2O microsensors and were used to estimate N_2O emissions via mass transfer calculations. The aim of the work was to assess the applicability of microelectrodes for direct gas-phase N_2O measurements from a full-scale WWTP and to assess two different methodologies to estimate N_2O gas emissions from dissolved N_2O measurements.

4.2 MATERIALS AND METHODS

4.2.1 Experimental setup for full-scale sensor calibration

A Clark-Type N_2O gas sensor was used to measure N_2O emissions and a liquid N_2O microsensor was used for the liquid phase N_2O measurements in this study (Unisense Environment A/S, Denmark). Both sensors contained an internal reference

and a guard cathode and before use, were connected to individual amplifier systems (Unisense Environment A/S, Denmark) and polarised overnight following manufacturer instructions (Unisense, 2014). The Clark-Type N_2O gas sensor was modified, as compared with the lab-scale version (Chapter 3), to be more robust and prepared for handling shock impacts, and a temperature sensor was integrated within it to measure the variation of temperature in the gas phase along the measurement period (Figure 4.1 A).

Figure 4.1 – A– Full-scale N_2O gas sensor and controller box; **B** – Full-scale dissolved N_2O sensor and controller box; **C** – Close-up of the gas sensor placed in the sampling hood; **D** – Sampling hood placed in the full-scale activated sludge SBR.

To validate the N_2O concentration in the tests described below, a commercial N_2O online gas analyser (VA-3000, Horiba, Japan) was also used as well as a GC-ECD (Thermo Fisher Scientific, Trace GC Ultra, USA) with a column (TracePLOT TG-BOND Q, 30 m x 0.32 mm x 10 µm). Three ranges of calibration curves (up to: 422.3 ppmv of N_2O, 50 ppmv of N_2O and 10 ppmv of N_2O) were tested according to the methodology described in Chapter 3. Four different commercial N_2O gas mixtures were used in this experiment, 100% N_2O, 422.3, 104.3 and 83.7 ppmv N_2O (Linde, Spain). Mass flow controllers (Applikon Biotechnology, Netherlands) were used to achieve other desired N_2O concentrations using nitrogen as dilution gas. A 3 L vessel was used to perform the sensor calibration tests described below. The vessel was immersed in a water bath to control the temperature at the desired set-point. Temperature was measured with a temperature probe connected to an ez-control box (Applikon Biotechnology, Netherlands). The vessel was connected via gas tight tubing to a commercial N_2O analyser. Gas tight valves were used to seal the chamber after the

volume of gas was fluxed to reach the desired N_2O concentration. A commercial hood (AC 'SCENT® Flux Hood, USA) was used to collect the gas from the full-scale wastewater reactor. The full-scale gas N_2O sensor was attached to the hood and the gas collected was directed to the commercial analyser via gas tubing.

4.2.2 Experimental Procedure

Several sets of tests were conducted to validate the most influential parameters on the sensor signal, as described in Chapter 3, including calibration curves at different N_2O concentrations, the sensor signal saturation, sensor drift and temperature dependence of the sensor were characterized prior to monitoring the wastewater treatment plant.

Full-scale gas sensor validation

The linearity of the sensor was tested with three different N_2O concentration ranges (High range: 0-422.3 ppmv N_2O; Medium range: 0-50 ppmv N_2O; Low range: 0-10 ppmv N_2O) using nitrogen as dilution gas. The methodology used was similar to that described in Chapter 3. The sensor signal saturation was then tested with three different concentrations (1000, 2000 and 3000 ppmv of N_2O) to identify the upper N_2O detection limit of the sensor. The concentrations of the gas flow were simultaneously assessed by a commercial gas analyser and GC-ECD. The drift over time in the signal of the Clark-Type N_2O gas sensor was measured during 5h in a N_2O-free environment at a controlled temperature of 25 °C. The sensor drift was very low (0.016 mV/h) indicating that this sensor is suitable for long-term experiments with negligible influence on the target signal. Nevertheless, routine recalibration is recommended when measurements are performed for several days.

The temperature dependency was characterized using 3 different concentrations of N_2O. A zero current gas mixture, 25.5 ppmv of N_2O and 50.1 ppmv of N_2O. Calibration curves were performed within the range of 15-33 °C. To describe the influence of temperature on the sensor signal, a double exponential equation was used as described by Jenni et al., (2012) and Chapter 3 (Equation 4.1):

$$S_{N_2O}(T, C) = a_1 \times e^{b_1 T} + a_2 \times C \times e^{b_2 T} \quad (4.1)$$

where T is the temperature and C the concentration measured by the sensor, where a_i and b_i are the fitting parameters.

Full-scale liquid sensor and online commercial analyser calibration

The full-scale liquid sensor was calibrated according to the instructions present in the Unisense N_2O sensor manual. Briefly, the sensor was connected to an amplifier and polarized overnight following manufacturer instructions. A saturated solution with N_2O was obtained thought bubbling, at a flow rate of 5L/min, 100% N_2O during 5 minutes. A three-point calibration was obtained by adding twice 0.1 mL to 100 mL of free N_2O water. The online commercial analyser (VA-3000, Horiba, Japan) was calibrated with nitrogen gas free of N_2O to obtain a zero N_2O calibration point and with a gas mixture of 422.3 ppmv of N_2O to perform a two-point calibration curve. Both systems were calibrated before and after monitoring the WWTP.

Full-scale monitoring tests

N_2O emission dynamics were monitored online at a domestic WWTP of 48000 population equivalents (P.E) (WWTP of La Roca del Vallès, Barcelona, Spain) in order to validate the full-scale N_2O measurements from the gas sensor with a commercial analyser, and also with a liquid phase N_2O sensor (Figure 4.1 A,B). The plant consists of four identical SBRs with an operational volume of 4684.2 m^3 each that were operated for COD and N removal (More details can be found at Rodriguez-Caballero et al., 2015). The N_2O gas emissions were captured by a hood placed in one of the SBRs (Figure 4.1 C, D) and were compared between the N_2O gas sensor and a commercial analyser. Simultaneously, a liquid-phase N_2O sensor was applied in the same zone of the SBR as the gas sensor. Temperature in the liquid-phase varied between the range of 16.9 to 17.9 °C.

Data acquisition and N_2O emission calculation

N_2O emission measured by the Gas sensor and Commercial analyser:

On-line process data from the SBR tank was acquired from the data acquisition system of the WWTP. These values were used to calculate N_2O emissions during the reactor monitoring. The N_2O gas emitted in the aerated phases was calculated using the following equation 4.2:

$$N_2O\ gas\ emitted_{(aerated)} = \left[\sum \left(C_{N_2O} \times Q_{gas(aerated)} \times \Delta t\right)\right] \quad (4.2)$$

Where,

- N_2O gas emitted $_{(aerated)}$ – N_2O gas emitted during aerated operational times (mg N-N_2O);
- C_{N2O} (mg N-$N_2O.m^3$) = C_{N2O} (ppmv N_2O) × 1/0.08205 atm.L.$mol^{-1}.K^{-1}$ × (28/T(K));
- $Q_{gas(aerated)}$ – gas flow coming out of the reactor during aerated zones ($m^3.d^{-1}$);
- Δt – time interval by which the off-gas concentration was recorded (d);

While during the non-aerated phases the gas emitted was calculated according to the following equation 4.3:

$$N_2O\ gas\ emitted\ _{(\text{non}-aerated)} = \left[\left(\sum \left(C_{N_2O} \times Q_{in(\text{non}-aerated)} \times \Delta t\right)\right) \times \left(\frac{A_{Tank}}{A_{hood}}\right)\right] \quad (4.3)$$

Where,

- N_2O gas emitted$_{(non\text{-}aerated)}$ – N_2O gas emitted during non-aerated operational times (mg N-N_2O);
- A_{hood} – Area of the tank covered by the hood (m^2);
- A_{Tank} – Aeration field size (m^2);
- Q_{in} (L/min) - Flow at which the sample conditioning system pumps gas into the analyser (0.5 L/min);

N_2O emissions calculated using liquid-phase measurements:

Estimation based on the dissolved N_2O sensor data and the K_La of N_2O was also applied to this full-scale SBR WWTP. During the cycle the reactor was operated with both aerated and non-aerated phases. The aeration was performed using diffused aerators situated near the bottom of the tank. The N_2O gas emitted during aeration was calculated based on the mass transfer coefficient, the input of the air flow, the volume of the reactor, the Henry's coefficient and the concentration of dissolved N_2O through applying Equation 4.4 (Schulthess and Gujer, 1996):

$$Gas\ emitted_{(aerated)}=H_{N_2O,T_{process}}\times S_{N_2O_{T_{Comp.}}}\times\left[1-e^{-\frac{K_La_{N_2O_{T_{Process}}}}{H_{N_2O,T_{process}}}\times\frac{V_R}{Q_{gas}}}\right]\times Q_{gas(aerated)}\times\Delta t \quad (4.4)$$

Where,

- Gas emitted (aerated) – Emissions of N_2O during the aerated phases (mg N-N_2O);
- $S_{N2O}T_{Comp}$ – Concentration of N_2O in the liquid measured by the N_2O liquid microsensor, after temperature compensation (mg N-$N_2O.m^{-3}$);
- $H_{N2O,}T_{process}$ – Henry`s constant at the process temperature (dimensionless);
- $K_LaN_2O_{Tprocess}$ – N_2O mass transfer coefficient at the process temperature (d^{-1});

For non-aerated periods, a typical K_La for N_2O of $2d^{-1}$ for an anoxic tank was first chosen (Schulthess and Gujer, 1996), and later estimated as described below (equation 4.6). The rate of N_2O emissions were then calculated using equation 4.5 (Schulthess and Gujer, 1996):

$$Gas\ emitted_{(non-aerated)}=K_La_{N_2O(non-aerated)}\times\left(S_{N_2O_{T\_Comp.}}-\frac{C_{N_2O,air}}{H_{N_2O,}T_{process}}\right)\times V_R\times\Delta t \quad (4.5)$$

Where,

- Gas emitted (non-aerated) – Emissions of N_2O during the non-aerated phases (mg N-N_2O);
- $K_LaN_2O_{Tprocess\ (non\text{-}aerated)}$ – N_2O mass transfer coefficient during non-aerated phases (d^{-1});
- C_{N2O}, air - average concentration of N_2O in the atmosphere of the northern hemisphere, 0.326 mg-N/m^3 according to (Blasing, 2009);

Through rearranging equation 4.5, the mass transfer coefficient was estimated for non-aerated operational times using the N_2O emissions measured in the gas-phase and in the liquid-phase sensors, as shown in equation 4.6:

$$K_L a_{N_2O(non-aerated)} = \frac{S_{N_2O\,Gas\ sensor}}{\left(S_{N_2O\,Liquid\ sensor} - \frac{C_{N_2O,air}}{H_{N_2O,}T_{process}}\right)} \quad (4.6)$$

Where,

- $S_{N2O\ Gas\ sensor}$ – Concentration of N_2O in the gas measured by the N_2O gas sensor, after temperature compensation (mg N-N_2O.m^{-3}).
- $S_{N2O\ Liquid\ sensor}$ – Concentration of dissolved N_2O measured by the N_2O liquid microsensor, after temperature compensation (mg N-N_2O.m^{-3}).

This dynamic estimation of K_La during non-aeration conditions was applied during the anoxic phases of WWTP operation, where negative K_La values were assumed to be zero.

The K_La during aeration is related with many factors, including reactor geometry (particularly aerator immersion depth), aeration bubble size, diffuser layout and liquid viscosity (Foley et al., 2010; Gillot et al., 2005). The methodologies used to estimate the K_La during aeration are described in detail in the supplementary information. Briefly, the methodologies applied to assess the K_La during aeration and non-aeration operational times are described below:

- Method 1:
  - (aerated phase) based on the superficial gas velocity of the reactor (Appendix B, Equation B1 and B2) as described by Foley et al., (2010);
  - (non-aerated phase) based on a typical K_La for N_2O of $2d^{-1}$ for an anoxic tank (Schulthess and Gujer, 1996);
- Method 2:
  - (aerated phase) based on the superficial gas velocity of the reactor (Appendix B, Equation B1 and B2) as described by Foley et al., (2010);
  - (non-aerated phase) based on Equation 4.6;
- Method 3:
  - (aerated phase) based on the oxygen transfer rate (OTR) of the reactor, assuming pure water (Appendix B, Equation B4);

- (non-aerated phase) based on a typical K_La for N_2O of $2d^{-1}$ for an anoxic tank (Schulthess and Gujer, 1996);

- Method 4:
  - (aerated phase) based on the OTR of the reactor, integrating fouling, salinity and impurity factors in the estimation (Appendix B, Equation B5);
  - (non-aerated phase) based on a typical K_La for N_2O of $2d^{-1}$ for an anoxic tank (Schulthess and Gujer, 1996);
- Method 5:
  - (aerated phase) based on the OTR of the reactor integrating fouling, salinity and impurity factors in the estimation (Appendix B, Equation B5);
  - (non-aerated phase) based on Equation 4.6;

After obtaining the K_La of O_2 at 20ºC for each of the OTR methods (3-5) for the aerated phase, Higbie`s penetration model was applied to calculate the K_La of N_2O applying equation B7 (Appendix B) (Foley et al., 2010; Van Hulle et al., 2012) (Appendix B, Equation B7). Due to temperature variation along the day, K_La and Henry's constant estimations were corrected for temperature, as described in detail in the Appendix B.

4.3 RESULTS AND DISCUSSION

4.3.1 Full-scale N_2O sensor calibration

The sensor linearity was tested in three different concentration ranges (0-422.3 ppmv; 0-50 ppmv; 0-10 ppmv) with nitrogen used as dilution gas. The sensor showed high linearity and stability within the ranges tested. No saturation of the signal was observed up to the maximum concentration tested, nor was a decrease in linearity observed at the lower range tested (Appendix B, Figure B1). Overall, the sensor was shown to respond linearly over a wide concentration range of N_2O, which is in accordance with the results obtained in Chapter 3 for the lab-scale N_2O gas sensors.

In order to evaluate the sensor and commercial analyser responses at high N_2O levels, as well as the signal saturation of each system, a series of standards were performed at concentrations above 1000 ppmv and compared with GC-ECD. A pure 100% N_2O gas bottle was used and the gas diluted in order to have three gas streams with concentrations of approximately 1000, 2000 and 3000 ppmv of N_2O. The results

(Table 4.1) showed that at the first concentration tested, 1000 ppmv of N_2O, the commercial analyser was already saturated and not able to determine this concentration correctly. The N_2O gas sensor was able to follow the trend and measure the gas stream well at this level. The sensor was also able to correctly measure the N_2O in the gas stream at 2000 ppmv (Table 4.1). A final gas stream of 3000 ppmv of N_2O was used and showed that the sensor was not able to adequately measure it at this very high level. Further results showed that the sensor was able to measure concentrations up to 2750 ppmv of N_2O (through additional testing), while the commercial analyser was not able to adequately describe any of the high concentrations tested. This validates the applicability of the sensor to measure very high concentrations of N_2O in gas streams.

Table 4.1 – Comparison between the gas sensor, commercial analyser and GC-ECD between 3 different mixtures with approximate concentrations of 1000, 2000 and 3000 ppmv of N_2O.

	Gas Sensor (ppmv)			Commercial Analyser (ppmv)			GC-ECD (ppmv)		
	1000	2000	3000	1000	2000	3000	1000	2000	3000
Average	1072	2029	2829*	774	946	NT	1036	2115	3037
STD (%)	0.05	0.32	0.01	0.06	0.66	NT	8.81	0.81	0.06

NT- concentration not tested with this equipment; * - saturation of the N_2O gas sensor reached

The temperature dependency of the sensor was tested for the zero current and for selected N_2O concentrations. There was an exponential temperature dependency on the zero current and the tested N_2O concentrations for the sensors. The influence of temperature was well described by an exponential equation and the coefficient of determination had a value of ≥0.96 (Figure 4.2, A). A similar dependency was also found for the commercially available N_2O microsensors in lab-scale tests for liquid and gas phase measurements (Jenni et al., 2012 and Chapter 3).

Since the N_2O sensor measurements depend on temperature, and the air experiences higher temperature fluctuations along the day as compared to the liquid phase, the gas sensor can experience high temperature fluctuations throughout the day. Correct characterization and prediction of the temperature effect on the sensors is essential for their application in full scale systems. A double exponential equation (equation 4.1) was used to predict the sensor signal, using calibration curves at different temperatures (Figure 4.2, B), where only 6 measurements were needed to accurately calibrate the sensor, validating the strategy proposed with the lab-scale gas sensor (Chapter 3). The fitting was performed with 3 different concentrations (0, 25.5

and 50.1 ppmv of N_2O) at 2 different temperatures (15.5 and 33.1 °C), though the equation also described well the sensor signal for these 3 concentrations at 2 additional temperatures (22.6 and 25.5°C) to validate the temperature dependency. High coefficient of determination values > 0.999 were obtained in this case between the measured and the predicted signal. The maximum difference between the measured and the predicted sensor signal values was 3.0 %. Therefore, the temperature influence on all sensors was effectively predicted using only 6 points of experimental data for calibration. When temperature variations are unavoidable (e.g. at a full-scale WWTP), the correction of the sensor signal should be performed to obtain valid results.

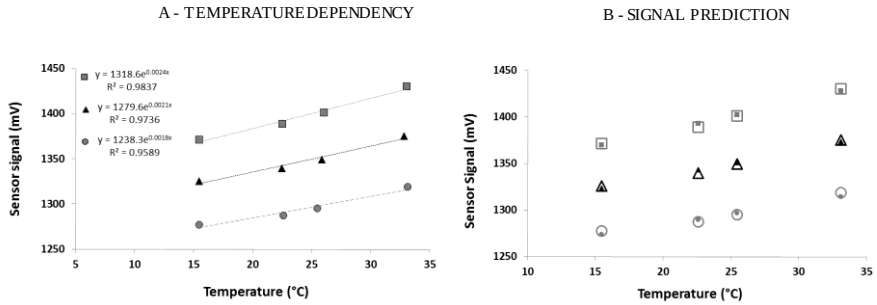

Figure 4.2 – A - SBR Exponential variation of sensor signal with three different N_2O gas mixtures (● 0 ppmv, ▲25.5 ppmv, ■ 50.1 ppmv) as a function of temperature at a range of 15 to 35 °C; **B** - Measured (open symbols) and predicted (close symbols) signal values for concentrations of 0 (●,○), 25.5 (▲,Δ), and 50.1 (■,□) ppmv of N_2O for the sensor. Prediction equation for the sensor was S_{N2O} (T,C) = $1238.3e^{0.002T}+1.638Ce^{0.009T}$.

4.3.2 Comparing the N_2O gas sensor with the online gas analyser at full-scale

The sensor was attached to the hood and placed in the SBR at the WWTP. The N_2O gas emissions were collected and characterized during 4 days. The sensor signal was corrected for the temperature variations using equation 3.1. Figure 4.3 shows the results obtained with the sensor and the commercial N_2O gas analyser. The sensor was able to describe very well the trend in the emissions when compared with the commercial analyser. Due to saturation of the commercial analyser at N_2O concentrations above 500 ppmv (as indicated by the manufacturer), the higher emission peaks were in fact much better described by the full-scale gas sensor (Figure 4.3). This shows that the wide detection range of the microelectrode can result in

improved ability to estimate N_2O emissions, and that N_2O peaks measured by conventional analysers may be underestimating the true emissions in cases where the concentration exceeds their upper detection limit (in the case of this study, 500 ppmv). Rodriguez-Caballero et al., (2014) also reported the importance of correctly characterizing peak emissions in their study, where even isolated peak emissions had a significant impact on the global emissions of a WWTP.

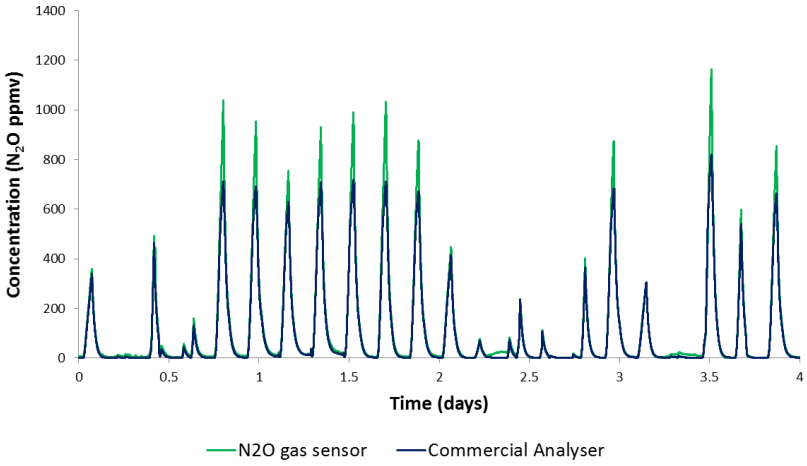

Figure 4.3 – N_2O emissions over a 4 day monitoring period at the full scale SBR with the gas sensor (green line) and the commercial analyser (blue line).

The emissions from the full-scale SBR were calculated using equation 4.2 for aerated phases and equation 4.3 for non-aerated phases, where the phases were differentiated based on the measured DO concentration in the liquid after aeration commenced or ceased. When comparing the overall N_2O emissions between the sensor and the commercial analyser, there was a difference of 14.1% between both (Table 4.2). As shown in Figure 4.3, this difference is mainly due to the underestimated N_2O peaks in the case of the commercial analyser, which had already exceeded its saturation signal. This difference decreases significantly when analysing the emissions as assessed by the sensor and commercial analyser below 500 ppmv, where the difference was only 2.0 %. Thus, at levels below 500 ppmv, the sensor and commercial analyser achieved highly comparable results, supporting the applicability of either methodology in this concentration range. Further, peak emissions should be correctly characterized because the N_2O peak emission events can significantly increase the overall N_2O emission factor of a WWTP. The high variability of peak emissions (very high and low), under aerated and non-aerated conditions, varying DO, temperature, nutrient concentrations and aeration flow rates (Appendix B, Figure B3), validate the

use of the gas sensor to accurately quantify the N_2O emissions when subjected to the variable conditions present in a WWTP. Overall, the results validate the use of the gas sensor to measure N_2O emissions in a WWTP, even achieving a wider range of emission rates than currently achieved by a commercial analyser.

Table 4.2 – Comparison between the gas sensor, commercial analyser and GC-ECD between 3 different mixtures with approximate concentrations of 1000, 2000 and 3000 ppmv of N_2O. Comparison between the total emissions and emissions limited up to 500 ppmv between the N_2O gas sensor and the commercial analyser.

Total emissions	Gas Sensor (KgN-N_2O)	Commercial analyser (KgN-N_2O)	Difference (%)	
Total emissions	19.69	16.91	14.11	
Aerobic	18.93	16.27	14.04	a
Anoxic	0.76	0.64	15.82	
Emissions (<500 ppmv)	**Gas Sensor (KgN-N_2O)**	**Commercial analyser (KgN-N_2O)**	**Difference (%)**	
Total emissions	8.42	7.71	2.04	
Aerobic	7.84	7.68	2.03	b
Anoxic	0.58	0.50	13.88	

The anoxic emissions measured with both techniques were very similar (Table 4.2a, 2b). When comparing the total emissions between the aerobic and anoxic phases, the aerobic phase was the main contributor with over 96.1% of the total emissions. These results agree with the studies of Ahn et al., (2010) and Ye et al., (2014), where the aerobic phase contributes with higher N_2O emissions as compared with the anoxic due to the higher rate of N_2O production and stripping during aeration.

4.3.3 N_2O gas sensor estimation through dissolved N_2O measurements

The total emissions were calculated for the aerated and non-aerated periods using the dissolved N_2O sensor data, with five different approaches to estimate the K_La of N_2O during aeration. The first approach consisted on using the superficial gas velocity in the liquid (Method 1) resulting in a difference of 19.5 % between the calculated emissions based on dissolved N_2O data and the measured emissions with the N_2O gas sensor (Table 4.3). During the four days of monitoring, a higher difference was observed in the emissions predicted by the liquid sensor for the first 2 days (period_a: 32.7%), as compared to the last 2 days (period_b: 4.4%), when comparing the results to the gas sensor emissions (Table 4.3 – Method 1). This difference was likely due to the accumulation of particles on the liquid sensor observed during the

monitoring of period_a (first 2 days), while during period_b (last 2 days) the sensor was cleaned once per day.

Table 4.3 – Emission comparison between N_2O measured with the Gas sensor, Commercial analyser and the methodologies used to estimate the gas emissions using the N_2O liquid sensor. The difference between the N_2O measured with the gas sensor and the respective methodology used to estimate the N_2O emission using the liquid sensor is shown in brackets.

Emissions	Gas sensor	Commercial analyser	Liquid sensor (Method 1)	Liquid sensor (Method 2)	Liquid sensor (Method 3)	Liquid sensor (Method 4)	Liquid sensor (Method 5)
	Emissions	Emissions	Emissions	Emissions with K_La (non-aerated) estimated)	Emissions (pure water)	Emissions (with α, β and F)	Emissions (with α, β, F and K_La (non-aerated) estimated)
	(KgN-N_2O)	(KgN-N_2O)	(KgN-N_2O)	(KgN-N_2O)	(KgN-N_2O)	(KgN-N_2O)	(KgN-N_2O)
Total emissions	19.69	16.91	15.85 (19.5)	13.48 (31.5)	17.15 (12.9)	18.07 (8.2)	15.70 (20.2)
Aerated	18.93	16.27	12.92 (31.7)	12.92 (31.7)	14.22 (24.8)	15.14 (20.0)	15.14 (20.0)
Non-Aerated	0.76	0.64	2.93	0.56	2.93	2.93	0.56
Period_a	12.75	10.81	8.58 (32.7)	7.45 (41.6)	9.32 (26.9)	9.81 (23.0)	8.67 (31.9)
Period_a (aerated)	12.28	10.40	7.09 (42.2)	7.09 (42.2)	7.83 (36.2)	8.32 (32.2)	8.32 (32.2)
Period_a (non-aerated)	0.47	0.41	1.49	0.35	1.49	1.49	0.35
Period_b	6.94	6.10	7.26 (4.4)	6.04 (13.0)	7.83 (11.4)	8.26 (16.1)	7.03 (1.3)
Period_b (Aerated)	6.65	5.87	5.83 (12.4)	5.83 (12.4)	6.39 (3.9)	6.82 (2.4)	6.82 (2.4)
Period_b (non-aerated)	0.29	0.23	1.44	0.21	1.44	1.44	0.21

The second approach consisted of calculating the K_La based on the OTR (Method 3). A difference of 12.9 % between the total emissions measured by the gas sensor and the calculated emissions based on dissolved N_2O data was found (Table 4.3 – Method 3). As observed in the previous approach, the difference in the emissions was higher during period_a as compared to period_b. To increase the applicability of the model equation using the Method 3 estimation methodology, the main factors affecting liquid-gas mass transfer in wastewater systems were taken into account, including salinity (β), impurities (α) and fouling (F). The total estimated emissions obtained with this approach (Method 4) were closer (8.2%) to the emissions measured by the N_2O gas sensor (Table 4.3 – Method 4).

When evaluating the aerated emissions, considering each methodology, higher agreement with the gas sensor emissions was achieved for period_b, with differences of 4.4, 11.4 and 16.1 % for Method 1, Method 3 and Method 4, respectively. While for period_a the differences between the emissions measured by the gas sensor with each methodology (Method 1, Method 3 and Method 4) were 32.7, 26.9 and 23.0 %,

respectively. Furthermore, the total predicted emissions in the non-aerated phase were substantially higher as compared with the ones measured by the gas sensor. This overestimation in the non-aerated phase can be related with the use of a typical K_La for N_2O of $2d^{-1}$ for anoxic tanks (Method 1, 3 and 4), which was originally determined for continuous activated sludge processes (Schulthess and Gujer, 1996). This estimation of K_La was thus not applicable to the present WWTP, a full-scale SBR, and required reassessment to avoid overestimation of the N_2O emissions. To correct this, the K_La for non-aerated phases was calculated based on the dynamic emissions measured by the N_2O gas and liquid sensors (Equation 4.6, Method 2 and 5). The average non-aerated K_La throughout the experimental period was 0.39 d^{-1}, five times smaller than the previously applied value. The SBR configuration of the studied WWTP clearly influenced this mass transfer coefficient, as there was lower turbulence in the SBR as compared to continuous-flow WWTPs. Dynamic estimation of the non-aerated K_La increased the confidence of the model equations to estimate the emissions calculated using dissolved N_2O data, particularly for the Method 5.

A comparison between the dynamic N_2O emissions as assessed by the gas sensor and estimated via the liquid sensor is shown in Figure 4.4 for 3 typical cycles during the monitoring of the plant (period_b). By applying equation 4.6, the non-aerated kLa was corrected according with the emission measure by the N_2O gas sensor (Method 2 and 5). The predicted emissions based on the dissolved N_2O data using estimation Method 5 agreed very well with the emissions captured by the hood and measured with the N_2O gas sensor. The prediction of N_2O emissions during period_a show higher deviation as compared to the gas-phase analysis (Appendix B, Figure B2), highlighting the importance of sensor cleaning. It is also clear from Figure 4.4 that the N_2O emissions were mainly attributed to aerobic production mechanisms rather than anoxic production and subsequent aerobic stripping. Indeed, while the dissolved N_2O concentrations were initially high anoxically, they were gradually reduced along the anoxic and settling phases, contributing little to the total N_2O emissions during this time period due to the very low non-aerated K_La. Aerobically, the initial N_2O emissions were consistently negligible, revealing near-complete denitrification during the previous anoxic and settle/decant phases, with minimal carryover of the anoxically produced N_2O to the subsequent aerobic phase where it would be more readily emitted. The amount of N_2O that was reduced during the settling/decant phases in a typical cycle was 75.5 mg $N\text{-}N_2O/m^3$, which would have increased the N_2O emissions by 21.6±1.8% if it were emitted (assuming the typical aeration flow rate applied during the aerobic

periods). These results highlight that estimation of both the aerobic and anoxic K_La can be useful to both quantify the total N_2O emissions using dissolved N_2O measurements and identify operational factors that lead to these emissions.

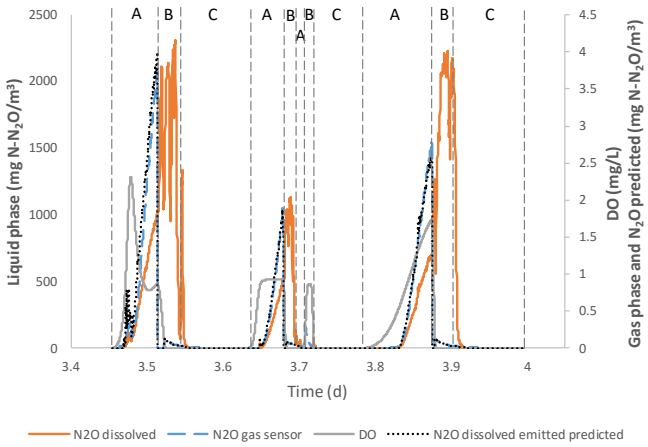

Figure 4.4 – Typical SBR profile at La Roca del Vallès WWTP of N2O gas emissions (blue dashed line), liquid N_2O concentration (orange line), DO concentration (grey line) and N2O dissolved emitted predicted (black dashed line) (Method 5 – period_b). A – aerobic phase, B – anoxic phase and C-settling and decant phase.

The total emissions obtained from the SBR analysed in this study were 48.6 and 41.8 gN-N_2O/kg N-NH_4^+ removed for the N_2O gas sensor and the online commercial analyser, respectively, during the total measurement period (Table 4.4).

Table 4.4 – Emissions of N_2O per ammonia removal measured by the gas sensor, commercial analyser, and liquid-phase sensor.

Emissions (g N-N_2O/kg NH_4)	Total	Period_a	Period_b
Gas sensor	48.6	55.7	39.5
Commercial analyser	41.8	47.2	34.7
Liquid sensor (Method 2)	33.3	32.5	34.3
Liquid sensor (Method 5)	38.8	37.9	40.0

Underestimation of the emissions was evident when comparing these two methodologies due to the high peak emissions that could not be effectively quantified by the commercial analyser. The total estimated emission values obtained using the dissolved N_2O measurements were 33.3 and 38.8 gN-N_2O/kg N-NH_4^+ for the methodologies using Method 2 and Method 5, respectively (Table 4.4). However, when taking into account only period_b, the emissions of the liquid sensor (Method 2) underestimated the gas sensor emissions by 13.0 %, while the liquid sensor (Method 5) emissions agreed within 98.7 %. The estimation of the emissions using the OTR-

based method, where both the aerobic and non-aerobic K_La are calculated, was shown to be a reasonable means of providing a good estimation of the total N_2O emissions, where regular cleaning of the sensor can increase the validity of these estimations.

4.3.4 Comparison of N_2O monitoring methodologies

The results of this study showed that the gas sensor is advantageous over conventional online gas analysers due to its higher measurement range. The gas sensor signal has a very low drift over time and by applying the drift correction, the sensor could be continuously used without performing additional calibration during several weeks, which is comparable to conventional analysers. The additional step required for the application of N_2O gas sensors as compared to conventional gas analysers is the calibration step at different temperatures. Nevertheless, this study showed that this can be effectively achieved with 6 experimental measurements, minimising labour. The gas sensor does not require regular cleaning, although it has a limited lifetime (~6 months). Unlike conventional analysers, however, the gas sensor does not require pre-conditioning of the gas sample prior to measurement. This increases maintenance requirements to the measurement system, as regular maintenance checks are required in conventional analysers. Thus, both systems require occasional maintenance and/or replacement of parts.

The dissolved N_2O sensor signal is also very stable over time, and, as suggested by the manufacturer (Unisense Environment, Denmark), requires only a bimonthly calibration, which takes around 10 minutes and does not involve measurements at different temperatures. Regarding the cleaning of the sensor, we observed an improvement of the signal if the sensor was cleaned on a daily basis. However, an improved version of this sensor to be used for full-scale measurements is now commercially available, and the manufacturer claims that no regular cleaning is needed (Unisense Environment, Denmark). The liquid and gas-phase N_2O sensors have a similar lifetime. In this study it was found that emissions were effectively estimated within a reasonable error based on dissolved N_2O sensor signals.

For highest rigour, the simultaneous utilisation of an N_2O sensor in both the gas and liquid phases is recommended, as it also enables estimation of the relative importance of the aerobic or anoxic N_2O production mechanisms. Furthermore, both signals can be measured using only one multimeter controller, decreasing total cost of the equipment. Overall, this work shows that the analytical methodology employed to

assess N_2O emissions can have a significant influence on the N_2O emission factor obtained for WWTPs. We recommend that this new methodology also be applied to assess N_2O emissions at other full-scale WWTPs.

4.4 CONCLUSIONS

The main conclusions of this work are summarised below:

- The N_2O Clark-type full-scale gas sensor proved to be a reliable alternative to standard methods for online detection of N_2O emissions in the gas phase of WWTPs.
- The sensor was linear at both low and high ranges of N_2O concentrations, reaching an upper detection limit of 2750 ppmv N_2O. Routine calibrations should be performed, and the temperature influence on the sensor signal must be adequately predicted.
- Emissions were successfully described by the gas sensor, being even more accurate than the values given by the commercial analyser at N_2O concentrations above 500 ppmv. Total N_2O emissions were underestimated by 14.0 % by the commercial analyser in this study.
- The two proposed methodologies to estimate N_2O emissions using dissolved N_2O measurements performed by a full-scale liquid N_2O sensor with best results agreed by 98.7% (Method 5) or 87.0 % (Method 2) with the emissions measured by the gas sensor. This is the first study showing a reliable estimation of gas emissions based on dissolved N_2O online data in a full-scale wastewater treatment facility.
- This proposed methodology has the added advantage of simultaneously analysing the N_2O dynamics in the liquid and gaseous phases, in only one experimental setup, and can in this way contribute to improve the characterisation of the N_2O emission mechanism in the WWTP.

Acknowledgements

This study was funded by the Spanish Government (MINECO) (CTM 2011-27163 and CTM2015-66892-R), European Commission (FP7-PEOPLE-2011-CIG 303946) and the Portuguese Fundação para a Ciência e Tecnologia (PTDC/AAC-AMB/12058/2010, UID/Multi/04378/2013, PhD grant SFRH/BD/74515/2010). Spanish and Portuguese Governments are also acknowledged for Acciones Integradas (PRI-

AIBPT-2011-1232) and Luso-Espanhola action E-61/12. M. The European Commission is also acknowledged through COST action ES1202 (Water 2020). M. Pijuan acknowledges the Ramon y Cajal Research fellowship (RYC-2009-04959) from the Spanish Government. We thank Dr. Mikkel Holmen Andersen (Unisense Environment, Denmark) for providing the sensors and helpful comments.

REFERENCES

Aboobakar, A., Cartmell, E., Stephenson, T., Jones, M., Vale, P., Dotro, G., 2013. Nitrous oxide emissions and dissolved oxygen profiling in a full-scale nitrifying activated sludge treatment plant. Water Res. 47, 524–34.

Ahn, J.H., Kim, S., Park, H., Rahm, B., Pagilla, K., Chandran, K., 2010. N2O emissions from activated sludge processes, 2008-2009: results of a national monitoring survey in the United States. Environ. Sci. Technol. 44, 4505–4511.

Blasing, T.J., 2009. Recent Greenhouse Gas Concentrations. [WWW Document]. URL http://digital.library.unt.edu/ark:/67531/metadc11963/

Daelman, M.R.J., De Baets, B., van Loosdrecht, M.C.M., Volcke, E.I.P., 2013. Influence of sampling strategies on the estimated nitrous oxide emission from wastewater treatment plants. Water Res. 47, 3120–3130.

Daelman, M.R.J., van Voorthuizen, E.M., van Dongen, L.G.J.M., Volcke, E.I.P., van Loosdrecht, M.C.M., 2013. Methane and nitrous oxide emissions from municipal wastewater treatment - results from a long-term study. Water Sci. Technol. 67, 2350–5.

Daelman, M.R.J., van Voorthuizen, E.M., van Dongen, U.G.J.M., Volcke, E.I.P., van Loosdrecht, M.C.M., 2015. Seasonal and diurnal variability of N2O emissions from a full-scale municipal wastewater treatment plant. Sci. Total Environ. 536, 1–11.

De Haas, D., Hartley, K., 2004. Greenhouse gas emission from BNR plants-do we have the right focus? In: Paper Presented at the Proceedings of EPA Workshop: Sewage Management, Risk Assessment & Triple Bottom Line. Cairns, Australia, 5-7 April 2004

Ferrell, R.T., Himmelblau, D.M., 1967. Diffusion coefficients of nitrogen and oxygen in water. J. Chem. Eng. Data 12, 111–115.

Foley, J., de Haas, D., Yuan, Z., Lant, P., 2010. Nitrous oxide generation in full-scale biological nutrient removal wastewater treatment plants. Water Res. 44, 831–44.

Gillot, S., Capela-Marsal, S., Roustan, M., Héduit, a., 2005. Predicting oxygen transfer of fine bubble diffused aeration systems - Model issued from dimensional analysis. Water Res. 39, 1379–1387.

IPCC, Stocker, T.F., Qin, D., Plattner, G.-K., Tignor, M.M.B., Allen, S.K., Boschung, J., Nauels, A., Xia, Y., Bex, V., Midgley, P.M., 2013. Climate Change 2013 - The Physical Science Basis, Intergovernmental Panel on Climate Change.

Jenni, S., Mohn, J., Emmenegger, L., Udert, K.M., 2012. Temperature dependence and interferences of NO and N_2O microelectrodes used in wastewater treatment. Environ. Sci. Technol. 46, 2257–66.

Kampschreur, M.J., Temmink, H., Kleerebezem, R., Jetten, M.S.M., van Loosdrecht, M.C.M., 2009. Nitrous oxide emission during wastewater treatment. Water Res. 43, 4093–103.

Law, Y., Ye, L., Pan, Y., Yuan, Z., 2012. Nitrous oxide emissions from wastewater treatment processes. Philos. Trans. R. Soc. B Biol. Sci. 367, 1265–1277.

Mampaey K.E., van Dongen U.G.J.M., van Loosdrecht M.C.M., Volcke E.I.P., 2015. Novel method for online monitoring of dissolved N2O concentrations based on gas phase measurements. Environmental Technology, 36(13), 1680-1690.

Metcalf & Eddy, I., 2003. Wastewater engineering: Treatment and Reuse, 4th ed, McGraw-Hill Education. New York.

Rodriguez-Caballero, a., Aymerich, I., Marques, R., Poch, M., Pijuan, M., 2015. Minimizing N2O emissions and carbon footprint on a full-scale activated sludge sequencing batch reactor. Water Res. 71, 1–10.

Rodriguez-caballero, A., Aymerich, I., Poch, M., Pijuan, M., 2014. Evaluation of process conditions triggering emissions of green-house gases from a biological wastewater treatment system. Sci. Total Environ. 493, 384–391.

Schulthess, R., Gujer, W., 1996. Release of nitrous oxide (N 2 O) from denitrifying activated sludge: Verification and application of a mathematical model. Water Res. 30, 521–530.

Stenstrom, M.K., Gilbert, R.G., 1981. Effects of alpha, beta and theta factor upon the design, specification and operation of aeration systems. Water Res. 15, 643–654.

Tamimi, A., Rinker, E.B., Sandall, O.C., 1994. Diffusion Coefficients for Hydrogen Sulfide, Carbon Dioxide, and Nitrous Oxide in Water over the Temperature Range 293-368 K. J. Chem. Eng. Data 39, 330.

Unisense, 2014. Nitrous Oxide Sensor User Manual. Unisense, Aarhus.

Van Hulle, S.W.H., Callens, J., Mampaey, K.E., van Loosdrecht, M.C.M., Volcke, E.I.P., 2012. O and NO emissions during autotrophic nitrogen removal in a granular sludge reactor – a simulation study. Environ. Technol. 1–10.

Ye, L., Ni, B.J., Law, Y., Byers, C., Yuan, Z., 2014. A novel methodology to quantify nitrous oxide emissions from full-scale wastewater treatment systems with surface aerators. Water Res. 48, 257–268.

5

METABOLISM AND ECOLOGICAL NICHE OF *TETRASPHAERA* AND *ACCUMULIBACTER* IN ENHANCED BIOLOGICAL PHOSPHORUS REMOVAL

SUMMARY: *Tetrasphaera* and *Candidatus* Accumulibacter are two abundant polyphosphate accumulating organisms in full-scale EBPR systems. However, little is known about the metabolic behaviour and ecological niche that each organism exhibits in mixed culture communities. In this study, an enriched culture of *Tetrasphaera* and *Ca.* Accumulibacter was obtained using casein hydrolysate as sole carbon source. This culture was able to achieve a high phosphorus removal efficiency (>99%), storing poly-p while consuming amino acids anaerobically. MAR-FISH confirmed that *Tetrasphaera* were responsible for amino acid consumption while *Ca.* Accumulibacter likely survived on fermentation products. *Tetrasphaera* performed the majority of the P removal in this culture, and batch tests showed that the metabolism of some carbon sources could actually lead to anaerobic P uptake through energy generated by fermentation of glucose and amino acids. This anaerobic P uptake may lead to lower net P release to C uptake ratios and reduce the P needed to be removed aerobically in WWTPs. Intracellular metabolites such as amino acids, sugars, VFAs and small amines were observed as storage products, which may serve as energy sources in the aerobic phase. The culture showed a preference towards the uptake of certain amino acids, while the intracellular amino acids that were accumulated during the anaerobic phase accounted for 20% of the total amino acids consumed. Evidence of the urea cycle was found, which could be involved in reducing the intracellular nitrogen content. This study improves our understanding of how phosphorus is removed in EBPR systems and can enable novel process optimisation strategies.

IN PREPARATION: Portions of this work will be submitted to international peer reviewed scientific journals, including: Marques, R., Santos, J., Nguyen, H., Carvalho, V., Carvalho, G., Freitas, E., Noronha, J. P., Nielsen, P. H., Reis, M. A. M., Oehmen, A., 2016. Metabolism and ecological niche of *Tetrasphaera* and *Accumulibacter* in enhanced biological phosphorus removal.

5.1 INTRODUCTION

The EBPR process is an efficient, relatively inexpensive and environmentally sustainable option for P removal in WWTP (Oehmen et al., 2007a). *Candidatus* Accumulibacter (hereafter *Accumulibacter*) is the most widely known polyphosphate accumulating organism (PAO), able to store large amounts of poly-P aerobically after taking up organic substrates anaerobically, unlike ordinary heterotrophic organisms. *Accumulibacter* PAOs take up VFAs anaerobically and store them as PHAs, with energy obtained from hydrolysis of intracellular poly-P and energy and reducing power from glycolysis of intracellular glycogen. In the subsequent aerobic or anoxic phase, PAOs degrade PHA as the energy source for orthophosphate (PO_4^{-3}-P) uptake and poly-P production, glycogen regeneration, biomass growth and cell maintenance. The phosphate removal is obtained through a higher P uptake in the aerobic phase as compared with the anaerobic P release, and through the removal of waste activated sludge containing high poly-P content.

Besides *Accumulibacter*, *Tetrasphaera*-related organisms are also putative PAOs present in a higher abundance than *Accumulibacter* in full-scale EBPR systems, up to 30% of the total biomass in EBPR plants in Denmark and Portugal (Kong et al., 2005; Lanham et al., 2013a; Nguyen et al., 2011). Nguyen et al., (2011) found that the genus *Tetrasphaera* is comprised of three clades. Clade 1 includes clones related to sequences of *T. elongata* and *T. duodecadis*, and clade 2 contains four isolated species: *T. jenkinsii*, *T. australiensis*, *T.veronensis* and the filamentous "*Candidatus Nostocoida limicola*", while clade 3 contains only sequences from uncultured clones. *Tetrasphaera*-related PAOs can take up P aerobically and store it intracellularly as poly-P, while assimilating different organic substrates (such as glucose and amino acids) under anaerobic conditions, as assessed through MAR-FISH of full-scale EBPR sludge (Kong et al., 2005; Nguyen et al., 2011). It has been shown that *Tetrasphaera*-related organisms cannot store PHAs, although some can take up acetate, and they can synthesize glycogen, are capable of fermenting glucose, and can express extracellular surface-associated amylases for degradation of starch (Kong et al., 2008; Kristiansen et al., 2013; Nguyen et al., 2011; Xia et al., 2008). Recently, Kristiansen et al., 2013) proposed a metabolic model based on glucose metabolism for members of the genus *Tetrasphaera* involved in EBPR systems. They suggested that under anaerobic conditions the *Tetrasphaera*-related organisms take up glucose and ferment it to succinate and other components. Furthermore, glycogen is produced as a storage

polymer and the energy required for these anabolic reactions is obtained from fermentation and poly-P degradation. Aerobically, the stored glycogen is degraded to provide carbon and energy for growth, P uptake and poly-P formation. Nguyen et al., (2015), using amino acids as carbon sources, showed that during the anaerobic phase glycine labelled was consumed and the majority was stored intracellularly as free glycine and fermentation products. In the subsequent aerobic phase, the stored glycine was consumed. The uptake of glycine took place along with the release of PO_4^{-3}-P while the oxidation of intracellular metabolites was linked with the uptake of P.

While some isolates within the *Tetrasphaera* genus are available, this is a rather broad group of organisms with a diverse metabolism that possesses metabolic differences on a species level. Due to the high diversity of *Tetrasphaera* typically found in EBPR plants (Nguyen et al., 2011), understanding their role in mixed cultures in the presence of other relevant organisms in WWTPs is of importance. The metabolism of *Accumulibacter* has been frequently studied using enriched cultures of microorganisms, although so far, no enriched cultures of *Tetrasphaera*-related PAOs have been reported. Little is known about the P removal efficiency of *Tetrasphaera*-related PAOs in EBPR systems, as compared to *Accumulibacter*, which is a key point when investigating the importance of *Tetrasphaera* for EBPR. Much remains to be learned regarding their metabolic behaviour, as it is difficult to distinguish their activity from *Accumulibacter*, particularly in full-scale systems where both PAO groups are present in comparatively low abundance. Furthermore, the potential synergy that may exist between *Tetrasphaera* and *Accumulibacter* has never before been studied. A better understanding of the ecophysiology of *Tetrasphaera* is needed to understand their function, and improve our understanding of the EBPR process and our ability to optimise it.

This study focuses on enriching *Tetrasphaera*-related PAOs from EBPR sludge, in order to investigate their metabolic transformations and their ability to metabolise different carbon sources. Tools such as MAR-FISH and energetic balances were used in order to differentiate the niche of *Tetrasphaera* and *Accumulibacter* in the enriched culture through a series of anaerobic-aerobic batch tests fed with either an amino acid, VFA or glucose. Since wastewater typically comprises a complex combination of these and other carbon sources, this work provides important insight into how P removal is achieved in EBPR WWTPs.

5.2 MATERIALS AND METHODS

5.2.1 SBR operation

A sequencing batch reactor (SBR) with 0.5 L working volume was inoculated with sludge from a WWTP in Setubal, Portugal. The SBR was operated with 8 h cycles, including an anaerobic phase (4 h), a settling/decant phase (1 h) and an aerobic phase (3 h). A synthetic medium containing sodium casein hydrolysate (Fluka, USA) (hereafter referred to as Cas aa) and yeast extract (Panreac, Spain) was fed during an acclimatisation period of 105 days. Thereafter, the yeast extract was removed from the feed, and the reactor operated for an additional 9 months period. During the first 3 h of the anaerobic phase, the SBR was fed continuously with 150 mL of synthetic carbon medium. It was also fed with 50 mL of mineral medium and 50 mL of phosphate medium (300 mg P/L) during the first 3 minutes in the beginning of the aerobic phase. The reactor was operated with a HRT (Hydraulic Retention Time) and SRT (Sludge Retention Time) of 16 h and 19 d, respectively. To maintain anaerobic conditions, argon was bubbled at an approximate flow rate of 0.2 mL/min, while during the aerobic phase, air was bubbled at an approximate flow rate of 0.5 L/min. Temperature was controlled at 20 $\pm$ 1 ºC and the pH was controlled at 7.1 $\pm$ 0.1 by automatic addition of HCl 0.1 M when the pH was above the set point. The stirring rate was kept constant at 300 rpm during the anaerobic and aerobic phases.

The reactor performance was assessed through biological and chemical analyses. SBR cycle studies were performed to analyse the carbon source, PHA, glycogen, ammonia and phosphate, where samples were taken every hour throughout a cycle and analysed via chemical analytical methods, and total suspended solids (TSS) and volatile suspended solids (VSS) were analysed at the end of the cycle to follow the cell concentration in the reactor (Section 5.2.4). Fluorescence *in situ* hybridisation (FISH) analysis was also performed to assess the microbial community dynamics (Section 5.2.5).

5.2.2 Batch test

Batch tests were performed in order to investigate the preferred carbon sources (acetate, propionate, glucose and amino acids) by the culture in the SBR. Three different types of experiments were carried out: 1) assessing the anaerobic uptake of each carbon source fed individually; 2) assessing the anaerobic/aerobic metabolism of

carbon sources fed individually (glucose and amino acids), or in combination (acetate, propionate and Cas aa); 3) assessing the capacity of the culture to anaerobically take up and store a mixture of amino acids.

Test 1: Seven anaerobic batch tests were carried out, one for each carbon source (acetate, propionate, glucose, glutamate, aspartate and glycine), as well as a blank without carbon feeding. Flasks with a working volume of 50 mL were inoculated with approximately 17 mL of sludge collected from the main SBR at the end of the cycle, plus 33 mL of mineral medium. Prior to feeding of the carbon source (5 mL), argon was bubbled to ensure anaerobic conditions and a sample of 5 mL was taken (Time 0). The stirring rate in all batch tests was 250 rpm, the room temperature was 21 ± 1 ºC, the pH of the culture media was 7.4 ± 0.1 and the pH of sludge before inoculation was 6.95. Samples were taken to analyse the carbon sources, phosphate, ammonia, poly-P concentration, as well as for FISH, TSS and VSS.

Test 2: Seven batch tests were performed following experimental conditions similar to the main SBR, operated with anaerobic and aerobic conditions, and with settling between both phases. Each test was seeded with 95 mL of sludge from the main SBR at the end of the cycle. The sludge used from the parent reactor at the end of the aerobic phase was centrifuged at 6000 rpm for 10 min and rinsed with mineral media without carbon source, with the procedure being repeated twice. The sludge was re-suspended with a final volume of 95 mL using mineral media. The culture media pH was adjusted to 7.0 prior to carbon addition.

- Four of the batch tests were performed with carbon sources added individually (glucose, glutamate, aspartate and glycine). The 95 mL of washed/re-suspended sludge was added to 355 mL of effluent from the main SBR. The cycle started with a pulse feed of each carbon source (50 mL, initial concentration of 2mM for glucose and each amino acid, respectively). Between the end of the anaerobic phase (4 h) and the beginning of the aerobic phase, the supernatant was totally removed. The biomass was re-suspended with 250 mL of effluent from the main SBR and 50 mL of mineral medium. A pulse addition of phosphate media (50 mL) was added at the beginning of the aerobic phase.
- An additional anaerobic/aerobic batch test was performed under similar conditions as those fed with individual carbon sources, where a combination of VFA and Cas aa was fed. The 95 mL of washed/re-suspended sludge was added to 255

mL of SBR effluent and 150 mL of synthetic medium containing acetate, propionate and casein hydrolysate.

- Two batch tests without carbon source feeding were operated for 7 h, one under anaerobic conditions and the other under aerobic conditions, to assess the processes used for maintenance energy generation. These tests were inoculated with 95 mL of washed/re-suspended sludge and 405 mL of effluent from the main SBR was added in the aerobic test. In the anaerobic test, the sludge was added to 155 mL of effluent, 50 mL of mineral medium and 50 mL of phosphate medium.

The anaerobic and aerobic conditions were maintained by bubbling continuously argon and air, respectively. The pH was controlled at 7.1 $\pm$ 0.1 by the addition of 1 M HCl and 0.1 M NaOH, and the room temperature was 22 $\pm$ 1ºC. Samples were taken to analyse the carbon sources, PHA, glycogen, phosphate, ammonia, poly-P concentration, as well as for FISH, MAR-FISH, TSS and VSS.

Test 3: A mixture of 22 amino acids (Arginine, Ornithine, Lysine, Glutamine, Citrulline, Asparagine, Alanine, Threonine, Glycine, Valine, Serine, Proline, Isoleucine, Leucine, Methionine, Histidine, Phenylalanine, Glutamic acid, Aspartic acid, Cysteine, Tyrosine and Tryptophan) were fed anaerobically in order to assess amino acid uptake and storage. The test was performed for 4h, and 200 mL of sludge from the main SBR was used to seed this batch test. The sludge was taken from the parent reactor at the end of the aerobic phase, centrifuged at 6000 rpm for 10 min and rinsed with mineral media without carbon source, with the procedure being repeat twice. The sludge was re-suspended to a volume of 200 mL using mineral media. Then, 100 mL of mineral media and 100 mL of phosphorus solution were added, while argon was bubbled to ensure anaerobic conditions. The culture media pH was adjusted to 7.0 prior to carbon source addition (100 mL). The pH was controlled at 7.1 $\pm$ 0.1 by the addition of 0.1 M HCl and 0.1 M NaOH, and the temperature was controlled by a water bath at 20 $\pm$ 1ºC. Samples were taken to analyse amino acids, VFAs, P, ammonia, poly-P concentration, glycogen, PHAs, FISH, TSS and VSS.

5.2.3 Culture media

The composition of the SBR culture media is described as follows: the synthetic carbon medium contained per litre 0.53 g Cas aa; the mineral medium contained per litre: 0.74 g NH_4Cl, 1.19 g $MgSO_4.7H_2O$ g, 0.55 g $CaCl_2.2H_2O$, 0.01 g N-Allylthiourea (ATU), 0.04 g ethylene-diaminetetraacetic (EDTA) and 3.96 mL of micronutrient solution. The micronutrient solution was based on Smolders et al., 1994a) and contained per litre: 1.5 g $FeCl_3.6H_2O$, 0.15 g H_3BO_3, 0.03 g $CuSO_4.5H_2O$, 0.18 g KI, 0.12 g $MnCl_2.4H_2O$, 0.06 g $Na_2MoO_4.2H_2O$, 0.12 g $ZnSO_4.7H_2O$ and 0.15 g $CoCl_2.6H_2O$. The phosphate medium contained 0.95 g K_2HPO_4 and 0.58 g KH_2PO_4 per litre. The synthetic carbon and mineral media, as well as the micronutrient solution were autoclaved, but prior to this, the pH was set to 7.4 $\pm$ 0.1 in the Cas aa and the mineral media. In the batch tests, the mineral and phosphate media had the same composition described for the SBR. For the batch tests with only one carbon source performed in flasks (1st test) and in reactors (2nd test), it was selected an initial concentration of 2 mM for each of the carbon sources (glucose, glutamate, aspartate and glycine). For the test with combination of carbon sources, it was selected an initial concentration in the reactor of 2.90 C-mM for each carbon source (acetate, propionate and casein hydrolysate). The mixture of 22 amino acids (Arginine, Ornithine, Lysine, Glutamine, Citruline, Asparagine, Alanine, Threonine, Glycine, Valine, Serine, Proline, Isoleucine, Leucine, Methionine, Histidine, Phenylalanine, Glutamic acid, Aspartic acid, Cysteine, Tyrosine and Tryptophan) had a final concentration of 22 C-mmol/L in the reactor equally divided by the number of amino acids present in the composition. In all carbon source media, the pH was set to 7.4 $\pm$ 0.1 by the addition of 1.0 M NaOH.

5.2.4 Chemical analyses

Inorganic phosphate and ammonia were analysed by segmented flow analysis (Skalar 5100, Skalar Analytical, The Netherlands). For Total P concentration, an acid digestion of a sample from the end of the aerobic period was performed with 0.3 M H_2SO_4 and 73 mg/L of $K_2S_2O_8$ and analysed using the segmented flow analyser. The poly-P content was determined by subtracting the supernatant phosphate concentration from the total phosphate concentration obtained by sample digestion. The VFAs concentration in the supernatant was determined by high-performance liquid chromatography (HPLC) using a Metacarb 87 H (Varian) column and a refractive index detector (RI-71, Merck). Sulphuric acid (0.005 M) was used as eluent at a flow rate of

0.6 mL/min and 50 ºC was the operating temperature. Glycogen was determined as described by Lanham et al., (2013), briefly, using a CarboPac PA10 column (Dionex), equipped with an amperometric detector. After digestion (2 mg biomass, HCl 0.9 M during 3 h) the analysis was performed at 30 ºC, with sodium hydroxide (NaOH 18 mM) as eluent, at a flow rate of 0.8 mL/min. PHA was determined by GC (gas chromatography) according to the methodology described by Lanham et al., (2013b), using a Bruker 430-GC gas chromatograph equipped with a FID detector and a BR-SWax column (60 m, 0.53 mm internal diameter, 1 mm film thickness, Bruker, USA). The casein hydrolysate uptake was assessed through the analysis of total organic carbon (TOC) by a Shimadzu TOC-VCSH (Shimadzu, Japan). Individual amino acids were quantified by HPLC with gold electrochemical detector (DIONEX ICS3000, USA) equipped with an Aminopac PA10 DIONEX 4x250 mm column, eluent NaOH/CH_3COONa ate a flow of 0,8 ml/min and 30ºC and 20µL of samples injected samples. GC-MS analysis was performed using an Agilent 6850 GC fitted with a 5975 VL MSD (Triple Axis Detector) Agilent mass spectrometric detector, with a DB-5MS 5% phenyl- and 95% dimethylpolysiloxane capillary column (30 m x 0.25 mm i.d., 0.25 µm film thickness) from Agilent and a helium flow of 1 mL/min. The injection port was operated in splitless mode, during 5 min. The injection port temperature was 250ºC. The ion source, the quadrupole and the transference line were kept at 230, 150 and 280ºC, respectively. The oven temperature was maintained at 70ºC for 1.3 min, programmed to 280ºC, at an increase of 12ºC/min, then increased to 315ºC at 25ºC/min, and held for 3.3 min. The MS spectrum was obtained with electron energy 70 eV, mass range *m/z* 40-800 and using MSD Chem Station software (Agilent). The identification of the metabolites was performed by the use of mass spectrum database libraries of NIST (2005) and Wiley (2005) that suggest possible chemical structures for metabolites, which were confirmed by the injection of the derivatised standards. The ChemStation library of the MS search uses a probability based matching (PBM) algorithm. For TSS and VSS at the end of each aerobic phase, standard methods were used (APHA, 2005).

Intracellular metabolites

To evaluate intracellular metabolite accumulation, samples were taken every hour along a typical SBR cycle. While the supernatant was analysed directly after filtration (0.20 µm), the internal amino acids present in the biomass was analysed after

cold ethanol quenching based on Börner et al., (2007) and Spura et al., (2009) by High-performance liquid chromatography (HPLC) and Gas chromatography–mass spectrometry (GC-MS).

Briefly: 5 mL samples were centrifuged during 5 min at 3940 x g (4 ºC), the supernatant was then removed, filtered (0.20 µm) and stored (-20ºC) for amino acids analysis. Biomass was washed twice with cold NaCl (8%, 4ºC) and centrifuged during 5 min at 3940 x g (4ºC) and the supernatant removed. An ethanol solution (ethanol-sodium chloride solution 0.8% W/V, -20 ºC) was used to re-suspend the cells 40% (V/V) and was stored for 30 min at -20 ºC, which was followed by centrifugation during 10 min at 3940 x g and the supernatant removed. A volume of 1.5 mL of ethanol solution (1.5 mL Ethanol + 60 µL ethanol + 60µL ribitol (0.2 mg/mL)) was added and mixed by inversion and immersed in an ultrasonic bath during 15 min at 70 ºC, then put on ice for 2 min, and 1.5 mL of MilliQ water was added and mixed. 1 mL of chloroform (total volume 4 mL) was then added and mixed with a vortex. The mixture was centrifuged during 10 min at 3940 x g (4 ºC) to achieve phase separation with the polar phase transferred to a vial for GC-MS and HPLC analysis of the intracellular metabolites in the cells. 1 mL of the polar phase was added to a conical shaped vial, and dried with low nitrogen gas flow. The same procedure was applied for HPLC amino acids quantification, except sample drying low nitrogen gas flow. 25 µL of methoxyamine hydrochloride solution (20 mg/mL in pyridine) was added to the dried sample, and digested at 35 ºC for 125 min. Then 32 µL of BSTFA (Aldrich, USA) was added and the sample was incubated for 125 min at 35 ºC.

5.2.5 Microbial characterisation and MAR-FISH

FISH was performed at the end of the anaerobic and aerobic phases using the following oligonucleotide probes: EUBMIX (equimolar concentrations of EUB338, EUB338II, and EUB338III, see (Amann et al., 1990; Daims et al., 1999)) that target all *Bacteria*; PAOMIX (PAO651, PAO462 and PAO846, see (Crocetti et al., 2000)) that target most members of the *Accumulibacter* cluster; and Tet1-266, Tet2-892, Tet2-174 and Tet3-654 that target most *Tetrasphaera*-related PAOs (Nguyen et al., 2011). GAOmix (GAOQ431, GAOQ989 and GB_G2) targeting *Competibacter* GAOs (Crocetti et al., 2000; Kong et al., 2002); DEF1mix (TFO_DF218 and TFO_DF618) targeting *Defluviicoccus vanus*-related GAOs cluster I (Wong et al., 2004); DEF2mix (DF988 and DF1020) targeting *D. vanus*-related GAOs cluster II (Meyer et al., 2006); DF1013 and

DF1004 targeting phylotypes within cluster III *Defluviicoccus* (Nittami et al., 2009) and indicated as putative GAOs (McIlroy et al., 2010), were also assessed (Appendix C, Table C1). FISH samples were observed using an Olympus BX51 epifluorescence microscope. FISH quantification was performed by image analysis taken with a Zeiss LSM 710 confocal laser scanning microscope. The biomass quantification was obtained as the area covered by the specific probe divided by the area covered by EUBmix. Standard error of the mean was obtained as the standard deviation divided by the square root of the number of images (20 in each quantification). MAR-FISH was also used to investigate the substrate uptake of probe-defined members of *Tetrasphaera* and *Accumulibacter*, following the methodology applied in Nguyen et al. (2011). Briefly, fifteen 9-mL serum bottles containing 2 mL sludge samples from the SBR were incubated 1 h anaerobically. 10 μCi per 2 mL of labelled and non-labelled substrates (glucose, glutamic acid, aspartate, glycine and control-pasteurized: 4 serum bottles for each substrate and 1 for control), to get a final concentration of 2 mM, were added and incubated anaerobically for 3 h. The samples were homogenised by rubbing two gelatine-coated cover glass slides against each other with a 30-μL sample in between, allowed to dry, and hybridised with oligonucleotide probes labelled with fluorescent dyes (Cy3 and FLUOS). Hybridisation was carried out at 46ºC for 1.5 h. The cover glasses were carefully dipped in pre-warmed (42 ºC) LM-1 emulsion (Amersham Bioscience) and exposed at 4 ºC for 3 days; this was followed by development (0.5 to 4 min) in a Kodak L-19 developer. Microscopic examinations of MAR-FISH samples were performed with an epifluorescence microscope (Axioskop 2 Plus; Zeiss) equipped with a charge-couple device camera (CoolSNAP HQ; Photometrics, Oberkochen, Germany).

5.2.6 Mass and energy balances

Contribution of *Accumulibacter* and Tetrasphaera towards P-uptake

The contribution of *Accumulibacter* or *Tetrasphaera* towards aerobic P-uptake was calculated during SBR operation by first calculating the yield of PHA utilisation for Poly-P formation by *Accumulibacter* according to the model of Lopez-Vazquez et al. (2009), where the remaining P taken up was linked to *Tetrasphaera* activity (Appendix C, Table C2). The model developed by Lopez-Vazquez et al. (2009) was chosen due to the presence of a high polyhydroxyvalerate (PHV) content in the biomass, where the

aerobic PAO model of Smolders et al., (1994a) describes only polyhydroxybutyrate (PHB) utilisation.

Glucose and amino acid fermentation

Adenosine triphosphate molecule (ATP) energy balances were performed for the 2nd batch test during the anaerobic phase fed with glucose, glutamate, aspartate and glycine. For the glucose test, the balances were based on the metabolism described by Kristiansen et al., (2013), where glucose uptake and P-release produce the ATP that is used for glycogen formation and anaerobic maintenance. Since P uptake was observed instead of P release, the glucose uptake was considered to be the only energy source responsible for ATP formation in the ATP balance. As described in the model of Kristiansen et al., (2013), glucose is fermented to acetate, where the amount that is converted is obtained by the difference of the total glucose uptake minus the glucose converted to glycogen. The ATP coefficients used in this balance are described in Table C3 of the Appendix C. Glucose uptake, P-uptake, glycogen utilization and anaerobic cell maintenance were obtained using rates calculated from the experimental data. Glutamate, aspartate and glycine degradation by *Tetrasphaera* has not yet been described by metabolic models. However, these amino acids can also be fermented to different organic acids, obtaining ATP. Acetate was assumed to be the end product of amino acids fermentation for the purposes of energy balances. Glutamate can be degraded as the sole carbon source through a pathway generating acetate directly, or involving the formation of pyruvate that is then converted to acetate. The overall reaction for this pathway involves the production of 2 moles of ATP per mole of glutamate consumed (Equation 5.1) (Ramsay, 1997). Aspartate can be degraded by a Stickland reaction or through uncoupled reactions. It can be degraded through pyruvate, generating acetate as the final product, or to alanine firstly and then to pyruvate and acetate. The overall equation leads to a production of 2 moles of ATP per mole of aspartate (Equation 5.2) (Brock et al., 2012; Ramsay, 1997). As a simple amino acid, glycine can be degraded by a Strickland reaction or can be fermented as the only carbon source. The overall reaction of glycine can either generate ¼ ATP mol per mol of glycine, or zero ATP (Equation 5.3) (Lebertz and Andreesen, 1988; Ramsay, 1997). The more energetically favourable pathway was chosen for glycine degradation in the energy balances performed in this study. Glycogen can be formed through the TCA cycle by gluconeogenesis, where all 4 clades of *Tetraphaera*-related PAOs are

able to perform gluconeogenesis, according to Kristiansen et al., (2013). The gluconeogenesis pathway varies according to the type of amino acid (Harvey and Ferrier, 2011). Glutamate can be enzymatically converted by *Glutamate dehydrogenase* to α-ketoglutarate by oxidative deamination. α-ketoglutarate is converted to oxaloacetate through the TCA cycle. Oxaloacetate can be further converted to phosphoenolpyruvate by the *Phosphoenolpyruvate carboxykinase* enzyme. Phosphoenolpyruvate is further converted to glyceraldehyde 3-phosphate that can easily be isomerised to dihydroxy-acetone-P. Glyceraldehyde 3-phosphate can combine with dihydroxy-acetone-P to form Fructose 1,6-bis-P by the enzyme *Fructose bisphosphate aldose*. A final isomerization to Glucose 6-phosphate is achieved. Glucose 6-phosphate is then converted by a *hexokinase* to glycogen as the final product. A consumption of 1 ATP mol per mol of glutamate is needed for glycogen production (Harvey and Ferrier, 2011). Aspartate is primarily converted to oxaloacetate by enzymatic transaminase. The following conversion to glycogen follows the previously described pathway for glutamate. A consumption of 2 ATP is needed to achieve this conversion (Harvey and Ferrier, 2011).

$$(Asparate)C_5H_9O_4N + 2H_2O \rightarrow 2C_2H_4O_2(Acetate) + NH_3 + CO_2 + H_2 + 2ATP \quad (5.1)$$

$$(Glutamate)C_4H_7O_4N + 2H_2O \rightarrow C_2H_4O_2(Acetate) + NH_3 + 2CO_2 + 2H_2 + 2ATP \quad (5.2)$$

$$(Glycine)C_2H_5O_2N + \frac{1}{2}H_2O \rightarrow \frac{3}{4}C_2H_4O_2(Acetate) + NH_3 + \frac{1}{2}CO_2 + \frac{1}{4}ATP \quad (5.3)$$

5.3 RESULTS AND DISCUSSION

5.3.1 SBR performance and microbial composition

Both PAO groups, *Tetrasphaera*-related PAOs and *Accumulibacter*, were identified by FISH in the enriched culture as shown in Figure 5.1 and Table 5.1. None of the GAOs were detected. The culture was mainly constituted by *Tetrasphaera*, comprising a volume fraction of over 60% of the total microbial community (Table 5.1).

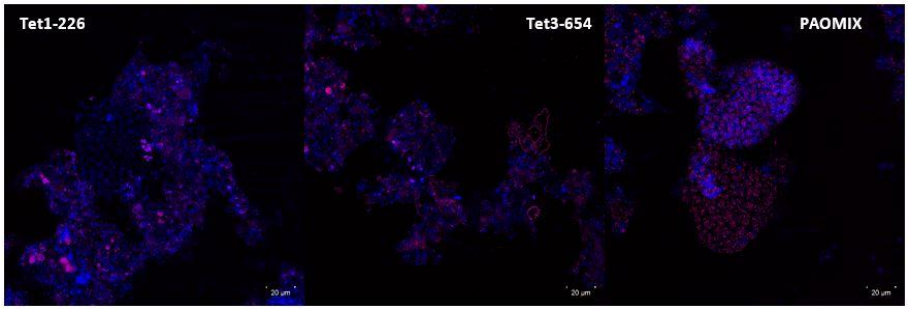

Figure 5.1 – FISH images of the dominant PAOs in SBR sludge. Bacteria targeted by Tet1-226, Tet3-654 and PAOMIX are in magenta, whereas the remaining Bacteria are in blue. The sample was taken on Day 233 after inoculation.

Accumulibacter was also detected in this culture, with an average volume fraction close to 20%. During the SBR operation, cycle studies were performed to evaluate reactor performance and to ensure steady state operation was achieved, before the batch tests with different carbon sources were performed. Cas aa was taken up during the slow feeding period of the anaerobic phase, which was accompanied by P release and glycogen hydrolysis (Figure 5.2a). In the subsequent aerobic phase, the culture was able to replenish their poly-p and glycogen pools. A very low PHA production, and consequently, consumption, was detected in the anaerobic and aerobic phases, respectively. PHV was the major PHA fraction produced (Appendix C, Figure C1). A high P removal efficiency was maintained in the SBR (>99%). This mixed culture also showed a high intracellular P content, accounting between 8-19% of the TSS concentration.

Table 5.1 – Different morphologies observed by FISH in the SBR sludge and % of volume fraction of each *Tetraphaera*-related PAOs clade and *Accumulibacter*. Results shown are an average of 3 samples taken during the experimental period.

Probe	Morphology	%vol. fraction
Tet1-266	Branched rods, short rods, clusters of tetrads, thin filaments and irregular cocci	38.5±1.4
Tet2-892	Clusters of tetrads, filaments, short rods, small cocci	<1
Tet2-174	Small cocci and irregular cocci	<1
Tet3-654	Branched rods, short rods in clusters, irregular cocci, thin filaments	31.0±4.3
PAOMIX	Rods and coccobacilli in clusters	21.7±8.8
GAOMIX		NT

NT – not detected

Upon comparing the results from this *Tetrasphaera*-enriched culture with typical *Accumulibacter* behaviour, the culture displayed comparable levels of intracellular P, glycogen degradation and P release, while much lower PHA production was found (Table 5.2). This agrees with previous studies, which refer that most *Tetrasphaera*-related PAOs are not able to produce and oxidise PHA, except in filamentous species and *Tetrasphaera japonica* (Kristiansen et al., 2013; McKenzie et al., 2006). Contrarily

to what Kristiansen et al., (2013) observed in their studies, in this study glycogen is degraded anaerobically and regenerated aerobically. This contrast is likely due to the fact that glucose, instead of Cas aa, was fed to *Tetrasphaera elongata* Kristiansen et al. (2013). Since the ratios of P release and glycogen hydrolysis per carbon mol of substrate uptake was very similar to the *Accumulibacter* ratios, this suggests that the energy required for substrate uptake comes mainly from the cleavage of poly-P and release of phosphate from the cell. If this energy were to be mainly generated from glycogen hydrolysis, the glycogen to substrate ratio would be higher, as in the case of GAOs (Zeng et al., 2003b). Furthermore, methylene blue staining was employed to confirm the anaerobic/aerobic cycling of stored poly-P. More poly-P was stored in the end of the aerobic phase than in the anaerobic phase (data not shown). Aerobically, this mixed culture was able to take up P and produce poly-P as shown by the data in (Table 5.2), wherein the percentage of P per TSS was very similar to *Accumulibacter*-enriched cultures.

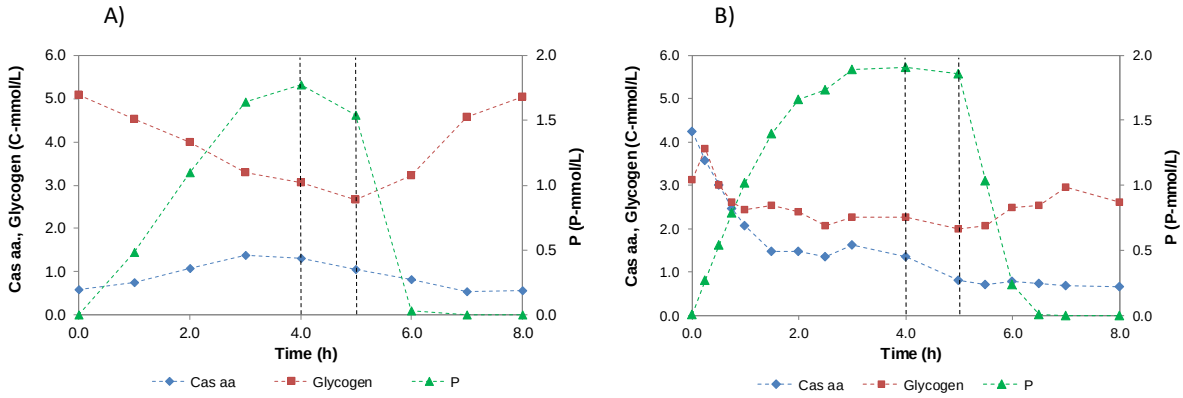

Figure 5.2 – Typical cycle study during SBR operation with continuous feed (A) and with pulse-feed (B). Between the dashed lines, the settling and decant phases occurred.

Different morphologies of *Tetrasphaera*-related PAOs were observed, matching the diversity of morphotypes observed by Nguyen et al., (2011), which correspond to different *Tetrasphaera* populations (see Table 5.2, note that not all of these morphologies are visible in Figure 5.2). The *Tetrasphaera* population was mainly constituted by 2 clades, detected by probes Tet1-266 and Tet3-654 (Table 5.1). Clade 2 of the *Tetrasphaera*-related PAOs was only present in low abundance in this study. A study in the same WWTP (Setubal) used for the SBR inoculation by Lanham et al., (2013a) showed the presence of clade 2 in this plant, suggesting that the reactor operational conditions were not conducive towards their enrichment. Nguyen et al.,

(2011) showed that not all morphological groups within clade 2 *Tetrasphaera* could take up casamino acids. Another study performed by Muszyński and Miłobędzka, (2015) detected clade 2 in aerobic granular sludge, mostly Tet2-892, when feeding acetate and with a low COD:P ratio (10). Since in this study, a low COD:P (close to 5) was used and only Cas aa was fed, the few organic substrates might be produced via fermentation by *Tetrasphaera*. *Accumulibacter* have been suggested to be more competitive for acetate uptake as compared to *Tetrasphaera*-related PAOs (Nguyen et al., 2011), which would imply that clade 2 of *Tetrasphaera* may have been outcompeted. Also, clade 1 of *Tetrasphaera*-related PAOs were reported to not take up acetate, while clade 3 covers a wide range of bacteria and only a fraction can take up acetate (Nguyen et al., 2011), being more competitive for casamino acids, glutamic acid and glucose. This might explain the natural selection of clades 1 and 3 in this SBR.

Table 5.2 – Anaerobic/aerobic activity from a typical cycle study during SBR operation, and comparison with literature from studies with *Accumulibacter* fed with acetate and propionate.

Anaerobic results			
	Accumulibacter + *Tetrasphaera* (this study)	*Accumulibacter*	
Carbon source	Casein hydrolysate	Acetate	Propionate
P release/substrate uptake (P-mol/C-mol)	0.35±0.08	0.48[a]	0.40[b]
Glycogen cons./substrate uptake (C-mol/C-mol)	0.38±0.12	0.50[a]	0.33[b]
PHB prod./substrate uptake (C-mol/C-mol)	0.03±0.01	1.33[a]	0.00[b]
PHV prod./substrate uptake (C-mol/C-mol)	0.09±0.02	0.00[a]	0.56[b]
PH2MV prod./substrate uptake (C-mol/C-mol)	0.03±0.01	0.00[a]	0.67[b]
PHA prod./substrate uptake (C-mol/C-mol)	0.15±0.04	1.33[a]	1.23[b]
Anaerobic pH	6.7±0.1	7	7
Aerobic results			
P uptake (Pmmol/L)	1.76 ±0.25	2.50[c]	2.20[c]
% P in TSS	8-19	7-17[d]	7-17[d]
Glycogen Production (C-mmol/L)	1.38±0.70	3.62[e]	3.78[f]
PHA Consumption (C-mol/L)	0.75±0.24	7.60[c]	5.10[c]
PHA Oxidation/P (C-mol/P-mmol)	0.44±0.17	3.00[c]	2.30[c]

[a] (Smolders et al., 1994a); [b] (Oehmen et al., 2005a); [c] (Oehmen et al., 2005b); [d](Oehmen et al., 2007a); [e] (Smolders et al., 1994b) and [f] .(Oehmen et al., 2007b)

Contribution of *Accumulibacter* and Tetrasphaera towards P uptake

Since these two different PAO groups were both present in the culture, it was necessary to estimate the contribution of each group towards P-uptake. For this purpose, metabolic model predictions of *Accumulibacter* metabolism were firstly used to estimate its contribution towards P uptake (Lopez-Vazquez et al., 2009). With PHAs being a divergent factor between *Accumulibacter* and *Tetrasphaera*, PHA synthesis and oxidation was assumed to be only performed by *Accumulibacter* during the anaerobic and aerobic phase, respectively, in the SBR. This assumption is validated by previous findings showing that *Tetrasphaera*-related PAOs are not able to produce PHAs (Kristiansen et al., 2013; Nguyen et al., 2011). Also, no GAOs were detected in this culture, further supporting this assumption. An average P uptake per PHA utilisation yield in the SBR of 3.94±0.01 P-mol Poly-P/C-mol PHA was calculated according to the SBR data shown in Table C2 of the Appendix C. This value agrees very well with the yield obtained by Smolders et al., (1994a) assuming only PHB utilisation (3.6 g P-mol Poly-P/C-mol PHA) and shows that different PHA compositions have only a small impact on this yield coefficient. Assuming all PHA (0.75±0.24 C-mol/L, Table 5.2) is consumed by *Accumulibacter* for P uptake, an average of 2.95±0.18 P-mmol/L of the Poly-P stored during the aerobic phase can be directly associated with the activity of the *Accumulibacter* present in the culture, which corresponds to approximately 35.1 % of the total Poly-P formed by this culture. This agrees very well with the weighted average abundance of *Accumulibacter* per total PAO (i.e. *Tetrasphaera* + *Accumulibacter*) present in the culture of 23.8 %, as quantified by FISH (Table 5.1). In this way, it can be concluded that the *Tetrasphaera*-related PAOs are the main group responsible for P removal in this culture when fed with Cas aa. This result is of significance since close to 30% of the COD in domestic wastewater influents are composed of proteins and amino acids (Nielsen et al., 2010). These results suggest that *Tetrasphaera*-related PAOs can contribute substantially towards P-removal in EBPR plants.

5.3.2 Understanding the metabolism of *Tetrasphaera* with different carbon sources

Individually carbon sources feeding

Tetrasphaera has been found to take up different carbon sources as compared to *Accumulibacter*. In order to understand the influence of carbon source on the metabolism of each group and its contribution towards P-removal, various batch tests were performed with a view to differentiate the niche of each group of PAOs. Batch tests were performed with sludge from the main SBR and one of the following carbon sources: glucose, acetate, propionate, glutamate, aspartate and glycine.

Acetate and propionate batch tests led to anaerobic carbon consumption and P release (Figure 5.3). As expected, anaerobic glycogen consumption was observed during propionate and acetate uptake (Figure 5.3). Also, the obtained P-release and PHA production ratios are comparable with those typical of *Accumulibacter* cultures fed with acetate and propionate, respectively (Table 5.3). PHB was the fraction most produced when acetate was fed as sole carbon source, and PHV and polyhydroxy-2-methylvalerate (PH2MV) were the most produced when propionate was fed as sole carbon source (Table 5.3, Appendix C Figure C2), which is also consistent with the metabolic models for *Accumulibacter*. Moreover, the maximum specific acetate and propionate uptake rates were observed to be 0.040 and 0.068 C-mol/(C-mol·h), respectively, which are substantially lower than those observed for *Accumulibacter* enriched cultures. Lopez-Vazquez et al., (2009) estimated these maximum uptake rates as 0.2 C-mol/(C-mol·h) each, meaning that the maximum acetate uptake rate was approximately 20% of that observed for *Accumulibacter* and the maximum propionate uptake rate was 34%. This was once again within the range of activity expectable from the *Accumulibacter* that existed in the culture. Therefore, the results suggest that the percentage of *Accumulibacter* present in this culture was mainly responsible for acetate and propionate uptake, due to the relative VFA uptake rates, where *Tetrasphaera* have been suggested to be less competitive for these substrates. Moreover, the PHA production was similar as compared to that which would be expected for *Accumulibacter* cultures, and *Tetrasphaera* are not capable of PHA production.

Regarding the other carbon sources tested, glucose, glutamate, aspartate and glycine consumption anaerobically led to either a negligible or very small level of anaerobic P-release (Table 5.3). The P release in the glycine and aspartate

experiments was not directly linked with carbon uptake, since it occurred after carbon was fully consumed, suggesting that this P release was linked with energy generation for cell maintenance. While glutamate led to a small P-release and uptake in the same anaerobic phase, no change in the phosphorus was linked with glucose uptake (Figure 5.3). Very low PHA formation was obtained with these carbon sources, agreeing with the SBR cycles when Cas aa was fed (Appendix C, Figure C2). Interestingly, while glycine consumption was associated with glycogen consumption, aspartate, glutamate and glucose led to glycogen production (Table 5.3, Appendix C Figure C2). These results suggest that *Tetrasphaera*-related PAOs were mainly responsible for taking up these four carbon sources. Indeed, previous studies have demonstrated the capacity of *Tetrasphaera* isolates to take up glucose, glutamate, glycine and aspartate, while *Accumulibacter* are not able to metabolise these carbon sources (Kristiansen et al., 2013; Nguyen et al., 2015). The profiles obtained when feeding these different carbon sources raised two main questions: 1) Could *Tetraphaera*-related PAOs be confirmed as the main organisms involved in the consumption of amino acids and glucose?; 2) Was P-release needed to generate energy for amino acid and glucose uptake? To clarify these issues, a second set of tests was performed with these carbon sources, using tools such as MAR-FISH and energetic balances to examine their metabolism in greater depth.

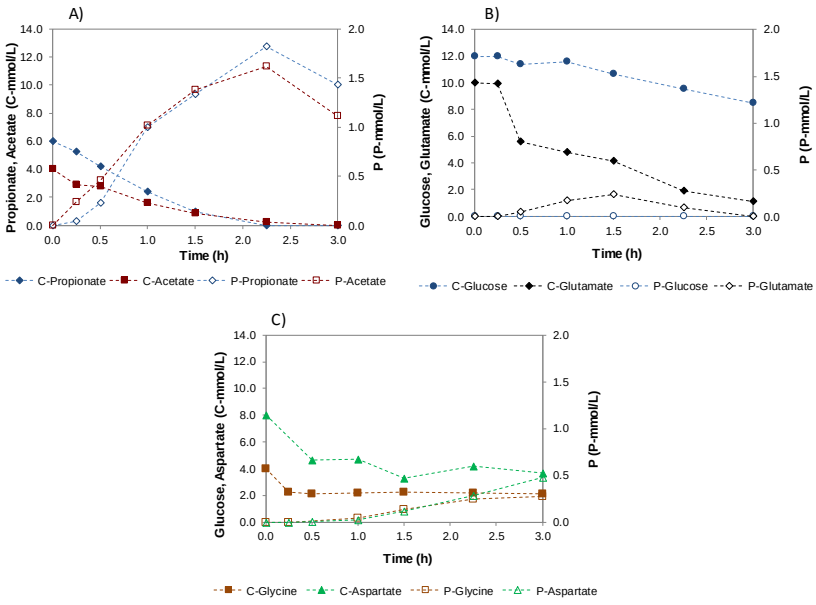

Figure 5.3 – Comparison of carbon source and P profiles under anaerobic conditions for the 1st batch experiments performed with different carbon sources of acetate, propionate, glucose, glutamate, aspartate and glycine: acetate and propionate (A); glucose and glutamate (B); glycine and aspartate (C). Carbon profiles are represented as C-carbon, while P profiles are represented as P-carbon. Glycogen and PHA profiles observed during these tests are shown in Figure C2 of the Appendix C.

The second set of experiments was performed by replicating a full SBR cycle study, with an anaerobic followed by an aerobic phase, to fully characterise the metabolism observed with each carbon source. In parallel, MAR-FISH was used to clarify the PAO, *Accumulibacter* or *Tetrasphaera*, responsible for taking up the carbon sources that were tested. The MAR-FISH results confirmed that glucose and amino acids (aspartate, glutamate and glycine) were mainly taken by *Tetrasphaera*-related PAOs. The *Tetrasphaera* clades dominant in this culture, clade 1 and 3, showed that more than 90% of the cells were capable of taking up the tested substrates. Meanwhile, *Accumulibacter* showed a negative signal for glucose and amino acids uptake, except for a low positive signal for glutamate. This supports the idea that in this culture, *Tetrasphaera* were mainly responsible for amino acid fermentation, while *Accumulibacter* were likely surviving on fermentation products (Table 5.4, Appendix C Figures C3-C6).

Table 5.3 – Comparison of anaerobic biochemical transformations between batch experiments and metabolic models of *Accumulibacter*.

	Parameter	*Accumulibacter + Tetrasphaera* (this study)							*Accumulibacter*	
		Acetate	Propionate	Glucose	Aspartate	Glutamate	Glycine	No Carbon	Acetate	Propionate
1st Batch Tests	PHB production (C-mmol/C-mmol substrate)	1.38	0.02	0.00	0.04	0.01	0.02	0.00	1.33[a]	0.00[b]
	PHV production (C-mmol/C-mmol substrate)	0.15	0.74	0.00	0.17	0.08	0.09	0.00	0.00[a]	0.56[b]
	PH2MV production (C-mmol/C-mmol substrate)	0.00	0.71	0.00	0.03	0.02	0.01	0.00	0.00[a]	0.67[b]
	PHA production (C-mmol/C-mmol substrate)	1.53	1.47	0.00	0.25	0.11	0.12	0.00	1.33[a]	1.23[b]
	Glycogen consumption (C-mmol/C-mmol substrate)	0.13	0.31	-0.34	-0.24	-0.06	0.56	-0.34	0.50[a]	0.33[b]
	P release (P mmol/C-mmol substrate)	0.40	0.30	0.00	0.01	0.04	0.00	0.00	0.48[a]	0.40[b]

[a] (Smolders et al., 1994a); [b] (Oehmen et al., 2005a); [c] (Oehmen et al., 2005b); [d](Oehmen et al., 2007a); [e] (Smolders et al., 1994b) and [f].(Oehmen et al., 2007b)

In the anaerobic/aerobic batch tests (Figure 5.4), the consumption of glucose, aspartate, glutamate and glycine was accompanied by anaerobic P-uptake instead of the expected P-release. Anaerobic P-uptake was most evident with glucose as carbon source, where 18.5 mgP/L of removal was observed. Glycine, aspartate and glutamate fermentation led to an average P-uptake of 9.02 ± 2.06 mg-P/L. Considering that a typical concentration of P in wastewater influents is about 7-10 mg-P/L, these results show that the anaerobic P uptake achieved by some sugars and amino acids can be significant. As in the first tests, glucose, aspartate and glutamate led to glycogen

production in the anaerobic phase (Appendix C Figure C7), while in the glycine test, glycogen was consumed. Overall, the results suggest that anaerobically, *Tetrasphaera* were able to take up P through energy generated by fermentation of the carbon sources (glucose, aspartate, glycine and glutamate), avoiding the need to release P for energy generation.

Table 5.4 – *Accumulibacter* (PAOMIX) and *Tetrasphaera* (Tet1-266, Tet2-892, Tet2-174 and Tet3-654) MAR-FISH result summary from anaerobic incubation with different substrates (Yes: > 90% of cells can take up substrate; No: cells could not take up substrate).

Probes	Glucose	Glutamate	Aspartate	Glycine
PAOMIX	No	< 10% positive	No	No
Tet1-266	Yes	Yes	Yes	Yes
Tet2-892	Yes	< 10% positive	No	< 50% positive
Tet2-174	Yes	Yes	Yes	Yes
Tet3-654	Yes	Yes	Yes	Yes

To investigate this hypothesis further, energy balances were performed for the anaerobic phase in the batch tests fed with each carbon source (glucose, aspartate, glutamate and glycine), as described in section 5.2.6. Energy was assumed to be generated by carbon fermentation, while P-uptake, gluconeogenesis and anaerobic cell maintenance were the processes requiring ATP consumption (Table 5.5). Energy generated by fermentation could account for the energetic demands for P-uptake, glycogen production and anaerobic maintenance within 90.9 and 90.7% for glucose and aspartate carbon sources, respectively. In the glutamate test, glycolysis was observed instead of gluconeogenesis, contributing therefore to energy production in this case. The energy produced via glycolysis and fermentation could account for 85% of the energy required for P uptake and maintenance in the case of glutamate (Table 5.5). Thus, the energy balance could describe quite well the metabolism of the culture with these 3 substrates, as it closed within 89 ± 3%, suggesting that the main processes leading to ATP generation and consumption within the cells were taken into account. The glycine test, however, showed that the energy generated due to glycine fermentation and glycogen consumption accounted for only 34% of the energetic demands for P uptake and cell maintenance (Table 5.5). Indeed, glycine is a less favourable amino acid energetically and Nguyen et al., (2015) reported that *Tetrasphaera*-related PAOs are able to take up glycine and store it as free intracellular glycine. The imbalance between energy generation and consumption in this test suggests that other internal metabolites besides glycogen could be used to generate the necessary ATP for P-uptake and maintenance in this case.

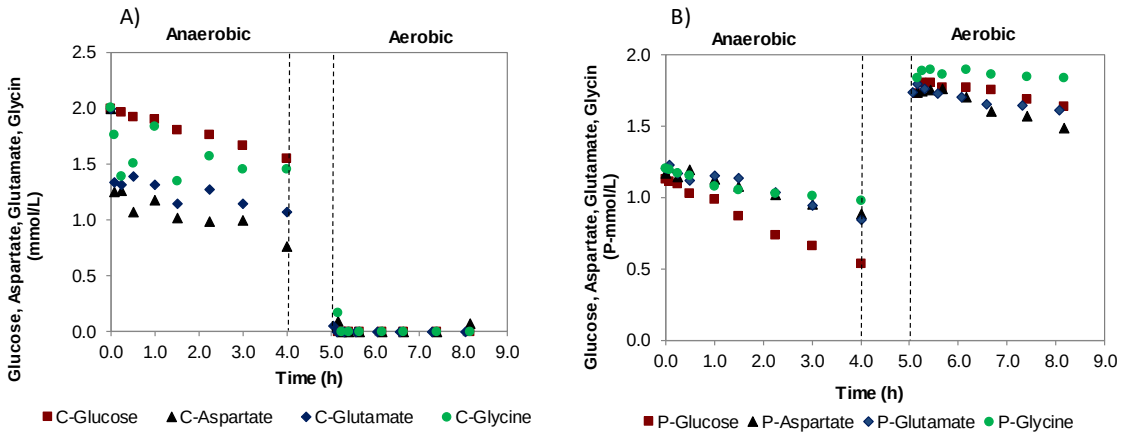

Figure 5.4 – Comparison of carbon source and P profiles for the 2nd batch experiments performed with different carbon sources (glucose, glutamate, aspartate and glycine): Carbon (A). Phosphorus (B); Glycogen and PHA from are shown in Figure 7 of the supplemental information.

In the following aerobic phase, the average P-uptake of each test was lower than that achieved in the previous anaerobic phase (3.61 ± 3.17 mg/L). The aerobic PHA consumption was negligible with each carbon source tested. Glycogen consumption observed in the aerobic phase was also small (0.45 ± 0.75 C-mmol/L). The low P uptake in the aerobic phase suggests that the cells depleted most of the energy produced by substrate fermentation during anaerobic P uptake and did not store a high quantity of each carbon source for subsequent aerobic P-uptake.

Table 5.5 – Energy balances for the 2nd experiment in the anaerobic phase with glucose, aspartate, glucose, aspartate, glutamate and glycine as carbon sources.

Carbon	Fermentation (ATP mol/L)	P-uptake (ATP mol/L)	Gluconeogenesis (ATP mol/L)	Maintenance (ATP mol/L)	ATP balance (produced/consumed)
Glucose	1.40	0.61	0.18	0.75	0.91
Aspartate	1.15	0.33	0.19	0.76	0.91
Glutamate	1.36	0.35	-0.11*	1.38	0.85
Glycine	0.13	0.23	-0.26*	0.93	0.34

*Glycolysis, not gluconeogenesis, was observed

It is noteworthy that when a mixture of amino acids was fed to the SBR (Figure 5.2), net P release was observed, but individual amino acid or glucose substrates led to anaerobic P uptake. Some possible explanations for this effect include, 1) fermentation of some amino acids not included in the individual tests require additional energy from P release in order to be metabolised and stored as carbon compounds that are later used for aerobic P uptake, 2) fermentation of multiple amino acids require

additional energy in order to activate the combination of enzymatic systems necessary for their simultaneous uptake, and 3) fermentation products such as acetate and propionate that are produced from amino acid or sugar fermentation by *Tetrasphaera* are taken up by *Accumulibacter*, which requires P release for carbon uptake, resulting in a net P-release. It is of interest that the metabolism of some carbon sources can actually lead to anaerobic P uptake through energy generated by fermentation of glucose and/or amino acids. This anaerobic P uptake may lead to lower net P-release to C-uptake ratios in WWTPs and reduce the P needed to be removed aerobically, representing a new P removal mechanism that has not previously been accounted for in EBPR systems.

Simultaneous feeding of amino acids and VFAs

To simulate a more complex carbon source composition, closer to that present in wastewater, a mixture of VFAs (propionate and acetate) with Cas aa was used to evaluate the substrate preferences and metabolism within the culture in an anaerobic/aerobic batch test (Figure 5.5).

Propionate was completely taken up by the culture, while 88% of the acetate and 64% of the Cas aa were consumed in this test. The uptake rate of acetate increased after propionate depletion, showing that propionate was preferred over acetate by the culture, which is consistent with the higher uptake rate of propionate over acetate when each was fed individually in the first tests. Anaerobic P-release was followed by aerobic P-uptake in this test (Figure 5.5). Anaerobic PHA production and aerobic PHA consumption were obtained, and the fraction mainly produced was PHV (Appendix C Figure C8). While *Accumulibacter* is known to perform anaerobic glycogen consumption, *Tetrasphaera* was observed in the previous tests to lead to glycogen consumption or production according to the carbon source fed. Glycogen production was followed by consumption in the anaerobic phase of this test (Figure 5.5). The same pattern was obtained in a cycle study of the parent SBR, when Cas aa was the only carbon source fed when carbon was fed as pulse as opposed to continuous feeding (Figure 5.1 a and b). This observation might be related to a preference of *Tetrasphaera* to firstly ferment carbon sources with higher energetic inputs to the cell, leading to simultaneous glycogen formation. The low ratio of glycogen consumption per C uptake (0.04 C-mol/C-mol) during the anaerobic phase in this test is likely explained by the simultaneous production and consumption in the

anaerobic phase by the two PAO groups. Aerobically, glycogen production was observed in this test (Figure 5.5).

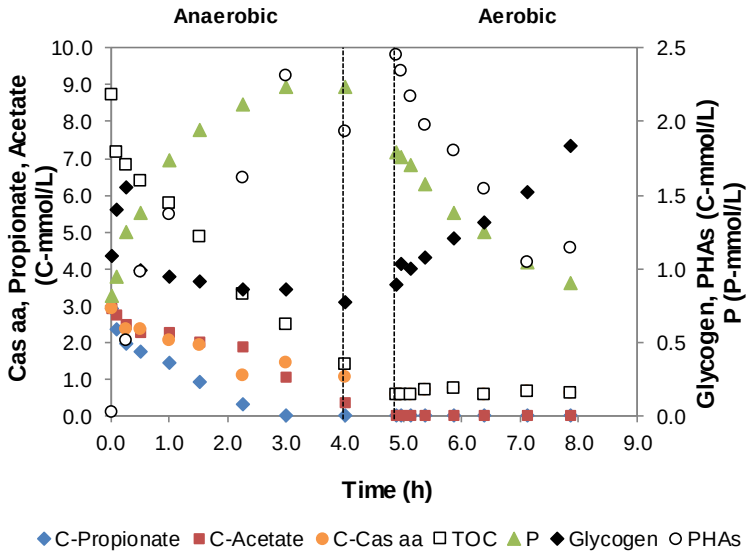

Figure 5.5 – Comparison of carbon, P and PHAs profiles for the 2nd batch experiment performed with a mixture of carbon sources (propionate, acetate and Cas aa).

Interestingly, the P release per C uptake in this test (0.19 P-mol/C-mol) was also somewhat lower than that observed with acetate or propionate feeding (0.40 and 0.30 P-mol/C-mol, respectively). This may be due to simultaneous P uptake from some amino acids present in the Cas aa by *Tetrasphaera*, in conjunction with the P release related to acetate and propionate uptake by *Accumulibacter*, supporting the hypothesis that *Tetrasphaera* activity can lead to lower net P-release to C-uptake ratios in WWTPs.

Anaerobic and aerobic cell maintenance

Also relevant to understanding the metabolism of the culture is to evaluate the energy source for cell maintenance. This was performed by conducting extended anaerobic or aerobic phase tests without external carbon source being fed. The results of these anaerobic and aerobic tests are presented in Figure 5.6 (A and B), respectively. As shown in this figure, the TOC profiles remained constant over time, due to the absence of carbon source. Interestingly, P release was not observed for energy generation for anaerobic cell maintenance, while glycogen consumption was observed. In the aerobic test, some P uptake (23.6 of mg-P/L) was found, in

conjunction with glycogen consumption, while the PHA concentration was stable. The results suggest that for anaerobic maintenance, *Tetrasphaera* prefer to consume glycogen as the primary source of energy source instead of P release. On the other hand, in the test of aerobic maintenance, it is observable that the cells were able to use the energy provided by glycogen consumption for P uptake.

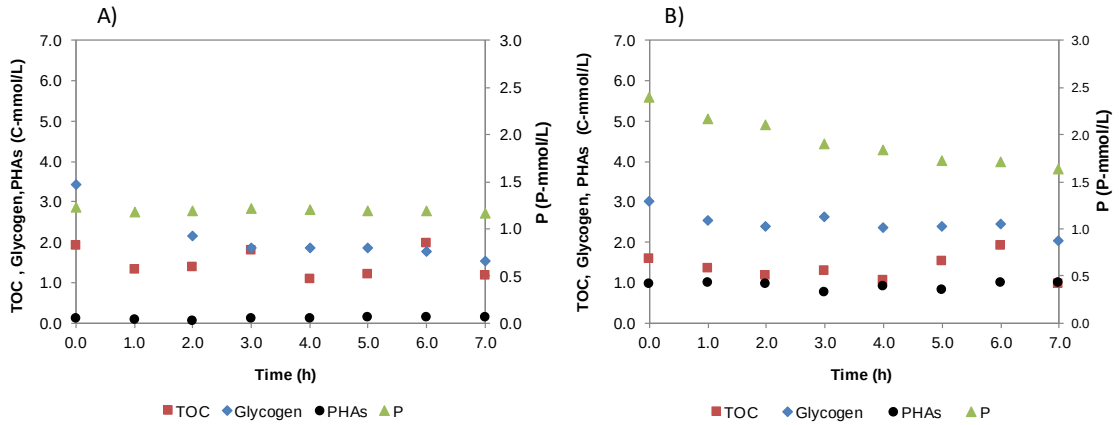

Figure 5.6 – Comparison of TOC, glycogen and P profiles for the 2nd batch experiments performed without carbon sources (control tests) under anaerobic (A) and aerobic (B) conditions, respectively.

5.3.3 Individual amino acids uptake and intracellular metabolites

In order to investigate the potential storage compounds used by *Tetrasphaera* for aerobic P uptake, the intracellular metabolites that were stored by the culture were assessed by GC-MS and HPLC. To allow identification of intracellular metabolites, a preliminary test was initially performed with biomass samples taken from the parent reactor.

Some amino acids, such as valine, threonine, aspartate, proline, glutamine, phenylalanine, lysine and ornithine were detected by GC-MS analysis during a cycle study fed with cas aa, although glycine was not detected (Table 5.6). These results support the hypothesis that other amino acids besides glycine can be stored as intracellular free amino acids and utilised in the following aerobic phase. Interestingly, ornithine was detected as a free intracellular metabolite. This amino acid is a substrate involved in the urea cycle and is utilised by cells to decrease the ammonia content inside the cells by converting it to urea, avoiding inhibition (Harvey and Ferrier, 2011). Urea was also detected as intracellular metabolite, supporting the existence of this metabolic pathway. There are no previous studies reporting the existence of the urea

cycle in *Tetrasphaera*, although the *Accumulibacter* genome has genes that could be active as urease in clade IIA (Flowers et al., 2013). However, while *Accumulibacter* do not typically take up amino acids (Kong et al., 2004; Kristiansen et al., 2013), *Tetrasphaera* might use the urea cycle to decrease the high content of nitrogen inside of the cells due to amino acids uptake and consumption. Small amines were also detected as intracellular metabolites in the cells. Other compounds associated as precursors of the TCA cycle, such as succinic acid and malic acid, were also found intracellularly. Both *Accumulibacter* and *Tetrasphaera* are known to employ the TCA cycle (Kristiansen et al., 2013; Oehmen et al., 2007a). Long chain fatty acids (LCFAs), such as palmitic acid, were also detected in this culture, and previous observations have shown that it is possible to increase its intracellular content up to 20% in *Accumulibacter*-dominated sludge during the anaerobic phase (Wexler et al., 2009). Stearic acid, one the most common LCFAs following palmitic acid, was also found as a free intracellular compound. The capacity of *Tetrapshaera* (or *Accumulibacter*) to store lipids is worthy of further study. Sugar compounds such as free glucose as well as turanose were also found, showing the high variety of different metabolites that could be involved as energy sources in *Tetrasphaera*.

Table 5.6 – Intracellular metabolites identified with GC-MS analysis during a cycle study.

Metabolite				
Amino aacids	Amines	Sugars	Acids	Others
Threonine	Acetamide	Glucose	Butanoic acid	Uridine
Valine	Silamine	Turanose	Propanoic acid	Adenosine
Aspartic acid		Inositol	Malic acid	Urea
Proline			Stearic acid	Phosphate
Serine			Palmitic acid	
Glutamine				
Phenylalanine				
Lysine				
Ornithine				

In order to further characterise the capacity of the culture to store amino acids, and to assess the preference of the culture for taking up different amino acids, an anaerobic test was performed with a mixture of 22 amino acids and the intracellular and extracellular amino acids quantified by HPLC. The individual amino acid consumption of this batch test revealed the preference of *Tetrapshaera* to take up certain amino acids. Arginine, lysine, alanine, glycine, serine, proline, isoleucine, phenylalanine, glutamic acid, aspartic acid, cysteine, tyrosine were the main amino acids consumed during these tests (Figure 5.7). The consumption of these 12 amino acids accounted for 75.4% of the total amino acids consumed in this batch test (9.3 C-

mmol/L). Proline, glycine and lysine were the only amino acids that were fully consumed.

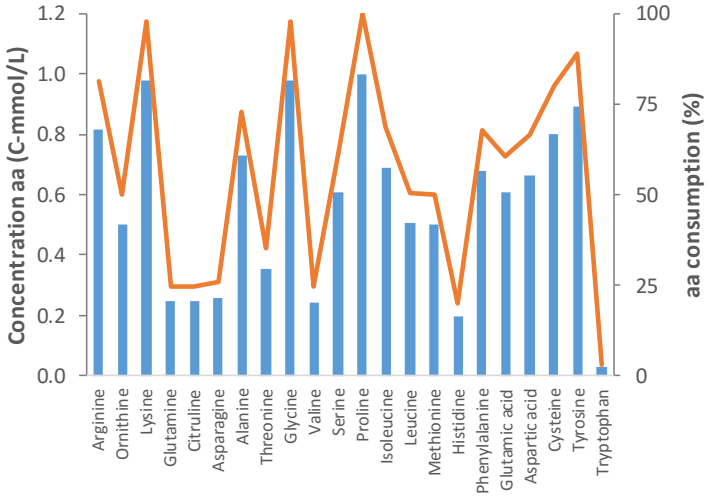

Figure 5.7 – Anaerobic batch test (test 3) comparing individual amino acids (aa) consumption (blue bars) versus % of amino acid consumption (orange line).

The solid phase samples from this test were also analysed by HPLC after applying cold ethanol quenching to assess intracellular amino acids storage. The culture had at the end of the anaerobic phase an increase in the free intracellular aa storage of 1.82 C-mmol/L, which accounted for 19.6% of all amino acids consumed. Nguyen et al., (2015) found that 9-15% of glycine taken up by *Tetrasphaera* was stored intracellularly. This study shows that numerous amino acids can be not only fermented, but stored by *Tetrasphaera*, likely for aerobic energy generation enabling P-uptake during the aerobic phase.

5.4 CONCLUSIONS

An enrichment was obtained of the two main PAOs groups commonly present in full-scale WWTPs: *Tetrasphaera* and *Accumulibacter*. Amino acids were consumed anaerobically and high aerobic P-removal was achieved by the culture. Anaerobically, this culture was able to perform casamino acids uptake, P release, glycogen hydrolysis, followed by aerobic P uptake and glycogen formation. Very low anaerobic PHA synthesis and aerobic PHA consumption were observed. *Tetrasphaera* performed the majority of the P removal in this culture, and batch tests showed that the metabolism of some carbon sources can actually lead to anaerobic P uptake through

energy generated by fermentation of glucose and amino acids. This anaerobic P uptake may lead to lower net P-release to C-uptake ratios and reduce the P needed to be removed aerobically in WWTPs. MAR-FISH confirmed that *Tetrasphaera*, not *Accumulibacter*, were responsible for amino acid and glucose consumption, while *Accumulibacter* likely survived on fermentation products. Intracellular metabolites such as amino acids, sugars, LCFAs and small amines were detected, and may contribute as energy sources in the aerobic phase. Storage of amino acids accounted for approximately 20% of the amino acids taken up, suggesting that the remaining 80% was fermented or stored as macromolecules. Evidence of the urea cycle was found, which could be involved in reducing the intracellular nitrogen content. *Tetrasphaera* and *Accumulibacter* contribute to P uptake through different ecological niches. The understanding of this synergy between *Tetrasphaera* and *Accumulibacter* improves our knowledge about how P removal is actually achieved in EBPR WWTPs and may lead to new cost-effective strategies for process optimisation.

Acknowledgements

The authors thank the Portuguese Fundação para a Ciência e Tecnologia (UID/Multi/04378/2013, AMB/120581/2010) and UCIBIO (FCT/MEC UID/Multi/04378/2013, POCI-01-0145-FEDER-007728) for financing. Ricardo Marques acknowledge the PhD grant SFRH/BD/74515/2010) provided by Portuguese Fundação para a Ciência e Tecnologia and the Danish Research Council (DFF – 4002-00455).

REFERENCES

Amann, R.I., Binder, B.J., Olson, R.J., Chisholm, S.W., Devereux, R., Stahl, D. a, 1990. Combination of 16S rRNA-targeted oligonucleotide probes with flow cytometry for analyzing mixed microbial populations. Appl. Environ. Microbiol. 56, 1919–25.

APHA, 2005. Standard methods for the examination of water and wastewater, 21st editi. ed. Washington, D.C.

Börner, J., Buchinger, S., Schomburg, D., 2007. A high-throughput method for microbial metabolome analysis using gas chromatography/mass spectrometry. Anal. Biochem. 367, 143–151.

Brock, T., Madigan, M.T.., Martinko, J.M.., Bender, K.S.., Buckley, D.H.., Stahl, D.A., 2012. Biology of Microorganisms, 13th ed. Benjamin Cumming, San Francisco.

Crocetti, G.R., Hugenholtz, P., Bond, P.L., Schuler, a, Keller, J., Jenkins, D., Blackall, L.L., 2000. Identification of polyphosphate-accumulating organisms and design of 16S rRNA-directed probes for their detection and quantitation. Appl. Environ. Microbiol. 66, 1175–82.

Daims, H., Brühl, a, Amann, R., Schleifer, K.H., Wagner, M., 1999. The domain-specific probe EUB338 is insufficient for the detection of all Bacteria: development and evaluation of a more comprehensive probe set. Syst. Appl. Microbiol. 22, 434–44.

Flowers, J.J., He, S., Malfatti, S., del Rio, T.G., Tringe, S.G., Hugenholtz, P., McMahon, K.D., 2013. Comparative genomics of two "*Candidatus* Accumulibacter" clades performing biological phosphorus removal. ISME J. 7, 2301–14.

Harvey, R.A., Ferrier, D.R., 2011. Lippincott's Illustrated Reviews, Biochemestry, 5th editio. ed. Lippincott Williams & Wilkins.

Kong, Y., Nielsen, J.L., Nielsen, P.H., Icrobiol, A.P.P.L.E.N.M., 2004. Microautoradiographic Study of Rhodocyclus -Related Polyphosphate- Accumulating Bacteria in Full-Scale Enhanced Biological Phosphorus Removal Plants. Appl. Environ. Microbiol. 70, 5383–5390.

Kong, Y., Nielsen, J.L.J.J.L., Nielsen, P.H.P.P.H., 2005. Identity and Ecophysiology of Uncultured Actinobacterial Polyphosphate-Accumulating Organisms in Full-Scale Enhanced Biological Phosphorus Removal Plants. Appl. Environ. Microbiol. 71, 4076–4085.

Kong, Y., Ong, S.L., Ng, W.J., Liu, W.T., 2002. Diversity and distribution of a deeply branched novel proteobacterial group found in anaerobic-aerobic activated sludge processes. Environ. Microbiol. 4, 753–757.

Kong, Y., Xia, Y., Nielsen, P.H., 2008. Activity and identity of fermenting microorganisms in full-scale biological nutrient removing wastewater treatment plants. Environ. Microbiol. 10, 2008–19.

Kristiansen, R., Nguyen, H.T.T., Saunders, A.M., Nielsen, J.L., Wimmer, R., Le, V.Q., Mcilroy, S.J., Petrovski, S., Seviour, R.J., Calteau, A., Nielsen, K.L., Nielsen, P.H.H., Thi, H., Nguyen, T., Saunders, A.M., Lund Nielsen, J., Wimmer, R., Le, V.Q., Mcilroy, S.J., Petrovski, S., Seviour, R.J., Calteau, A., Lehmann Nielsen, K., Nielsen, P.H.H., 2013. A metabolic model for members of the genus Tetrasphaera involved in enhanced biological phosphorus removal. Iternational Soc. Microb. Ecol. 7, 543–554.

Lanham, A.A.B., Oehmen, A.A., Saunders, A.M.A., Carvalho, G., Nielsen, P.H., Reis, M. a M., 2013. Metabolic versatility in full-scale wastewater treatment plants performing enhanced biological phosphorus removal. Water Res. 47, 7032–41.

Lanham, A.B., Ricardo, A.R., Albuquerque, M.G.E., Pardelha, F., Carvalheira, M., Coma, M., Fradinho, J., Carvalho, G., Oehmen, A., Reis, M. a M., 2013. Determination of the extraction kinetics for the quantification of polyhydroxyalkanoate monomers in mixed microbial systems. Process Biochem. 48, 1626–1634.

Lebertz, H., Andreesen, J.R., 1988. Glycine fermentation by Clostridium histolyticum. Arch. Microbiol. 150, 11–14.

Lopez-Vazquez, C.M., Oehmen, A., Hooijmans, C.M., Brdjanovic, D., Gijzen, H.J., Yuan, Z., van Loosdrecht, M.C.M., 2009. Modeling the PAO-GAO competition: effects of carbon source, pH and temperature. Water Res. 43, 450–62.

McIlroy, S.J., Nittami, T., Seviour, E.M., Seviour, R.J., 2010. Filamentous members of cluster III Defluviicoccus have the in situ phenotype expected of a glycogen-accumulating organism in activated sludge. FEMS Microbiol. Ecol. 74, 248–256.

McKenzie, C.M., Seviour, E.M., Schumann, P., Maszenan, a M., Liu, J.-R., Webb, R.I., Monis, P., Saint, C.P., Steiner, U., Seviour, R.J., 2006. Isolates of “Candidatus Nostocoida limicola” Blackall et al. 2000 should be described as three novel species of the genus Tetrasphaera, as Tetrasphaera jenkinsii sp. nov., Tetrasphaera vanveenii sp. nov. and Tetrasphaera veronensis sp. nov. Int. J. Syst. Evol. Microbiol. 56, 2279–90.

Meyer, R.L., Saunders, A.M., Blackall, L.L., 2006. Putative glycogen-accumulating organisms belonging to the Alphaproteobacteria identified through rRNA-based stable isotope probing. Microbiology 152, 419–429.

Muszyński, A., Miłobędzka, A., 2015. The effects of carbon/phosphorus ratio on polyphosphate- and glycogen-accumulating organisms in aerobic granular sludge. Int. J. Environ. Sci. Technol.

Nguyen, H.T.T., Kristiansen, R., Vestergaard, M., Wimmer, R., Nielsen, P.H., 2015. Intracellular Accumulation of Glycine in Polyphosphate-Accumulating Organisms in Activated Sludge, a Novel Storage Mechanism under Dynamic Anaerobic-Aerobic Conditions. Appl. Environ. Microbiol. 81, 4809–18.

Nguyen, H.T.T., Le, V.Q., Hansen, A.A., Nielsen, J.L., Nielsen, P.H.H., 2011. High diversity and abundance of putative polyphosphate-accumulating Tetrasphaera-related bacteria in activated sludge systems. FEMS Microbiol. Ecol. 76, 256–67.

Nielsen, P.H.H., Mielczarek, A.T., Kragelund, C., Nielsen, J.L., Saunders, A.M., Kong, Y., Hansen, A.A., Vollertsen, J., 2010. A conceptual ecosystem model of microbial communities in enhanced biological phosphorus removal plants. Water Res. 44, 5070–5088.

Nittami, T., McIlroy, S., Seviour, E.M., Schroeder, S., Seviour, R.J., 2009. Candidatus Monilibacter spp., common bulking filaments in activated sludge, are members of Cluster III Defluviicoccus. Syst. Appl. Microbiol. 32, 480–489.

Oehmen, A., Lemos, P.C., Carvalho, G., Yuan, Z., Keller, J.J., Blackall, L.L., Reis, M. a M., 2007a. Advances in enhanced biological phosphorus removal: From micro to macro scale. Water Res. 41, 2271–2300.

Oehmen, A., Teresa Vives, M., Lu, H., Yuan, Z., Keller, J.J., Vives, M.T., Lu, H., Yuan, Z., Keller, J.J., Teresa Vives, M., Lu, H., Yuan, Z., Keller, J.J., 2005a. The effect

of pH on the competition between polyphosphate-accumulating organisms and glycogen-accumulating organisms. Water Res. 39, 3727–37.

Oehmen, A., Yuan, Z., Blackall, L.L., Keller, J., 2005b. Comparison of acetate and propionate uptake by polyphosphate accumulating organisms and glycogen accumulating organisms. Biotechnol. Bioeng. 91, 162–8.

Oehmen, A., Zeng, R.J., Keller, J., Yuan, Z., 2007b. Modeling the aerobic metabolism of polyphosphate-accumulating organisms enriched with propionate as a carbon source. Water Environ. Res. 79, 2477–2486.

Ramsay, I.R., 1997. Modelling and Control of High-Rate Anaerobic Wastewater Treatment Systems., PhD. University of Queensland, Brisbane. The University of Queensland, Queensland.

Smolders, G.J., van der Meij, J., van Loosdrecht, M.C., Heijnen, J.J., 1994a. Model of the anaerobic metabolism of the biological phosphorus removal process: Stoichiometry and pH influence. Biotechnol. Bioeng. 43, 461–70.

Smolders, G.J., van der Meij, J., van Loosdrecht, M.C., Heijnen, J.J., 1994b. Stoichiometric model of the aerobic metabolism of the biological phosphorus removal process. Biotechnol. Bioeng. 44, 837–48.

Spura, J., Reimer, L.C., Wieloch, P., Schreiber, K., Buchinger, S., Schomburg, D., 2009. A method for enzyme quenching in microbial metabolome analysis successfully applied to gram-positive and gram-negative bacteria and yeast. Anal. Biochem. 394, 192–201.

Wexler, M., Richardson, D.J., Bond, P.L., 2009. Radiolabelled proteomics to determine differential functioning of Accumulibacter during the anaerobic and aerobic phases of a bioreactor operating for enhanced biological phosphorus removal. Environ. Microbiol. 11, 3029–3044.

Wong, M.T., Tan, F.M., Ng, W.J., Liu, W.T., 2004. Identification and occurrence of tetrad-forming Alphaproteobacteria in anaerobic-aerobic activated sludge processes. Microbiology 150, 3741–3748.

Xia, Y., Kong, Y., Thomsen, T.R., Halkjaer Nielsen, P., 2008. Identification and Ecophysiological Characterization of Epiphytic Protein-Hydrolyzing Saprospiraceae (“Candidatus Epiflobacter” spp.) in Activated Sludge. Appl. Environ. Microbiol. 74, 2229–2238.

Zeng, R.J., Van Loosdrecht, M.C.M., Yuan, Z., Keller, J., 2003. Metabolic Model for Glycogen-Accumulating Organisms in Anaerobic/Aerobic Activated Sludge Systems. Biotechnol. Bioeng. 81, 92–105.

6

DENITRIFYING CAPABILITIES OF *TETRASPHAERA* AND THEIR CONTRIBUTION TOWARDS NITROUS OXIDE PRODUCTION IN ENHANCED BIOLOGICAL PHOSPHORUS REMOVAL PROCESSES

SUMMARY: Denitrifying EBPR systems are an efficient means of removing P and NO_3^- with low carbon source and oxygen requirements. *Tetrasphaera* is one of the most abundant PAOs present in EBPR systems, but their capacity to achieve denitrifying EBPR has not previously been determined. An enriched *Tetrasphaera* culture, with over 80% of the total volume content of cells present, was obtained and achieved anoxic P-uptake with nitrate as the electron acceptor, but at lower levels than typically observed by *Accumulibacter* enrichments. Batch tests with different combinations of NO_3^-, NO_2^- and N_2O and without the presence of external carbon sources, revealed the preference of *Tetrasphaera* for NO_3^- and NO_2^- reduction over N_2O. The simultaneous addition of nitrite and N_2O appeared to augment the N_2O reduction rate. Electron competition was observed during the addition of multiple nitrogen oxide species, where P uptake also appeared to be favoured over glycogen production in these situations. This study increases our understanding of the role of *Tetrasphaera*-related organisms in denitrifying EBPR systems.

IN PREPARATION: This work will be submitted to an international peer reviewed scientific journal: Marques, R., Ribera-Guardia, A., Santos, J., Carvalho, G., Reis, M. A. M., Pijuan, M., Oehmen, A., 2016. Denitrifying capabilities of *Tetrasphaera* and their contribution towards nitrous oxide production in enhanced biological phosphorus removal processes

6.1 INTRODUCTION

Phosphorus and nitrogen are known key elements causing eutrophication of water bodies. Combining denitrification with EBPR can reduce both carbon source and aeration requirements of WWTPs. Anaerobically, some groups of PAO in these systems (particularly *Candidatus* Accumulibacter phosphatis) release P and take up organic carbon sources (e.g., acetate and propionate), consume glycogen and synthesize PHA (Louie et al., 2000; Oehmen et al., 2007a; Pereira et al., 1996; Wexler et al., 2009; Zhou et al., 2009). In the following anoxic (and/or aerobic) phase they reduce nitrate (NO_3^-, or oxygen), and oxidize PHA to obtain energy to replenish glycogen reserves, take up P and recover their intracellular poly-P level (Carvalho et al., 2007; Kuba et al., 1996). Another group of organisms is present in EBPR systems that compete for the same organic carbon sources as the *Accumulibacter* PAOs, which are known as GAOs. These bacteria are able to survive and grow under alternating anaerobic and anoxic/aerobic conditions with similar metabolic processes, but without contributing to P removal (Cech and Hartman, 1993; Oehmen et al., 2007a). Literature studies have enriched mixed cultures of dPAOs and dGAOs, achieving partial or total denitrification (Carvalho et al., 2007; Tsuneda et al., 2006; Wang et al., 2008; Zeng et al., 2003a, 2003b). Two groups of *Accumulibacter* PAOs were observed to reduce NOx. Type I *Accumulibacter* are generally able to reduce NO_3^- to N_2, while some members of Type II *Accumulibacter* are generally unable to reduce NO_3^- but could reduce NO_2^- to N_2 (Carvalho et al., 2007; Flowers et al., 2009). The main groups of GAOs present in WWTPs are *Candidatus* Competibacter phosphatis and *Defluviicoccus*. *Competibacter* GAOs can be grouped according to their denitrifying capabilities within the 6 subgroups identified: complete denitrification (subgroup 6), NO_3^- reduction (subgroup 1,4 and 5), and unable to denitrify (subgroup 3 and 7) (Kong et al., 2006). *Defluviicocus* cluster I can reduce NO_3^- but not NO_2^-, while cluster II was found to be unable to denitrify (Burow et al., 2007; Wang et al., 2008) (Table 6.1).

Tetrasphaera are also present in full-scale EBPR systems, reaching higher abundance than *Accumulibacter*, up to 30% of the total biomass (Kong et al., 2005; Lanham et al., 2013; Nguyen et al., 2011).These organisms can assimilate a wider range of carbon sources (amino acids, sugars, VFAs) during anaerobic conditions (Kong et al., 2008; Kristiansen et al., 2013; Nguyen et al., 2011). *Tetrasphaera* are capable of fermenting amino acids and sugars, storing either amino acids or glycogen anaerobically, and using it as an energy source for aerobic P uptake (Kristiansen et al.,

2013; Nguyen et al., 2015), and are believed to be less competitive for VFA uptake than *Accumulibacter* (Nguyen et al., 2015). With a *Tetrasphaera* enriched culture fed only with casein hydrolysate as carbon source, (detailed in Chapter 5) *Tetrasphaera* were responsible for amino acid consumption and performed the majority of the high level of aerobic P removal observed in this culture.

Table 6.1 – Denitrifying abilities of organisms present in EBPR systems

Microorganism	Reduction steps	Reference
Accumulibacter Type I	$NO_3^-\rightarrow NO_2^-\rightarrow N_2O\rightarrow N_2$	(Flowers et al., 2009)
Accumulibacter Type II	$NO_2^-\rightarrow N_2O\rightarrow N_2$	(Flowers et al., 2009)
Competibacter (Sub. 6)	$NO_3^-\rightarrow NO_2^-\rightarrow N_2O\rightarrow N_2$	(Kong et al., 2006)
Competibacter (Sub. 1,4, 5)	$NO_3^-\rightarrow NO_2^-$	(Kong et al., 2006)
Competibacter (Sub. 3, 7)	$NO_3^-\rightarrow X$	(Kong et al., 2006)
Defluviicoccus (Cluster I)	$NO_3^-\rightarrow NO_2^-$	(Wang et al., 2008)
Defluviicoccus (Cluster II)	$NO_3^-\rightarrow X$	(Burow et al., 2007)
Tetrasphaera (T.*australiensis*)	$NO_3^-\rightarrow NO_2^-\rightarrow N_2O$	(Kristiansen et al., 2013)
Tetrasphaera (T.*elongata*, T. *jenkinsii*)	$NO_3^-\rightarrow NO_2^-$	(Kristiansen et al., 2013)
Tetrasphaera (T.*japonica*)	$NH_4^+\leftarrow NO_3^-\rightarrow NO_2^-\rightarrow N_2O$	(Kristiansen et al., 2013)

Metagenomic results led to the observation that all four existing *Tetrasphaera* isolates (T. *australiensis*, T. *elongate*, T. *jenkinsii* and T. *japonica*) have the genomic capabilities to encode for enzymes to reduce NO_3^- to NO, while only two of them (T. *australiensis,* T. *japonica*) have the capability to reduce NO to N_2O (Kristiansen et al., 2013). Nevertheless, the capacity of *Tetrapshaera* to couple denitrification with P uptake has never been established, nor the kinetics of denitrification in the presence of different nitrogen oxides (Table 6.1).

Complete denitrification involves four consecutive reduction steps, starting with NO_3^-, leading to the sequential production of NO_2^-, NO, and N_2O as three obligatory intermediates, before producing N_2. N_2O is known as a potent greenhouse gas with a 300-fold stronger radiative force than carbon dioxide, and is the primary ozone-depleting substance of the 21st century (IPCC , 2013). Emissions from WWTPs have been found to contribute to over 80% of the total greenhouse gases emitted from some plants (Daelman et al., 2013a; Daelman et al., 2013b; Ye et al., 2014). The denitrification reduction process is mediated by four different denitrification reductases, NO_3^- reductase (Nar), NO_2^- reductase (Nir), NO reductase (Nor) and N_2O reductase (Nos) (Zumft, 1997). Unbalanced denitrification rates leads to the accumulation of intermediates in the denitrification process. This disturbance can be linked with the competition for electron demand between the four reduction steps when the electron supply rate is the limiting step. This was observed by Pan et al. (2013) for ordinary

heterotrophic denitrifiers using only methanol as carbon source, where the reduction rate of NO_2^- was prioritized over the other denitrification steps, consequently leading to N_2O accumulation. Ribera-Guardia et al., (2014) also observed electron competition on N_2O reduction rates in ordinary heterotrophic denitrifiers with multiple external electron donors (acetate, ethanol, and methanol). N_2O has been observed to accumulate in EBPR systems with enriched dPAO and dGAO cultures (Lemaire et al., 2006; Zeng et al., 2003a, 2003b). The consumption of PHAs as electron donor during the denitrification process has been associated with an increase in the production of N_2O in some cases (Li et al., 2013; Wang et al., 2011; Zhou et al., 2012). *Tetrasphaera* do not synthesise PHAs, and possibly use amino acids or glycogen as internal storage products (Kristiansen et al., 2013; Nguyen et al., 2015, 2011). The consumption of these internal products might lead to a different behaviour in the formation/consumption of N_2O within these bacteria.

This study focuses on the enrichment of a *Tetrasphaera*-EBPR culture under anaerobic-anoxic-aerobic conditions to evaluate and characterise their denitrifying capabilities and contribution towards anoxic P uptake. Anoxic batch tests with single or multiple electron acceptors were performed to investigate electron distribution and N_2O production without the presence of external carbon sources. This study contributes to clarify the potential role of *Tetrasphaera,* which are highly abundant organisms in biological nutrient removal plants, on N_2O accumulation during denitrification, as well as their impact on P removal. Increased understanding of the metabolism of *Tetrasphaera*-related PAOs may improve the removal efficiency of P and N with wastewaters with different compositions of organic carbon in EBPR WWTPs.

6.2 MATERIAL AND METHODS

6.2.1 Sequential batch reactor operation

A SBR, with 2L working volume, was operated for 196 days to enrich a denitrifying *Tetrasphaera* culture. The inoculum was obtained from the study described in Chapter 5. The SBR was fed with sodium casein hydrolysate (hereafter refer as Cas aa) as only carbon source, and operated with an 8-h cycle, including: anaerobic phase (3h), anoxic phase (2h), aerobic phase (2h) and settling/decant phase (1h). Three solutions were used to feed the SBR: A - Mineral media and carbon source (400 mL) was fed continuously during the first 2h of the anaerobic phase; B - Phosphate medium (600 mL) was fed at the start of the anaerobic phase during 3 min; C – Nitrate medium

was fed (50 mL) during 5 min in the start of the anoxic phase. The SBR was operated with a hydraulic retention time (HRT) and SRT of 16 h and 20 days, respectively. Anaerobic/anoxic or aerobic conditions were obtained by bubbling argon or air, respectively. pH was controlled at 7.1 ± 0.1 by automatic addition of 0.1 M HCl, while temperature was controlled at 20 ± 1ºC with a water bath. The reactor was stirred by via an overhead mixer at 300 rpm during the anaerobic/anoxic and aerobic phases. The performance and steady state of the SBR was assessed by biological and chemical analyses performed in samples taken during the weekly cycle studies. Samples were analysed for carbon source, PHAs, glycogen, ammonia and orthophosphate. Poly-P, TSS and VSS were analysed at the end of the cycle to follow P content and cell concentration in the reactor. Samples for FISH analysis were also taken to assess the microbial community composition of the culture.

6.2.2 Culture Media

The SBR culture media composition was similar as that used in Chapter 5, briefly: solution (A), mineral media with carbon source contained per litre: 0.79 g sodium casein hydrolysate, 0.37 g NH_4Cl, 0.59 g $MgCl_2.7H_2O$ g, 0.28 g $CaCl_2.2H_2O$, 0.07 g N-Allylthiourea (ATU), 0.2 g ethylene-diaminetetraacetic (EDTA) and 1.98 ml micronutrient solution. The micronutrient solution was prepared based on Smolders et al., 1994, and contained per litre: 1.5 g $FeCl_3.6H_2O$, 0.15 g H_3BO_3, 0.03 g $CuSO_4.5H_2O$, 0.18 g KI, 0.12 g $MnCl_2.4H_2O$, 0.06 g $Na_2MoO_4.2H_2O$, 0.12 g $ZnSO_4.7H_2O$ and 0.15 g $CoCl_2.6H_2O$; solution (B), Phosphate medium (30 ppm in the SBR) contained 0.32 g K_2HPO_4 and 0.19 g KH_2PO_4 per litre; solution (C), Nitrate medium (25 ppm in the SBR) contained 6.07 g $NaNO_3$ per litre. The pH of solution A was set to 7.4 ± 0.1, with addition of 1.0 M NaOH, before autoclaving.

6.2.3 Batch reactor setup and operation

The experimental procedure used for the batch tests was based on Ribera-Guardia et al., (2014) with minor modifications. A sealable reactor with a volume capacity of 330 mL was used for all batch tests. A 10 mL reservoir filled with the same mixed liquor concentration was connected to the lid to avoid the entrance of air into the vessel when samples were taken during each batch test. Online N_2O monitoring was performed with an N_2O liquid microsensor connected to an amplifier system (Unisense

Environment A/S, Denmark). The microsensor was calibrated before and after each test using a saturated solution obtained by bubbling pure N_2O gas during 5 min, at a flow rate of 5 L/min. A three-point calibration curve was performed by adding twice 0.1 mL of the saturated N_2O solution to 100 mL water free of N_2O. pH was manually controlled at 7.1±0.1 with addition of 0.5 M of NaOH and HCl. All tests were carried out in a temperature controlled lab with minor temperature variations (21-22ºC). The experiments were performed under anoxic conditions with no exchange of N_2O between the liquid and gas phase due to the absence of head space in the vessel.

To assess the denitrifying capabilities of the culture and evaluate the hypothesis of electron competition, seven batch tests with different combinations of nitrogen oxides were performed (Table 6.2).

Table 6.2 – Batch tests performed with different combinations of electron acceptors

Batch test	A	B	C	D	E	F	G
Electron acceptors	NO_3^-	NO_2^-	N_2O	NO_3^- N_2O	NO_2^- N_2O	NO_3^- NO_2^-	NO_3^- NO_2^- N_2O

All batch tests were performed in duplicate between days 139 and 164 of SBR operation. An additional batch test was also performed where external carbon was added (Cas aa at the same concentration fed to the parent SBR, but added as a pulse instead of continuous feeding). The tests were performed using sludge withdrawn from the end of the anaerobic phase, of the parent SBR. Sludge was washed twice with mineral media to remove any external carbon source present. The sludge was resuspended with mineral media to a final volume of 450 mL, equally divided between both replicate batch tests. Argon was bubbled to ensure all dissolved oxygen present was removed, prior to starting the experiment. A concentration of 20 mg N-NOx/L of each nitrogen oxide (NO_3^-, NO_2^- and N_2O depending on the test, see Table 6.2) was added initially as a pulse. Samples were taken along the batch tests to analyse NO_3-, NO_2-, NH_4^+ and phosphate. Biomass samples for PHA and glycogen were taken at the beginning and end of each test. Biomass concentration was assessed by VSS and TSS at the end of each cycle.

6.2.4 Contribution of *Tetrasphaera* and *Competibacter* to NOx reduction

The contribution of both *Tetrasphaera* and *Competibacter* GAOs to NOx reduction was evaluated by calculating the ratio of PHA utilisation to NOx reduction during the SBR and batch test operation. The model developed by Oehmen et al., (2010) was used to describe the GAOs PHA utilization to serve as electron donor for NOx reduction. The remaining NOx reduction was then linked with *Tetrasphaera* activity (Appendix D Table D1).

6.2.5 Calculation of the reduction rates

The maximum consumption rates of NO_3^-, NO_2^- and N_2O were determined by applying linear regression to the profiles of NO_3^-, NO_2^- and N_2O, respectively, which were obtained in each test. The specific degradation rate of nitrate (rNO_3^-,s), nitrite (rNO_2^-, s), and nitrous oxide (rN_2O, s) was calculated by dividing the rate data determined above by the VSS concentration present in each batch test. The specific degradation rate of (rNO, s) was assumed to be equal to the specific degradation rate of nitrite. The true reduction rate of each nitrogen oxide (mg N/(VSS.h)) was calculated as follows:

$$rNO_3^- = rNO_3^-,s \quad (6.1)$$

$$rNO_2^- = rNO_3^-,s \text{ – measured } NO_2^-,s \quad (6.2)$$

$$rNO = rNO_2^-,s \quad (6.3)$$

$$rN_2O = rNO,s \text{ – measured } N_2O,s \quad (6.4)$$

where, rNO_3^-, rNO_2^-, rNO, rN_2O are expressed in (mg N/(g VSS.h)).

The electron consumption rates for Nar, Nir, Nor and Nos were calculated as follows:

$$r_{Nar,e} = \frac{r_{NO_3^-}}{14} \cdot 2 \quad (6.5)$$

$$r_{Nir,e} = \frac{r_{NO_2^-}}{14} \cdot 1 \quad (6.6)$$

$$r_{Nor,e} = \frac{r_{NO}}{14} \cdot 1 \quad (6.7)$$

$$r_{Nos,e} = \frac{r_{N_2O}}{14} \cdot 1 \quad (6.8)$$

where, $r_{Nar,e}$, $r_{Nir,e}$, $r_{Nor,e}$, $r_{Nos,e}$ are expressed in (mmol e^-/(gVSS.h)).

Electron distribution was calculated through the ratio of electron consumption rate by each individual enzyme per total electron consumption rate, expressed as a percentage:

$$\text{Electron distribution (\%)} = \frac{r_{NOx,e}}{r_{Nar,e}+r_{Nir,e}+r_{Nor,e}+r_{Nos,e}} * 100 \quad (6.9)$$

6.2.6 Chemical analyses

Segmented flow analysis (Skalar 5100, Skalar Analytical, The Netherlands) was used for P, poly-P, ammonia, nitrate and nitrite analyses. Poly-P analysis was performed as described in Chapter 5. VFAs were analysed via HPLC using a Metacarb 87 H (Varian) column and a refractive index detector (RI-71, Merck) with sulphuric acid (0.005 M) as eluent at a flow rate of 0.6 mL/min and 50°C operating temperature. Glycogen was determined as described by Lanham et al., (2012). PHA was determined by GC according to the methodology described by Lanham et al., (2013), using a Bruker 430-GC gas chromatograph equipped with a FID detector and a BR-SWax column (60m, 0.53 mm internal diameter, 1 mm film thickness, Bruker,USA). The Cas aa consumption was assessed through the analysis of TOC by a Shimadzu TOC-VCSH (Shimadzu, Japan). TSS and VSS were assessed by standard methods (APHA, 2005).

6.2.7 Microbial characterisation

Microbial composition of the SBR was assessed by FISH according to Amann, (1995). The following oligonucleotide probes were used: EUBMIX (equimolar concentrations of EUB338, EUB338II, and EUB338III, see (Amann et al., 1990; Daims et al., 1999) that target all Bacteria; PAOMIX (PAO651, PAO462 and PAO846) (Crocetti et al., 2000) that target most members of the *Accumulibacter* PAO cluster; Tet1-266, Tet2-892, Tet2-174 and Tet3-654 that target most *Tetrasphaera*-related PAOs (Nguyen et al., 2011); GAOmix (GAOQ431, GAOQ989 and GB_G2) targeting

Competibacter GAOs (Crocetti et al., 2000; Kong et al., 2002); DEF1mix (TFO_DF218 and TFO_DF618) targeting *Defluviicoccus vanus*-related GAOs cluster I (Wong et al., 2004); DEF2mix (DF988 and DF1020) targeting *D. vanus*-related GAOs cluster II (Meyer et al., 2006); DF1013 and DF1004 targeting phylotypes within cluster III *Defluviicoccus* (Nittami et al., 2009), indicated as putative GAOs (McIlroy et al., 2010). FISH quantification was performed by image analysis taken with a Zeiss LSM 710 confocal laser scanning microscope. The biomass quantification was obtained as the area covered by the specific probe divided by the area covered by EUBmix. Standard error of the mean was obtained as the standard deviation divided by the square root of 20 of images per quantification.

6.3 RESULTS AND DISCUSSION

6.3.1 SBR performance and microbial composition

To evaluate the reactor performance, cycle studies were made regularly during reactor operation. Pseudo steady-state conditions were achieved in the SBR after 55 days of operation, and the reactor was operated under these conditions for 115 days prior to executing the batch tests. Two typical profiles of the reactor operation are displayed in Figure 6.1. During the typical reactor operation, 86% of the carbon, 30.0% of P and 91.0% of NO_3^- was removed.

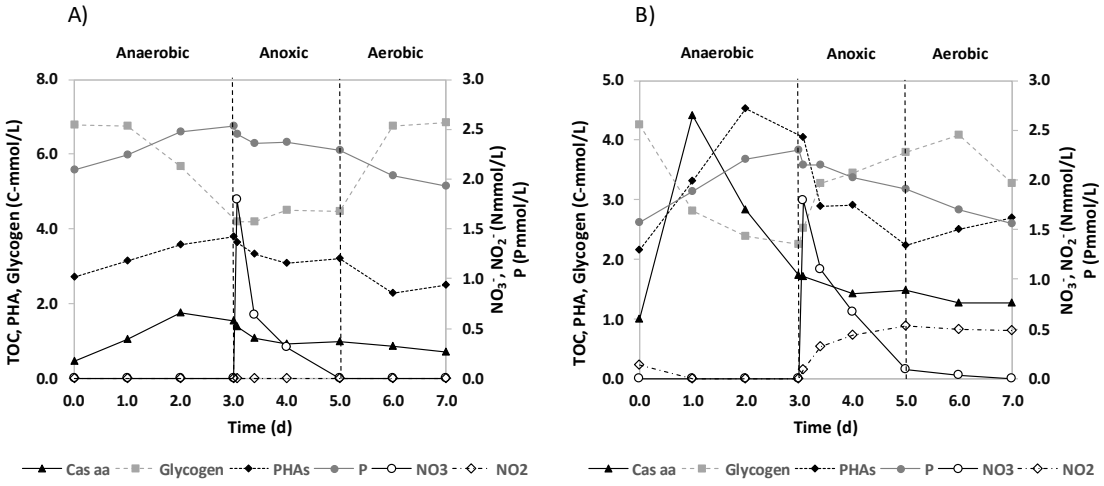

Figure 6.1 – Typical SBR cycle profile performed at day 82 (A) and 196 (B). Profiles of Cas aa (TOC), Phosphorous (P), Glycogen, PHAs, NO_3^- and NO_2^- are shown.

The main parameters analysed were compared with those obtained in an enriched *Accumulibacter* SBR and an SBR with a mixture of *Tetrasphaera* and *Accumulibacter* working under similar conditions. Table 6.3 presents a comparison among these three reactors. While the efficiency of carbon removal and NO_3^- reduced agree very well with the removals obtained for an *Accumulibacter* enriched culture operated with under similar conditions (Ribera-Guardia et al., 2016), the capacity of the *Tetrasphaera* enriched SBR to perform P-uptake was substantially lower as compared with the P-uptake obtained in the *Accumulibacter* enrichment. When comparing in more detail the P release/substrate ratios, *Tetrasphaera* SBR displayed a lower ratio (0.11±0.02 P-mmol/C-mmol) as compared with the *Accumulibacter* SBR (0.35±0.15 P-mmol/C-mmol). Furthermore, the P-uptake under anoxic and aerobic conditions was less effective in the *Tetrasphaera* SBR as compared to the *Accumulibacter* SBR. Also, this *Tetrasphaera* culture developed under anaerobic/anoxic/aerobic conditions also displayed less than half of the P uptake achieved by a *Tetrasphaera-Accumulibacter* culture operated with an anaerobic/aerobic cycle. Consequently, the intracellular P content displayed by this culture was also very low (Table 6.3).

The culture mainly consisted of *Tetrasphaera*-related organisms, where the four clades of *Tetrasphaera* comprised over 80% of the total microbial community. Contrary to the anaerobic/aerobic SBR study (Chapter 5), the Tet2-892 clade was the most abundant in this culture and clade Tet2-174 was also present, while the sum of Tet1-266 and Tet3-654 decreased slightly from 60% to 40% between studies (Table 6.4). Various morphologies were observed (short and branched rods, small cocci, cocci in tetrads, filaments, and thin filaments), which is consistent with the morphologies detected in the culture obtained under anaerobic/aerobic conditions discussed in Chapter 5. FISH quantification also confirmed the presence of *Competibacter* GAOs, with an abundance of 12% (Table 6.4). *Accumulibacter* PAOs was present in very low abundance (< 2%) and *Defluviicoccus* GAO were not detected.

Table 6.3 – Typical cycle study (anaerobic/anoxic/aerobic) obtained during SBR operation and comparison with *Accumulibacter* under similar operational conditions (Ribera-Guardia et al., 2016) and with *Tetrasphaera* + *Accumulibacter* under anaerobic/aerobic conditions.

Anaerobic results			
Dominant organisms	*Tetrasphaera* (this study)	*Accumulibacter*	*Tetrasphaera* + *Accumulibacter*
Carbon source	Casein hydrolysate	Propionate + Acetate	Casein hydrolysate
P release/substrate cons (P-mol/C-mol)	0.11±0.02	0.62±0.25[b]	0.35±0.08 [a]
Glycogen cons/substrate cons (C-mol/C-mol)	0.44±0.19	0.36±0.27[b]	0.38±0.12 [a]
PHB prod/substrate cons (C-mol/C-mol)	0.07±0.05	0.40±0.17[b]	0.03±0.01 [a]
PHV prod/substrate cons (C-mol/C-mol)	0.28±0.08	0.27±0.11[b]	0.09±0.02 [a]
PH2MV prod/substrate cons (C-mol/C-mol)	0.00±0.00	0.11±0.09[b]	0.03±0.01 [a]
PHA prod/substrate cons (C-mol/C-mol)	0.35±0.13	0.78±0.28[b]	0.15±0.04 [a]
Anaerobic pH	6.8±0.1	--	6.7±0.1 [a]
Anoxic results			
P uptake (Pmmol/L)	0.28 ±0.08	0.99 ±0.07[b]	
Glycogen Production (C-mmol/L)	1.37±0.17	-0.11±0.04[b]	
PHA Consumption (C-mmoL/L)	0.77±0.21	1.86±0.27[b]	
Aerobic results			
P uptake (Pmmol/L)	0.37 ±0.07	1.79 ±0.39[b]	1.76 ±0.25 [a]
% P in TSS	0.6-2.2	5-7[b]	8-19 [a]
Glycogen Production (C-mmol)	0.74±0.23	1.94±0.01[b]	1.38±0.70 [a]
PHA Consumption (C-mmol/L)	0.59±0.22	1.82±0.04[b]	0.75±0.24 [a]
Anoxic/Aerobic results			
P uptake (Pmmol/L)	0.65 ±0.06	2.79±0.43[b]	1.76 ±0.25 [a]
% P in TSS	0.6-2.2	5-7[b]	8-19 [a]
Glycogen Production (C-mmol/L)	2.11±0.06	1.82±0.03[b]	1.38±0.70 [a]
PHA Consumption (C-mmol/L)	1.36±0.06	3.69±0.30[b]	0.75±0.24 [a]

[a] (Chapter 5); [b] (Ribera-Guardia et al., 2016)

The absence of *Accumulibacter* PAOs and the presence of a small fraction of *Competibacter* GAOs likely contributed to the lower P uptake observed in this study as compared to the reactor previously operated under anaerobic/aerobic conditions described in Chapter 5. *Competibacter* would likely compete mostly for fermentation products such as acetate that would be produced by *Tetrasphaera*, although Kong et al., (2006) observed that *Competibacter* can take up certain amino acids. Since *Tetrasphaera* are not capable of PHA production (Kristiansen et al., 2013), the PHA produced under anaerobic conditions can be assumed to be stored by *Competibacter* through the uptake of fermentation products and certain amino acids. The slightly

higher anaerobic glycogen consumption and PHA production yields per C uptake and higher PHV fraction are consistent with GAO metabolism (Filipe et al. 2001) as opposed to PAO metabolism (Table 6.3).

Table 6.4 – Morphologies present in the SBR sludge and % volume fraction of *Competibacter* and each *Tetrasphaera*-related clade. Results obtained are an average of 3 samples taken during the experimental period.

Probe	Morphology	% vol. fraction
Tet1-266	Thin filaments, branched rods and cocci in tetrads	21.1±7.1
Tet2-892	Branched rods and filaments	9.1±3.8
Tet2-174	Filaments, tetrads and short rods/branched rods	32.6±8.8
Tet3-654	Branched rods and filament	19.3±6.9
GAOMIX	Rods and short rods in clumps	12.4±5.1
PAOMIX	cocci-bacilli and cocci	1.4±1.4
DFImix		<1

Accumulation of NO_2^- in the anoxic phase was also observed occasionally (Figure 6.1 b), where the NO_2^- remained during the aerobic phase. NO_2^- accumulation (more specifically in the form of free nitric acid) has been found to be inhibitory to anoxic and aerobic P uptake in PAOs, and is known to be toxic at different threshold levels to many organisms (Zhou et al., 2011). Nevertheless, NO_2^- accumulated only rarely, and at low levels (<7 mgN/L), where cycles without nitrite accumulation (Figure 6.1a) revealed a similar anoxic and aerobic P uptake level as compared to those with NO_2^- accumulation (Figure 6.1 b). Thus, it is unlikely that NO_2^- was present at levels that would lead to lower P-uptake in this anaerobic/anoxic/aerobic configuration as compared with the anaerobic/aerobic SBR (Chapter 5).

It should also be noted that the energy obtained from NO_3^- reduction by PAOs under anoxic conditions has been found to be typically 40% lower as compared to aerobic conditions, leading to lower P-uptake rates (Kuba et al., 1996). A reduction in energy generated anoxically by *Tetrasphaera* would both lower the P taken up under anoxic conditions, and may also deplete their storage compounds that would otherwise have been available for aerobic P uptake. This could also explain the lower P removal efficiency achieved by the *Tetrasphaera* enriched culture under anaerobic/anoxic/aerobic conditions as compared to anaerobic/aerobic conditions (Chapter 5).

6.3.2 Contribution of *Tetrasphaera* and *Competibacter* to NOx reduction

With both *Tetrasphaera* and *Competibacter* present in the culture, it was necessary to assess the contribution of each group to NOx reduction. To accomplish this, metabolic model predictions of denitrifying GAOs regarding the utilisation of PHA per NOx reduction were used. PHA is a differentiating factor between *Tetrasphaera* and *Competibacter*, since previous studies showed *Tetrasphaera*-related organisms are not able to produce PHAs (Kristiansen et al., 2013; Nguyen et al., 2011). Since very low *Accumulibacter* PAOs were detected in this culture, it was assumed that all PHA consumption for NOx reduction was associated with denitrification performed by GAOs.

During the anoxic phase, an average of 0.77±0.21 C-mmol/L of PHA was consumed during SBR operation. The ratio obtained of PHA utilisation to NOx reduction was 4.05 C-mmol/N-mmol, calculated according to the data shown in Table D1, Appendix D. Assuming all PHA is utilised by GAOs to perform NOx reduction, an average value of 0.19±0.05 N-mmol/L can be linked with these bacteria. An average of 1.67±0.05 N-mmol/L NO_3^- was reduced in the SBR and NO_2^- accumulation was considered negligible, thus it was assumed that NO_3^- was fully reduced to N_2O and N_2 gas. This led to 1.48 N-mmol/L reduction linked with *Tetrasphaera* (~90% of the total NOx) and 0.19 N-mmol/L (~10%) reduction to *Competibacter* GAOs. These results show that *Tetrasphaera*-related organisms were the main bacteria responsible for the N removal within this culture.

This result further validates the importance of *Tetrasphaera* in WWTPs, not only for P removal (Chapter 5), but also for denitrification. While the results of this study suggest that these organisms contribute relatively little to anoxic P removal, it is noteworthy that they are active anoxically for denitrification. This suggests an alternate route to achieve denitrification, even in non-EBPR systems. Supplementation of carbon sources to augment denitrification is an important issue in WWTPs, whereby amino acids are not typically added for this purpose. Addition of low-cost sources of amino acids, such as from residual streams, could represent an alternative means of achieving both N and P removal in WWTPs. One such example could be fish processing wastes (Ghaly, 2013), which have a high content of amino acids. The potential effectiveness of such a strategy in WWTPs requires further research.

6.3.3 Denitrification capabilities of *Tetrasphaera* culture

Individual electron acceptors

Batch tests with different electron acceptors were performed to study the denitrifying capacities of the *Tetrasphaera* enriched culture. In tests A, B and C electron acceptors NO_3^-, NO_2^- and N_2O were added individually. Similar reduction rates were obtained for NO_3^- (20.97 ± 2.31 mg N/gVSS.h) and NO_2^- (20.30 ± 3.10 mg N/gVSS.h), while the N_2O reduction rate (8.53 ± 0.22 mg N/gVSS.h) was slower (Figure 6.2, Appendix D Table D2 Supplemental Information). This clearly shows a preference of the culture for NO_3^- and NO_2^- reduction, while N_2O reduction had the lowest reduction rate of denitrification when fed individually. N_2O accumulation was also observed in both test A and B, although the N_2O reduction rates were higher as compared to the case when only N_2O was added. N_2O accumulation has also been observed in denitrifying PAO and GAO cultures with PHA as the electron donor (Lemaire et al., 2006; Ribera-Guardia et al., 2016; Wei et al., 2014; Zeng et al., 2003c), with either NO_3^- or NO_2^- as the electron acceptor. However, the increase of the N_2O reduction rate in the presence of NO_2^- vs NO_3^- addition, (20.20 ± 0.19 mg N/gVSS.h and 12.80 ± 0.76 mg N/gVSS.h, respectively) rules out this possibility (Figure 6.2, Appendix D Table D2).

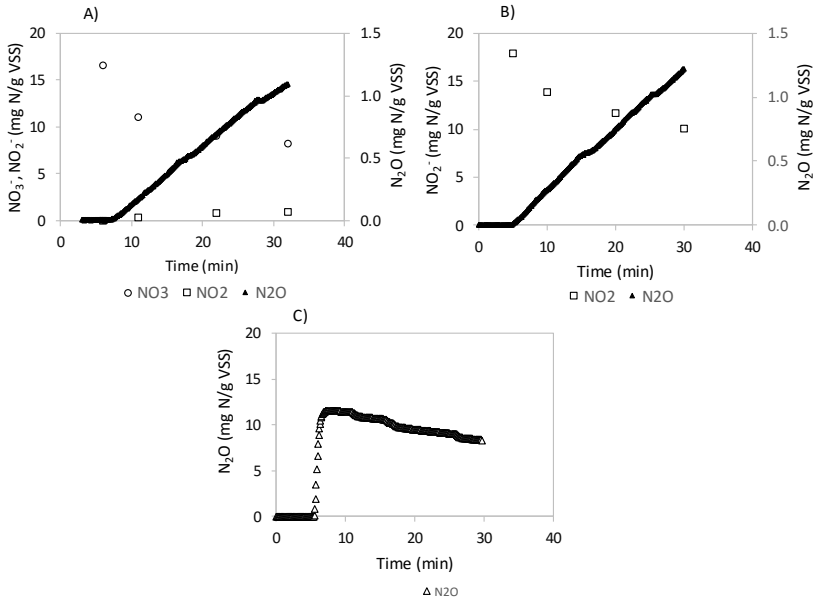

Figure 6.2 – Batch test profiles performed with different electron acceptors: Nitrate (A), Nitrite (B) and Nitrous oxide (C).

Higher reduction rates were obtained for NO_3^- (25.78 mg N/gVSS.h) in the external carbon source batch test. This result suggests the culture was carbon limited by the amount of internal metabolites (Figure D2 and Appendix D Table D2). Reduction rates of NO_2^- and N_2O were also higher (19.41 and 17.63 N/gVSS.h, respectively) as compared with test A. A decrease of 35% in N_2O accumulation at the end of external batch test when compared with the average accumulation obtained for test A. This result was further supported by a higher increase of N_2O reduction rate as compared with NO_2^-, in the external carbon source test (Appendix D Table D2). Limitation of intracellular carbon source during denitrification could potentially contribute to N_2O accumulation in this culture.

When fed alone, the N_2O reduction rate was significantly lower than when in presence of other NOx (Figures 6.2 and 6.3), which is in contrast to previous studies with ordinary heterotrophic denitrifiers fed with external carbon sources (Pan et al., 2013; Ribera-Guardia et al., 2014). One possible explanation for this lower N_2O reduction rate could be less efficient bioenergetics within the cell when metabolising this nitrogen oxide. N_2O reduction creates a lower amount of proton-motive force across the membrane to generate ATP. While reduction of NO_3^- to N_2 requires 10 electrons the reduction to N_2O requires 8. These 10 electrons are associated with translocation of 30 protons across the cytoplasmic membrane to drive ATP synthesis (~3.3 proton/ATP). The N_2O reduction can be associated with only 20% of energy generated by full denitrification, which will limit the bioenergetic advantage for a cell to perform this reduction (Richardson et al., 2009). This may explain why addition of N_2O as the only electron acceptor may lead to lower reduction rates as compared to situations where NO_3^- or NO_2^- are added, as once the N_2O is inside the cell, it is more readily reduced as compared to a situation where the cell must transport the N_2O prior to reduction, which generates comparatively little energy that does not compensate the transport step as readily.

When comparing the reduction rates obtained in this study with the results of Ribera-Guardia et al., (2016) for an enriched GAO culture and an enriched *Accumulibacter* PAO culture (Appendix D Figure D1), *Tetrasphaera* showed similar N_2O reduction than GAOs and lower than Accumulibacter PAO. On the other hand, nitrate reduction was higher in the *Tetrasphaera* culture as compared to the *Accumulibacter* or GAO cultures.

Combination of electron acceptors

The highest reduction rate of NO_3^- was observed in test A, while it decreased in tests D, F and G when other electron acceptors were added in combination (Figure 6.3, Appendix D Table D2). A similar pattern was observed for NO_2^- reduction rates, where the highest reduction rate of NO_2^- was observed in test B, while it decreased when other electron acceptors were also added (Figure 6.3, Appendix D Table D2). This suggests that *Tetrasphaera* has no preference for either NO_3^- or NO_2^-, reduction, while when both electron acceptors are present simultaneously the rates decrease. This suggests that electron competition could have an important role in these decreases of reduction rates.

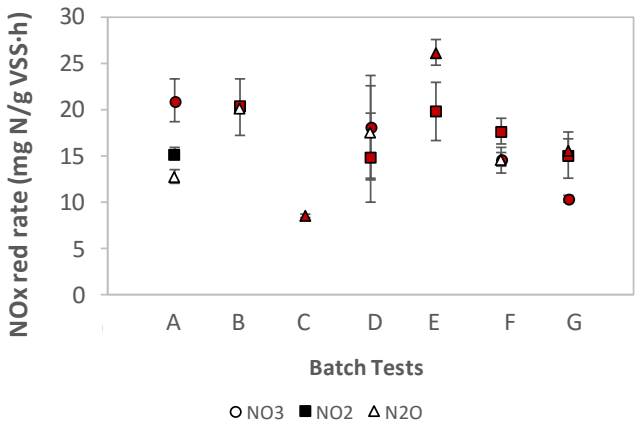

Figure 6.3 – Batch test profiles performed with different electron acceptors: Nitrate (A), Nitrite (B) and Nitrous oxide (C). (Red filled symbols, NOx added in each batch test).

The slowest N_2O reduction rate was obtained in test C, however, the rate increased in test D, E and G, respectively (Figure 6.3, Appendix D Table D2). This higher N_2O reduction rate with increased presence of NO_2^- and/or NO_3^- could be linked to an increased synthesis of enzymes responsible for N_2O reduction (Nos), perhaps caused by the increased available energy created by NO_2^- and/or NO_3^- reduction as explained above.

Interestingly, P-uptake had a similar rate in all tests performed with different combinations of electron acceptors (0.093±0.005 mmol-P/gVSS.h) (Table 6.5). When observing the ratio of P-uptake per NOx consumed, the ratio increased as a function of the number or nitrogen oxides provided (Table 6.5).

Table 6.5 – Rate of NOx consumed, glycogen production rate, P-uptake rate and ratio P-uptake/NOx and obtained during batch tests A, B, D, E, F and G with the *Tetrasphaera* enrichment.

Batch test type	NOx (mmol N/g VSS.h)	Gly Prod (C-mmol/g VSS.h)	P-uptake (P-mmol/ g VSS.h)	P-uptake/NOx (P-mmol/mmol N)
A	0.57±0.00	0.45±0.18	0.05±0.01	0.06±0.02
B	0.64±0.04	0.05±0.02	0.03±0.03	0.04±0.04
C	0.38±0.04	-0.07±0.05	0.01±0.00	0.02±0.00
D	0.86±0.24	0.19±0.13	0.10±0.01	0.15±0.04
E	1.14±0.01	0.25±0.01	0.09±0.01	0.08±0.01
F	0.57±0.10	0.10±0.02	0.09±0.03	0.17±0.08
G	0.71±0.10	0.20±0.04	0.09±0.01	0.13±0.03
Ext A	0.99	0.066	0.90	-0.043

6.3.4 Electron competition and distribution

The lower NO_3^- and NO_2^- reduction rates observed when multiple NOx were added as compared to the case where only one was added suggests that electron competition occurred within the culture. Previous studies have shown that electron competition occurs during ordinary heterotrophic denitrification either in conditions of limited or excess carbon substrates (Pan et al., 2013; Von Schulthess et al., 1994). This is the first study examining electron competition for an enriched *Tetrasphaera*-related PAO culture.

The total average electron consumption rate in the presence of two or more electron acceptors added simultaneously (tests D to G) was very similar (average of 5.27±0.55 mmol e-/gVSS.h) (Figure 6.4). This value was also very similar to the total electron consumption rate obtained in test A with NO_3^- (6.40 mmol e-/gVSS.h) (Figure 6.4). This indicates that these electron consumption rates were limited by the upstream electron supply from the carbon oxidation process of the internal metabolites, suggesting that the denitrification enzymes were competing for electron donors from a limited electron supply system originated from the same internal metabolites. In fact, a higher electron consumption rate (8.20 mmol e-/gVSS.h) was obtained in a test performed with external carbon source, at the same concentration as added to the main SBR, with NO_3^- added as sole electron acceptor (Figure 6.4). This result further supports the idea that cells were unable to supply sufficient electrons from internally stored sources and meet the energy demand to perform denitrification at their maximum rate.

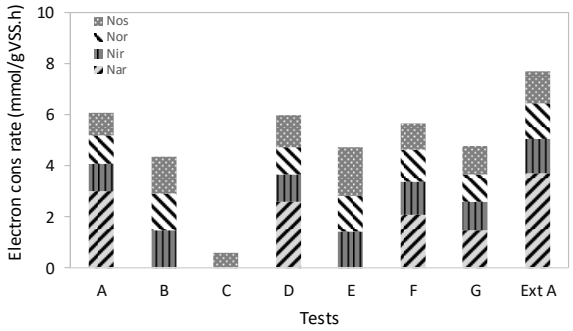

Figure 6.4 – Electron consumption rates for nitrate reductase (Nar), nitrite reductase (Nir), nitric oxide reductase (Nor) and nitrous oxide reductase (Nos) with the *Tetrasphaera* culture.

Another interesting observation is that the combination of NO_3^- and N_2O (test D) showed a higher electron consumption rate as compared to NO_2^- and N_2O (test E). It has been observed that Nar receives electrons directly from the ubiquinone/ubiquinol pool (UQ/UQH_2), while Nir, Nor and Nos receive their electrons from the cytochrome c550/pseudoazurin pool (Cyt c550/Ps az) by way of the UQ/UQH_2 pool. Due to this difference in electron flow, it is expected that the electron competition between Nar and Nos would be smaller as compared with Nir and Nos (Pan et al., 2013; Richardson et al., 2009). This hypothesis agrees very well with the results obtained in this study.

Table 6.6 shows the electron distribution between Nar, Nir, Nor and Nos within each batch test performed. A decrease in Nar activity was confirmed by the electron distribution between tests where NO_3^- was fed alone or in combination with other nitrogen oxides, decreasing from 49.1% to 43.4%, to 37.1% to 31.5% in tests, A, D, F and G, respectively. Similarly, both NO_3^- and N_2O had a similar impact on Nir activity as can be observed from the electron distribution (Table 6.6), being highest when NO_2^- was fed individually. This supports the hypothesis that both Nar and Nir activity were affected by electron competition. In the case of N_2O reduction, the total electron consumption rate obtained in test C was only about 1/10 of the value obtained in the other batch tests (Figure 6.4). This supports the fact that N_2O was energetically unfavourable for the culture when fed in isolation, which can be explained by the fact that N_2O reduction only comprises around 20% of the bioenergetic potential as compared to full denitrification.

When comparing the P-uptake/electron consumption ratio, higher P-uptake was obtained in tests D, E F and G. This shows that the culture channelled more energy obtained from the reduction of the NOx present to perform P-uptake, despite the similar total electron consumption rate (Figure 6.5). This could either be due to a lower activity

of GAOs when multiple NOx were added, or a shift in the metabolism employed by *Tetrasphaera*, prioritising P-uptake over glycogen production and/or biomass growth.

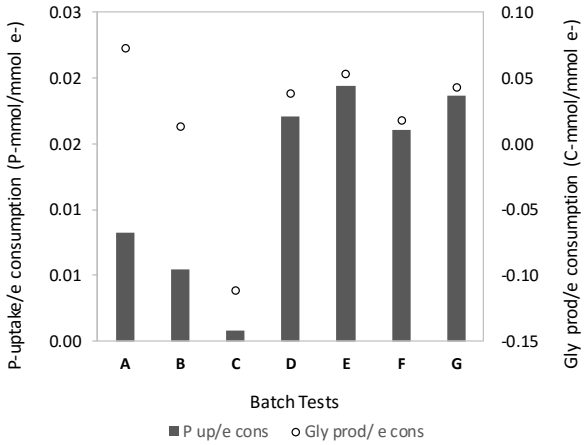

Figure 6.5 – Electron consumption rates for nitrate reductase (Nar), nitrite reductase (Nir), nitric oxide reductase (Nor) and nitrous oxide reductase (Nos) with the *Tetrasphaera* culture.

In this study it was not possible to link the internal carbon consumption of the *Tetrasphaera*-related bacteria with the electron consumption. The intracellular storage compound has not been entirely revealed, with glycogen, amino acids or macromolecules being observed as storage compounds (Kristiansen et al., 2013; Nguyen et al., 2015). The clarification of this issue would allow improvement in the understanding of the denitrification metabolism by these bacteria.

Table 6.6 – Rate of NOx consumed, glycogen production rate, P-uptake rate and ratio P-uptake/NOx and obtained during batch tests A, B, D, E, F and G with the *Tetrasphaera* enrichment.

Batch Test	electron distribution *Tetrasphaera*			
	Nar	Nir	Nor	Nos
	%			
A	49.1±3.9	17.9±1.3	17.9±1.3	15.1±1.3
B	0.0	33.2±1.6	33.2±1.6	33.6±3.2
C	0.0	0.0	0.0	100.0
D	43.3±0.3	17.7±0.0	17.7±0.0	21.2±0.4
E	0.0	30.0±1.2	30.0±1.2	40.0±2.5
F	37.1±0.8	22.3±0.2	22.3±0.2	18.4±0.2
G	31.5±2.3	22.5±1.5	22.5±1.5	23.5±0.6
Ext. A	49.4	16.9	16.9	16.9

6.4 CONCLUSIONS

Tetrasphaera was enriched in an EBPR system through an anaerobic/anoxic/aerobic cycle operation fed with amino acids. *Tetrasphaera* showed a good capacity for denitrification, being responsible for >85% of the denitrification in the SBR, although only little anoxic P uptake was observed. The results suggested that the organic carbon taken up anaerobically by *Tetrasphaera* appears to provide sufficient energy to achieve either anoxic denitrification or aerobic P removal rather than both denitrification and P removal simultaneously. Batch tests with individual electron acceptors revealed a preference for NO_3^- and NO_2^- reduction, with N_2O reduction being the limiting step. When two or more electron acceptors were present simultaneously, electron competition occurred, affecting the reduction rates achieved during the four reduction steps. The limitation of internal carbon source and the electron distribution within the electron carriers might affect and limit the enzyme activities. Increased anoxic P-uptake was linked with higher electron competition, suggesting a shift in the metabolism when multiple nitrogen oxides were present. The increased understanding of the metabolism of *Tetrasphaera*-related organisms may improve the efficiency of phosphorous and nitrogen removal in EBPR WWTPs.

Acknowledgements

The authors thank the Portuguese Fundação para a Ciência e Tecnologia (UID/Multi/04378/2013, AMB/120581/2010) and UCIBIO (FCT/MEC UID/Multi/04378/2013, POCI-01-0145-FEDER-007728) for financing. Ricardo Marques acknowledge the PhD grant SFRH/BD/74515/2010) provided by Portuguese Fundação para a Ciência e Tecnologia. Spanish and Portuguese Governments are acknowledged for Acciones Integradas (PRI-AIBPT-2011-1232) and Luso-Espanhola action E-61/12. The European Commission is also acknowledged through COST action ES1202 (Water 2020). M. Pijuan and A. Ribera-Guardia acknowledge the Ramon y Cajal research fellowship (RYC-2009-04959) and the FPIPhD grant (BES-2012-052753) respectively provided by the Spanish Government.

REFERENCES

Amann, R., 1995. In situ identification of micro-organisms by whole cell hybridization with rRNA-targeted nucleic acid probes. Mol. Microb. Ecol. 4, 331–345.

Amann, R.I., Binder, B.J., Olson, R.J., Chisholm, S.W., Devereux, R., Stahl, D. a, 1990. Combination of 16S rRNA-targeted oligonucleotide probes with flow cytometry for analyzing mixed microbial populations. Appl. Environ. Microbiol. 56, 1919–25.

APHA, 2005. Standard methods for the examination of water and wastewater, 21st editi. ed. Washington, D.C.

Burow, L.C., Kong, Y., Nielsen, J.L., Blackall, L.L., Nielsen, P.H., 2007. Abundance and ecophysiology of Defluviicoccus spp., glycogen-accumulating organisms in full-scale wastewater treatment processes. Microbiology 153, 178–185.

Carvalho, G., Lemos, P.C., Oehmen, A., Reis, M. a M., 2007. Denitrifying phosphorus removal: linking the process performance with the microbial community structure. Water Res. 41, 4383–96.

Cech, J.S., Hartman, P., 1993. Competition between polyphosphate and polysaccharide accumulating bacteria in enhanced biological phosphate removal systems. Water Res. 27, 1219–1225.

Crocetti, G.R., Hugenholtz, P., Bond, P.L., Schuler, a, Keller, J., Jenkins, D., Blackall, L.L., 2000. Identification of polyphosphate-accumulating organisms and design of 16S rRNA-directed probes for their detection and quantitation. Appl. Environ. Microbiol. 66, 1175–82.

Daelman, M.R.J., De Baets, B., van Loosdrecht, M.C.M., Volcke, E.I.P., 2013. Influence of sampling strategies on the estimated nitrous oxide emission from wastewater treatment plants. Water Res. 47, 3120–3130.

Daelman, M.R.J., van Voorthuizen, E.M., van Dongen, L.G.J.M., Volcke, E.I.P., van Loosdrecht, M.C.M., 2013. Methane and nitrous oxide emissions from municipal wastewater treatment - results from a long-term study. Water Sci. Technol. 67, 2350–5.

Daims, H., Brühl, a, Amann, R., Schleifer, K.H., Wagner, M., 1999. The domain-specific probe EUB338 is insufficient for the detection of all Bacteria: development and evaluation of a more comprehensive probe set. Syst. Appl. Microbiol. 22, 434–44.

Flowers, J.J., He, S., Malfatti, S., del Rio, T.G., Tringe, S.G., Hugenholtz, P., McMahon, K.D., 2013. Comparative genomics of two "*Candidatus* Accumulibacter" clades performing biological phosphorus removal. ISME J. 7, 2301–14.

Flowers, J.J., He, S., Yilmaz, S., Noguera, D.R., McMahon, K.D., 2009. Denitrification capabilities of two biological phosphorus removal sludges dominated by different "Candidatus Accumulibacter" clades. Environ. Microbiol. Rep. 1, 583–588.

Ghaly, A., 2013. Microbial & Biochemical Technology Fish Processing Wastes as a Potential Source of Proteins, Amino Acids and Oils: A Critical Review. J Microb Biochem Technol Amin. Acids Oils A Crit. Rev. J Microb Biochem Technol 54172, 107–129.

IPCC, Stocker, T.F., Qin, D., Plattner, G.-K., Tignor, M.M.B., Allen, S.K., Boschung, J., Nauels, A., Xia, Y., Bex, V., Midgley, P.M., 2013. Climate Change 2013 - The Physical Science Basis, Intergovernmental Panel on Climate Change.

Kong, Y., Nielsen, J.L.J.J.L., Nielsen, P.H.P.P.H., 2005. Identity and Ecophysiology of Uncultured Actinobacterial Polyphosphate-Accumulating Organisms in Full-Scale Enhanced Biological Phosphorus Removal Plants. Appl. Environ. Microbiol. 71, 4076–4085.

Kong, Y., Ong, S.L., Ng, W.J., Liu, W.T., 2002. Diversity and distribution of a deeply branched novel proteobacterial group found in anaerobic-aerobic activated sludge processes. Environ. Microbiol. 4, 753–757.

Kong, Y., Xia, Y., Nielsen, J.L., Nielsen, P.H., 2006. Ecophysiology of a group of uncultured Gammaproteobacterial glycogen-accumulating organisms in full-scale enhanced biological phosphorus removal wastewater treatment plants. Environ. Microbiol. 8, 479–489.

Kong, Y., Xia, Y., Nielsen, P.H., 2008. Activity and identity of fermenting microorganisms in full-scale biological nutrient removing wastewater treatment plants. Environ. Microbiol. 10, 2008–19.

Kristiansen, R., Nguyen, H.T.T., Saunders, A.M., Nielsen, J.L., Wimmer, R., Le, V.Q., Mcilroy, S.J., Petrovski, S., Seviour, R.J., Calteau, A., Nielsen, K.L., Nielsen, P.H.H., Thi, H., Nguyen, T., Saunders, A.M., Lund Nielsen, J., Wimmer, R., Le, V.Q., Mcilroy, S.J., Petrovski, S., Seviour, R.J., Calteau, A., Lehmann Nielsen, K., Nielsen, P.H.H., 2013. A metabolic model for members of the genus Tetrasphaera involved in enhanced biological phosphorus removal. Iternational Soc. Microb. Ecol. 7, 543–554.

Kuba, T., Murnleitner, E., Loosdrecht, M.C.M. Van, Heijnen, J.J., 1996. A Metabolic Model for Biological Phosphorus Removal by Denitrifying Organisms. Biotechnol. Bioeng. 52, 685–695.

Lanham, A.A.B., Oehmen, A.A., Saunders, A.M.A., Carvalho, G., Nielsen, P.H., Reis, M. a M., 2013. Metabolic versatility in full-scale wastewater treatment plants performing enhanced biological phosphorus removal. Water Res. 47, 7032–41.

Lanham, A.B., Ricardo, A.R., Albuquerque, M.G.E., Pardelha, F., Carvalheira, M., Coma, M., Fradinho, J., Carvalho, G., Oehmen, A., Reis, M. a M., 2013. Determination of the extraction kinetics for the quantification of polyhydroxyalkanoate monomers in mixed microbial systems. Process Biochem. 48, 1626–1634.

Lanham, A.B., Ricardo, A.R., Coma, M., Fradinho, J., Carvalheira, M., Oehmen, A., Carvalho, G., Reis, M. a M., 2012. Optimisation of glycogen quantification in mixed microbial cultures. Bioresour. Technol. 118, 518–525.

Lemaire, R., Meyer, R., Taske, A., Crocetti, G.R., Keller, J., Yuan, Z., 2006. Identifying causes for N2O accumulation in a lab-scale sequencing batch reactor performing simultaneous nitrification, denitrification and phosphorus removal. J. Biotechnol. 122, 62–72.

Li, C., Zhang, J., Liang, S., Ngo, H.H., Guo, W., Zhang, Y., Zou, Y., 2013. Nitrous oxide generation in denitrifying phosphorus removal process: Main causes and control measures. Environ. Sci. Pollut. Res. 20, 5353–5360.

Louie, T.M., Mah, T.J., Oldham, W., Ramey, W.D., 2000. Use of metabolic inhibitors and gas chromatography/mass spectrometry to study poly-β-hydroxyalkanoates metabolism involving cryptic nutrients in enhanced biological phosphorus removal systems. Water Res. 34, 1507–1514.

McIlroy, S.J., Nittami, T., Seviour, E.M., Seviour, R.J., 2010. Filamentous members of cluster III Defluviicoccus have the in situ phenotype expected of a

glycogen-accumulating organism in activated sludge. FEMS Microbiol. Ecol. 74, 248–256.

Meyer, R.L., Saunders, A.M., Blackall, L.L., 2006. Putative glycogen-accumulating organisms belonging to the Alphaproteobacteria identified through rRNA-based stable isotope probing. Microbiology 152, 419–429.

Muszyński, A., Miłobędzka, A., 2015. The effects of carbon/phosphorus ratio on polyphosphate- and glycogen-accumulating organisms in aerobic granular sludge. Int. J. Environ. Sci. Technol.

Nguyen, H.T.T., Kristiansen, R., Vestergaard, M., Wimmer, R., Nielsen, P.H., 2015. Intracellular Accumulation of Glycine in Polyphosphate-Accumulating Organisms in Activated Sludge, a Novel Storage Mechanism under Dynamic Anaerobic-Aerobic Conditions. Appl. Environ. Microbiol. 81, 4809–18.

Nguyen, H.T.T., Le, V.Q., Hansen, A.A., Nielsen, J.L., Nielsen, P.H.H., 2011. High diversity and abundance of putative polyphosphate-accumulating Tetrasphaera-related bacteria in activated sludge systems. FEMS Microbiol. Ecol. 76, 256–67.

Nittami, T., McIlroy, S., Seviour, E.M., Schroeder, S., Seviour, R.J., 2009. Candidatus Monilibacter spp., common bulking filaments in activated sludge, are members of Cluster III Defluviicoccus. Syst. Appl. Microbiol. 32, 480–489.

Oehmen, A., Lemos, P.C., Carvalho, G., Yuan, Z., Keller, J.J., Blackall, L.L., Reis, M. a M., 2007. Advances in enhanced biological phosphorus removal: From micro to macro scale. Water Res. 41, 2271–2300.

Oehmen, A., Lopez-Vazquez, C.M.M., Carvalho, G., Reis, M.A.M.A.M., van Loosdrecht, M.C.M.C.M., 2010. Modelling the population dynamics and metabolic diversity of organisms relevant in anaerobic/anoxic/aerobic enhanced biological phosphorus removal processes. Water Res. 44, 4473–4486.

Pan, Y., Ni, B.J., Bond, P.L., Ye, L., Yuan, Z., 2013. Electron competition among nitrogen oxides reduction during methanol-utilizing denitrification in wastewater treatment. Water Res. 47, 3273–3281.

Pereira, H., Lemos, P.C.P.C.P.C., Reis, M.A.M.A.M., Crespo, J.P.S.G., Carrondo, M.J.T., Santos, H., Cresp, J.P.S.G., Carrondo, M.J.T., Santos, H., 1996. Model for carbon metabolism in biological phosphorus removal processes based on in vivo13C-NMR labelling experiments. Water Res. 30, 2128–2138.

Ribera-Guardia, A., Kassotaki, E., Gutierrez, O., Pijuan, M., 2014. Effect of carbon source and competition for electrons on nitrous oxide reduction in a mixed denitrifying microbial community. Process Biochem. 49, 2228–2234.

Ribera-Guardia, A., Marques, R., Arangio, C., Carvalheira, M., Oehmen, A., Pijuan, M., 2016. Distinctive denitrifying capabilities lead to different N2O production in dPAO and dGAO. Bioresource Technology (in press, 2016).

Richardson, D., Felgate, H., Watmough, N., Thomson, A., Baggs, E., 2009. Mitigating release of the potent greenhouse gas N2O from the nitrogen cycle - could enzymic regulation hold the key? Trends Biotechnol. 27, 388–397.

Smolders, G.J., van der Meij, J., van Loosdrecht, M.C., Heijnen, J.J., 1994. Model of the anaerobic metabolism of the biological phosphorus removal process: Stoichiometry and pH influence. Biotechnol. Bioeng. 43, 461–70.

Tsuneda, S., Ohno, T., Soejima, K., Hirata, A., 2006. Simultaneous nitrogen and phosphorus removal using denitrifying phosphate-accumulating organisms in a sequencing batch reactor. Biochem. Eng. J. 27, 191–196.

Von Schulthess, R., Wild, D., Gujer, W., 1994. Nitric and nitrous oxides from denitrifying activated sludge at low oxygen concentration. Water Sci. Technol. 30, 123–132.

Wang, X., Zeng, R.J., Dai, Y., Peng, Y., Yuan, Z., 2008. The denitrification capability of cluster 1 Defluviicoccus vanus-related glycogen-accumulating organisms. Biotechnol. Bioeng. 99, 1329–1336.

Wang, Y., Geng, J., Ren, Z., He, W., Xing, M., Wu, M., Chen, S., 2011. Effect of anaerobic reaction time on denitrifying phosphorus removal and N2O production. Bioresour. Technol. 102, 5674–84.

Wei, Y., Wang, S., Ma, B., Li, X., Yuan, Z., He, Y., Peng, Y., 2014. The effect of poly-B-hydroxyalkanoates degradation rate on nitrous oxide production in a denitrifying phosphorus removal system. Bioresour. Technol. 170, 175–182.

Wexler, M., Richardson, D.J., Bond, P.L., 2009. Radiolabelled proteomics to determine differential functioning of Accumulibacter during the anaerobic and aerobic phases of a bioreactor operating for enhanced biological phosphorus removal. Environ. Microbiol. 11, 3029–3044.

Wong, M.T., Tan, F.M., Ng, W.J., Liu, W.T., 2004. Identification and occurrence of tetrad-forming Alphaproteobacteria in anaerobic-aerobic activated sludge processes. Microbiology 150, 3741–3748.

Ye, L., Ni, B.J., Law, Y., Byers, C., Yuan, Z., 2014. A novel methodology to quantify nitrous oxide emissions from full-scale wastewater treatment systems with surface aerators. Water Res. 48, 257–268.

Zeng, R.J., Lemaire, R., Yuan, Z., Keller, J.J., 2003a. Simultaneous nitrification, denitrification, and phosphorus removal in a lab-scale sequencing batch reactor. Biotechnol. Bioeng. 84, 170–178.

Zeng, R.J., Yuan, Z., Keller, J.J., 2003b. Enrichment of denitrifying glycogen-accumulating organisms in anaerobic/anoxic activated sludge system. Biotechnol. Bioeng. 81, 397–404.

Zhou, Y., Lim, M., Harjono, S., Ng, W.J., 2012. Nitrous oxide emission by denitrifying phosphorus removal culture using polyhydroxyalkanoates as carbon source. J. Environ. Sci. 24, 1616–1623.

Zhou, Y., Oehmen, A., Lim, M., Vadivelu, V., Ng, W.J., 2011. The role of nitrite and free nitrous acid (FNA) in wastewater treatment plants. Water Res. 45, 4672–4682.

Zhou, Y., Pijuan, M., Zeng, R.J., Yuan, Z., 2009. Involvement of the TCA cycle in the anaerobic metabolism of polyphosphate accumulating organisms (PAOs). Water Res. 43, 1330–40.

Zumft, W.G., 1997. Cell biology and molecular basis of denitrification. Microbiol. Mol. Biol. Rev. 61, 533–616.

7

GENERAL CONCLUSIONS AND FUTURE WORK

7.1 GENERAL CONCLUSIONS

This work contributed to the validation of a new N_2O monitoring methodology that will allow advances in the understanding of N_2O production and emissions in lab and full-scale systems. Moreover, this study established differences of the ecological niche of *Tetrasphaera* towards P and N removal in comparison with other organisms present in EBPR systems.

Lab-scale and full-scale Clark-type N_2O gas sensors proved to be a valid and reliable alternative to standard methods to quantify N_2O concentration in the gas phase of lab and full-scale systems. An exponential correlation between temperature and sensor signal was found, and N_2O was adequately predicted with few experimental measurements needed. The sensors displayed a linear response with different concentration ranges. The N_2O emission dynamics from two lab-scale sequencing batch reactors with different emission ranges were accurately described by the lab-scale sensor, supporting their application for assessing gaseous N_2O emissions. The full-scale sensor accurately described the N_2O gas emissions in a full-scale SBR, being even more accurate than a commercial analyser in monitoring high-level emissions. This methodology overcomes some limitations of conventional methods and includes a wider quantification range of N_2O emissions from lab and full-scale systems, increasing the accuracy of assessing greenhouse gas emissions. Moreover, a single measurement system can assess both liquid and gas-phase N_2O dynamics. The use of dissolved N_2O measurements was shown to provide a reasonable estimation of gaseous N_2O emissions in a full-scale WWTP facility. This was the first report showing on-line estimation of gas emissions based on dissolved N_2O online data.

Due to the high abundance of *Tetrasphaera* in full-scale BNR systems, their metabolism and contribution towards P and N removal was also addressed in this work. A culture enrichment was obtained with *Tetrasphaera* as the predominant PAO group, which consumed amino acids anaerobically and achieved high aerobic P-removal. *Tetrasphaera* performed the majority of the P removal in this culture, and batch tests showed that the metabolism of some carbon sources can actually lead to anaerobic P uptake through energy generated by fermentation of glucose and amino acids. Anaerobic P uptake may lead to lower net P-release to C-uptake ratios and reduce the P needed to be removed aerobically in WWTPs. MAR-FISH confirmed that *Tetrasphaera*, not *Accumulibacter*, were responsible for amino acid and glucose consumption, while *Accumulibacter* likely survive on fermentation products. Batch tests

demonstrated that *Tetrasphaera* had higher kinetics towards the uptake of certain amino acids. Different intracellular metabolites were detected, and may be stored anaerobically and contribute as energy sources in the aerobic phase. *Tetrasphaera* and *Accumulibacter* were found to contribute to P uptake through different ecological niches. The understanding of this synergy between *Tetrasphaera* and *Accumulibacter* improves our knowledge about how P removal is actually achieved in EBPR WWTPs and may lead to new cost-effective strategies for process optimisation.

Tetrasphaera enriched culture was also used in a BNR system through an anaerobic/anoxic/aerobic cycle operation fed with amino acids, where their denitrifying capacities were assessed. *Tetrasphaera* was the major organism responsible for denitrification in this culture, however, only little anoxic P uptake was observed. The culture revealed a preference for NO_3 and NO_2 reduction, with N_2O reduction being the limiting step. Electron competition occurred when 2 or more electron acceptors were present simultaneously. An increase in the anoxic P-uptake was linked with higher electron competition, suggesting a shift in the metabolism when multiple nitrogen oxides were present. The activity of *Tetrasphaera* could potentially be exploited by amino acid addition as a supplemental carbon source in WWTPs to achieve denitrification and/or aerobic P removal. The increased understanding of the metabolism of *Tetrasphaera*-related PAOs may improve the efficiency of phosphorus and nitrogen removal in EBPR WWTPs and/or their versatility for dealing with wastewaters with different compositions of organic carbon.

7.2 FUTURE WORK

The advances achieved with this work raised new questions, and some suggestions for future research are discussed below:

Numerous important questions remain regarding the role of *Tetrasphaera*-related PAOs in EBPR systems. The intracellular carbon storage products that are used under aerobic or anoxic conditions as well as the metabolic pathways employed by these organisms are still not fully understood. Further tests with analytical methods such as GC-MS, HPLC-MS and nuclear magnetic resonance (NMR) should be used to identify all intracellular storage compounds. Coupling this analysis with mass and energetic balances will allow characterization of the biochemical pathways employed by these organisms. The metabolism of other organisms present in WWTPs has been frequently studied using enriched cultures of microorganisms. These studies with mixed cultures

allowed identification of specific factors promoting their growth or activity. Systematic study to identify the optimal conditions (e.g. Temperature, pH, dissolved oxygen level, COD/P ratio in the influent, SRT, carbon composition) would allow us to establish optimal operational conditions for *Tetrasphaera* and optimization of P removal. Identification of optimal operational conditions for enriched *Tetrasphaera* mixed cultures should be confirmed by full-scale studies. This will allow us to close the gap between lab and full-scale studies and obtain comparative data. Anaerobic-aerobic batch tests with fresh sludge coupled with tools such as MAR-FISH should be performed to validate the identified parameters. This will allow to validate the extent of the findings achieved in lab-scale studies and the influence of environmental, operating conditions and wastewater characteristics on the performance of *Tetrasphaera* PAOs. A distinctive characteristic of *Tetrasphaera* as compared to *Accumulibacter* is the ability to ferment carbon sources and obtain energy to perform anaerobic P-uptake. This would be advantageous in full-scale, reducing the P needed to be removed aerobically in WWTPs, minimizing the extent of the aeration required. This has the added advantage of minimizing aeration costs and decreasing indirect GHG emissions from the facilities.

The denitrifying capacities of *Tetrasphaera* should also be further investigated. The effect of external carbon sources, high and low COD/N ratios, different carbon compositions and optimal operational factors should be investigated. As a final validation, operation of a bioreactor with real wastewater with optimal conditions identified will allow evaluation of the impact of wastewater characteristics on their anoxic metabolism. This will contribute to optimize the denitrifying efficiency of this bacterial group. Integration of this knowledge with the characterization of N_2O emissions in Full-scale EBPR plants can contribute to identify factors minimising N_2O accumulation and emission in WWTPs.

This work led to the development of a new method for on line monitoring N_2O emission from WWTPs. The added advantage of measuring the N_2O in the liquid and gas-phases should be further exploited at full-scale WWTPs. Measuring emissions in both phases will allow to assess the mechanisms of N_2O production and consumption and the impact on the emissions from WWTPs. This will allow us to develop new operational strategies designed to mitigate N_2O emissions Further measurement campaigns should be performed at WWTPs with different configurations, along different seasonal periods and for long measurement periods in order to characterise WWTP emissions using this technique.

The versatility of *Tetrasphaera* to utilize different carbon sources as compared with *Accumulibacter* should be better explored and exploited. Addition of low-cost sources of amino acids, such as from residual streams from fish processing industries (Source of Proteins, Amino Acids and Oils), could represent an alternative means of achieving both N and P removal in WWTPs. Performing batch tests with real wastewater sludge with and without supplementation of residual streams from the fish processing industry, rich in proteins and amino acids, would allow us to verify the feasibility of this possibility. The versatility of BNR systems to deal with wastewaters with different compositions of organic carbon can be an advantage to improve their efficiency. The activity of *Tetrasphaera* could potentially be better exploited by the addition of cheap sources of amino acids as a supplemental carbon source in WWTPs to achieve denitrification and/or aerobic P removal.

Metabolic models are also an interesting approach to simulate and predict the effect of different parameters on the growth and activity of microbial groups. Existing models already describe the biochemical activity of *Accumulibacter* PAOs and different groups of GAOs. This work as well as the continued identification of the important factors affecting P and N removal by *Tetrasphaera*, should be integrated into previously developed EBPR models in order to improve the characterization of full-scale EBPR systems and to better optimise them.

.

APPENDICES – A TO D

APPENDIX A

Appendix A1: Sensors used for the test

Six Clark-Type sensors provided by UNISENSE, with an internal reference and a guard cathode, were used for this study. All the sensors are presented in Figure A1.

Figure A1 - Clark type gas N_2O microsensors used in this study.

General experimental set-up used to perform most of the microsensor tests is shown in figure A2 and A3:

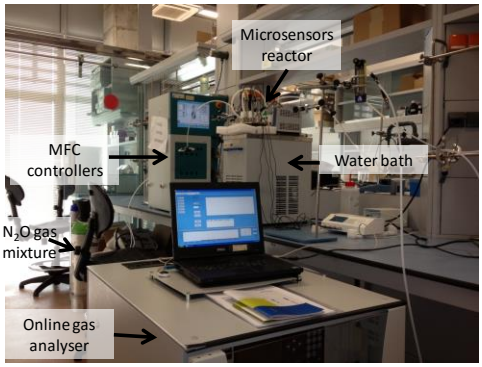

Figure A2 - General view of the experimental laboratory set-up.

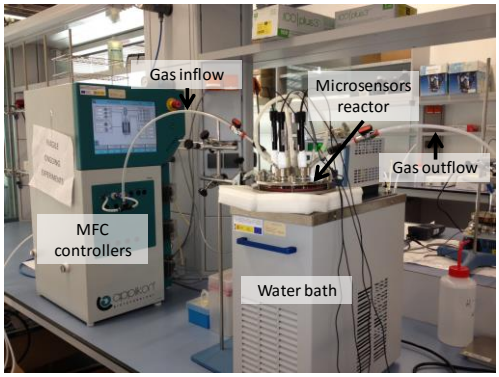

Figure A3 - Zoomed view of the microsensors reactor.

Appendix A2: Comparison between the four Sensors and the commercial analyser and GC-ECD.

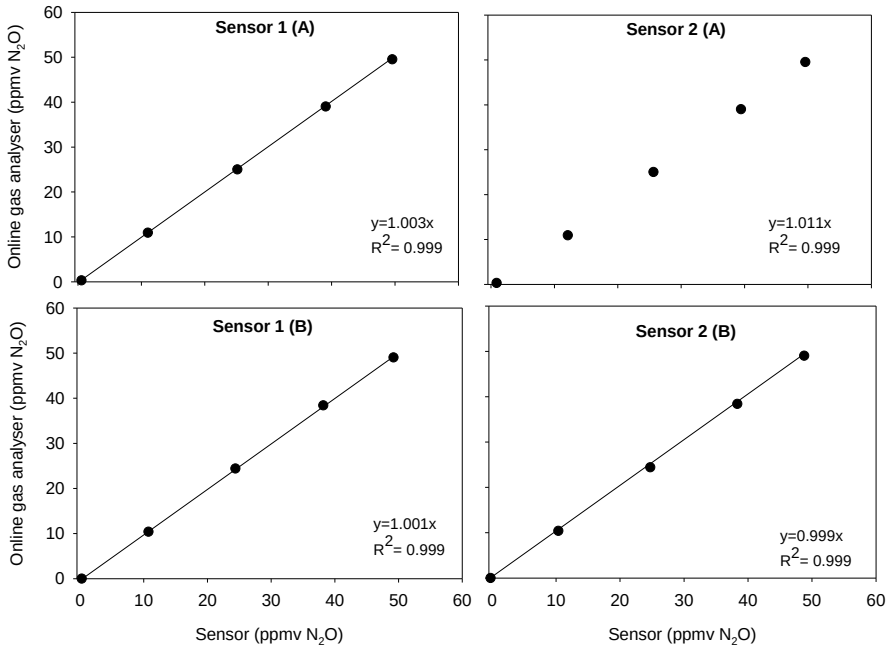

Figure A4 - Concentration measured by the commercial gas analyser vs Sensors at controlled temperature (25 °C) and with nitrogen (A) or air (B) as dilution gas.

Table A1 – Sensor 1 linear regression between sensor signal and concentration of N_2O within the range of 0 to 2 ppmv of N_2O, with temperature controlled at 25°C.

Type of Sensor	Equation	Coefficient of determination	Gas	Range (ppmv N_2O)
Sensor 1	Y=0.591x+9.96	R^2=0.984	N_2	0-2

Appendix A3: Random concentration peak test

A random concentration peak test, with a concentration range from 0 to 50 ppmv of N_2O with 8 different concentrations (0.0, 48.9, 10.4, 34.3, 41.3, 24.2, 18.1 and 44.0 ppmv of N_2O) was performed. A linear regression was performed between the sensor signal and the random peak concentrations, where the equations and coefficients of determination presented in Figure A5 were obtained.

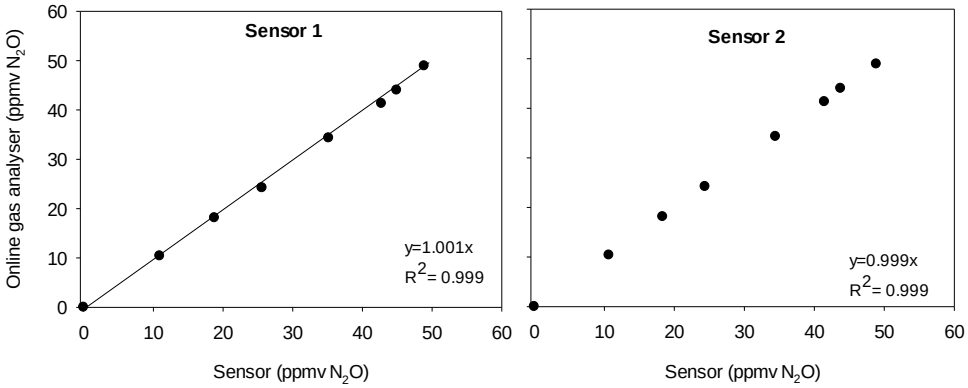

Figure A5 - Linear regression between sensor signal and concentration with random concentration peaks.

Appendix A4: Dilution gas and flow test

The influence of two different gases (Air and Nitrogen) on the sensor signal were evaluated, where negligible impact was observed (Table A2, A). Changes in the gas flow in the defined range (0.2-4 L/min) (Table A2, B) also did not affect the zero signal of the sensors. These results were obtained with nitrogen and air as dilution gases for Sensor 1 and Sensor 2.

Table A2 - Variation of the Sensor signal (1 and 2) with the change of the dilution gas (A). Variation of the sensor signal (1 and 2) with air and nitrogen within a range of flow from 0.2 to 4 L/min (B).

	Gas	Sensor 1 signal (mV)	Commercial gas analyser (N_2O ppmv)	Sensor 2 signal (mV)	Flow (L/min)
A	Air	7.25	0.3	25.09	1.5
	N_2	6.67	0	24.53	1.5
	Gas	**Average Sensor 1 signal (mV)**	**Std**	**Average Sensor 2 signal (mV)**	**Std**
B	Air	12.08	0.08	34.56	0.38
	N_2	11.21	0.23	33.50	0.25

Appendix A5.1: Sensor signal response time

The time required to reach 90% of a desired concentration (30 ppmv N_2O) was evaluated with five repeated experiments, where the results are presented in Table A3.

Table A3 - Signal response time required to reach 90% of the final sensor signal.

Test	Sensor 1 final signal (mV)	90% Sensor 1 signal (mV)	Time to reach 90% (s)
Average	19.31	18.43	15.4
Std	0.16	0.15	1.8

Appendix A5.2: Temperature Tests

The influence of temperature on sensor signals were tested within the range of 12.3 to 32.6°C and N_2O concentrations between 0 and 50.1 ppmv. Measured and modelled signal values are presented in Figure A6. Modelled values were obtained using all the measured parameters obtained in the test. Comparison between the measured and modelled values is presented in Figure A7, for four sensors used in this test.

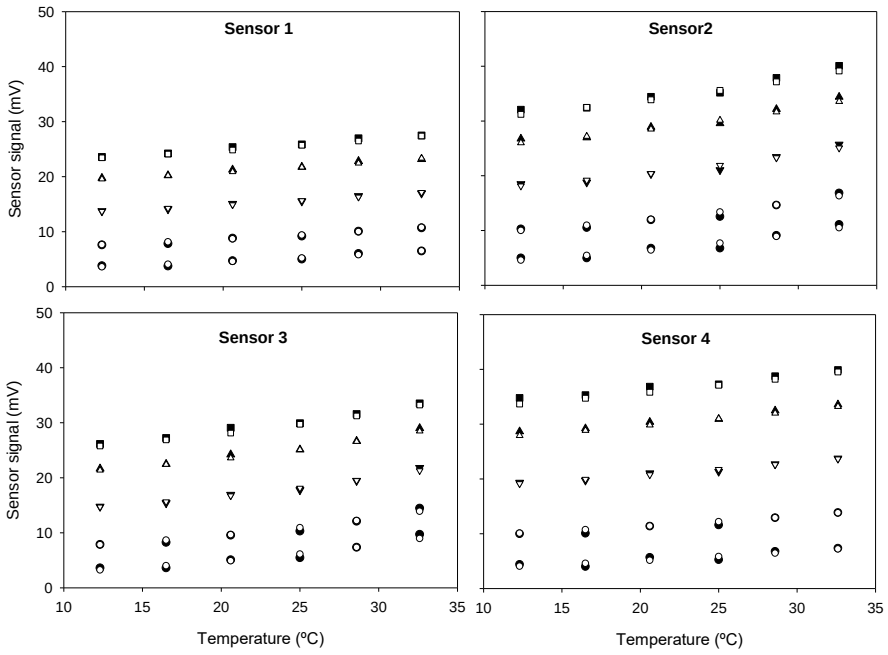

Figure A6 – Measured (black symbols) and predicted (white symbols) signal values for concentrations of 0 (● ○), 10.2 (▼ ▽), 25.5 (■□), 40.3 (♦ ◊) and 50.1 (▲ △) ppmv of N_2O for the four sensors. Prediction equations for each sensor were 1) $S_{N_2O}(T,C) = 2.502e^{0.029T}+0.384.C.e^{0.003T}$, 2) $S_{N_2O}(T,C) = 2.772e^{0.041T}+0.508.C.e^{0.004T}$, 3) $S_{N_2O}(T,C) = 1.743e^{0.050T}+0.430.C.e^{0.004T}$, 4) $S_{N_2O}(T,C) = 2.86e^{0.028T}+0.561.C.e^{0.004T}$.

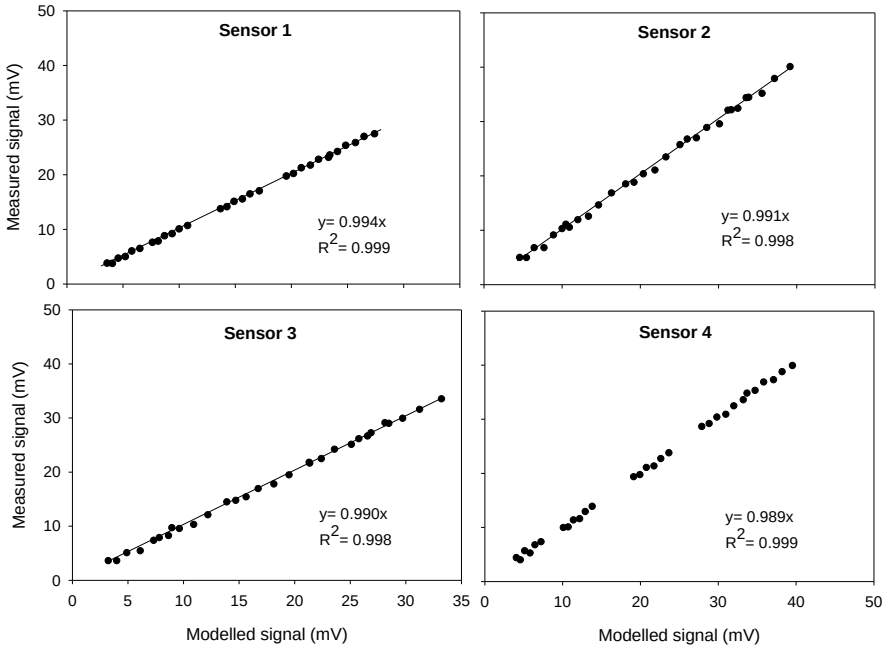

Figure A7 - Comparison between Measured *vs* Modelled values obtained. Modelled signal values obtained using all measured signal values.

A comparison between the measured and modelled values is also presented in Figure A8, for all 4 sensors. Modelled values were obtained for four sensors using calibration curves with 3 different concentrations each (0, 25.5 and 50.1 ppmv of N_2O) at 2 different temperatures (12.3 and 32.6 °C).

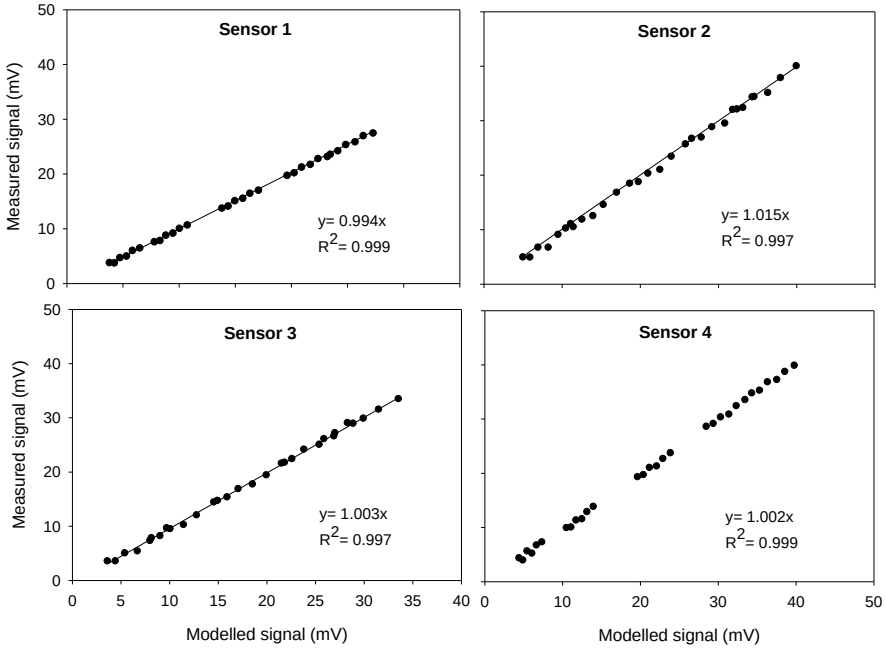

Figure A8 - Comparison between Measured *vs* Modelled values obtained. Modelled signal values obtained using 6 defined measurements.

APPENDIX B

Sensor calibration:

The N_2O concentration was compared with that given by a commercial online gas analyser. The sensor proved to be linear (i.e. y=ax) under different ranges of concentrations tested, where linear regression between the sensor measurements and the online analyser had very high coefficients of determination, $r^2 \geq 0.999$ for all the ranges tested (0-422.3 ppmv; 0-50 ppmv; 0-10 ppmv).

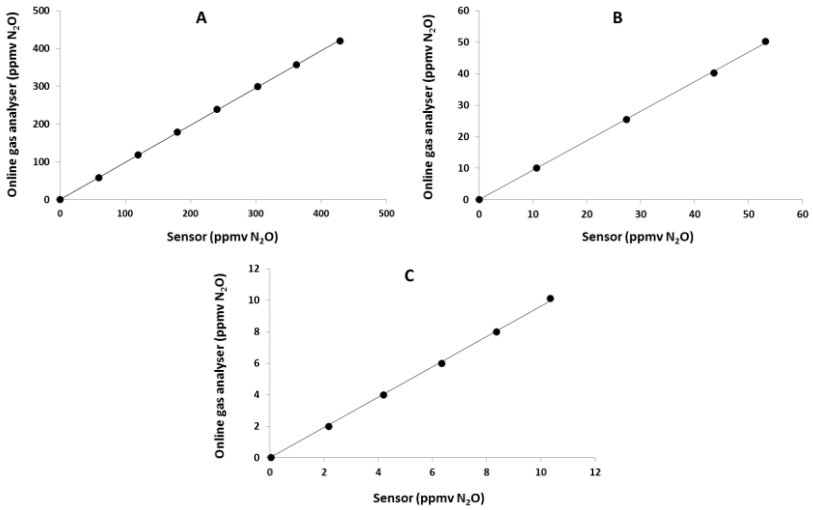

Figure B1 - Range of concentrations measured by the commercial gas analyser vs sensor (A: 0-422.3 ppmv N_2O; B: 0-50 ppmv N_2O; C: 0-10 ppmv N_2O) at controlled temperature (25 °C) and with nitrogen as dilution gas.

K_La Estimation Methodologies

Five methodologies were used to estimate the K_La of N_2O during aeration. The first one (Method 1) is based on the superficial gas velocity of the reactor and takes into account the correlation factor between the depth of a lab stripping column and the depth above the diffuser of the full-scale reactor, as described by Foley et al., (2010), in order to account for the increased depth of full scale WWTP reactors. This K_La estimation procedure is shown in equation B1:

$$K_L a_{N_2O}(20℃) = \left\{\frac{D_R}{D_L}\right\}^{-0.49} \times 34500 \times \left(v_g\right)^{0.86} \quad \text{(B1)}$$

Where,

- D_R - Depth over the diffuser of the reactor (m)
- D_L – Depth of lab stripping column (0.815 m)
- V_g – Superficial gas velocity of the reactor ($m^3.m^{-2}.s^{-1}$)

Since the total aeration field (676.47 m^2) and the Q_{gas} are known for the aerated reactor, the superficial gas velocity of the reactor (v_g) can be calculated assuming the following relation:

$$v_g \cong \frac{Q_{gas}}{Aeration\ field\ size} \quad \text{(B2)}$$

In Method 3, the K_La of O_2 was estimated for aerobic phases based on the oxygen transfer rate (OTR) of the reactor, using the following equation (B3):

$$OTR_{Liq.-Gas} = (K_L a_{O_2}(20℃)(DO_{sat.} - DO) - q_o.X) \times V \quad \text{(B3)}$$

Isolating the K_La_{O2} (20°C) the equation is converted to:

$$K_L a_{O_2}(20℃) = \left(\frac{OTR_{Liq.-gas}/V_R}{DO_{sat.} - DO}\right) + \left(\frac{q_o.X}{DO_{sat.} - DO}\right) \quad \text{(B4)}$$

Where,

- K_La_{O2} (20°C) – Oxygen mass transfer coefficient at the temperature of 20°C (d^{-1})
- $OTR_{Liq.-Gas}$ – Oxygen transfer rate (Kg $O_2.d^{-1}$) obtained from plant operators (12141.52 Kg $O_2.d^{-1}$);
- $DO_{sat.}$ – Oxygen saturation concentration in water at 20°C (Kg $O_2.m^{-3}$);
- DO – Oxygen concentration measured in the plant (Kg $O_2.m^{-3}$);
- $q_o.X$ = OUR – Oxygen uptake rate (Kg $O_2.d^{-1}$). This was obtained from the slope of oxygen concentration over time when the aerators were turned off, with an average value of 521.71±32.76 Kg $O_2.m^{-3}$. The measurements each lasted 5 min (on average) and the oxygen concentration was never limiting during the OUR estimation. The slope was linear in all three replicates with an average r^2 of 0.909±0.019.

The K_La estimation of equation B4 describes the mass transfer coefficient in pure water. In a WWTP, the presence of impurities, wastewater salinity, and fouling of the air diffusers are factors affecting this estimation and are typically incorporated in the estimation of K_La (Stenstrom and Gilbert, 1981; Tchobanoglous et al., 2003), as shown in equation B5 (Method 4):

$$K_L a_{O_2}(20℃) = \left(\frac{{}^{OTR}/_{V_R}}{\alpha(\beta DO_{sat} - DO).\ _F}\right) + \left(\frac{q_o.X}{\alpha(\beta DO_{sat} - DO).\ _F}\right) \quad \text{(B5)}$$

Where,

- α – Reduction in transfer rate caused by impurities in WWTP (typical WWTP value 0.65, dimensionless)
- β – Reduction in transfer rate caused by salinity (typical WWTP value 0.95, dimensionless);
- F – Reduction in transfer rate caused by fouling in the air diffusers (typical WWTP value 0.65-0.9, value used 0.78, dimensionless);

In accordance with Higbie`s penetration model, where the K_La of N_2O is calculated as a function of the ratio of molecular diffusivity of N_2O in water to the molecular diffusivity of O_2 in water, the K_La of N_2O was calculated using the following equation B6 (Foley et al., 2010; Van Hulle et al., 2012) (Method 3-5):

$$K_L a_{N_2O}(20℃) = K_L a_{O_2}(20℃) \times \sqrt{\frac{D_{F_{N_2O}}}{D_{F_{O_2}}}} \quad \text{(B6)}$$

Where,

- K_La_{N2O} (20°C) – N_2O mass transfer coefficient at a temperature of 20°C (d^{-1})
- D_{FN2O} – Molecular diffusivity of N_2O in water (1.84×10^{-9} $m^2.s^{-1}$ at 20°C) (Foley et al., 2010; Tamimi et al., 1994)
- D_{FO2} – Molecular diffusivity of oxygen in water (1.98×10^{-9} $m^2.s^{-1}$ at 20°C) (Ferrell and Himmelblau, 1967; Foley et al., 2010):

All five methodologies for K_La estimations were corrected for temperature based on a standard factor (Θ) of 1.024 (Foley et al., 2010; Tchobanoglous et al., 2003) (Method 1-5):

$$K_L a_{N_2O_{T_{Process}}} = K_L a_{N_2O}(20℃) \times (1.024)^{(T_{Process}-20℃)} \quad \text{(B7)}$$

Liquid N_2O microsensor signals also depend on process temperature ($T_{Process}$) and must be corrected for temperature differences from the original calibration temperature ($T_{Calibration}$) (equation B8) (Unisense, 2014);

$$S_{N_2O_{T\_Comp.}} = S_{N_2O_{T\_Proc.}} \times (1.033)^{(T_{Process}-T_{calibration})} \quad \text{(B8)}$$

Where,

- $S_{N2O}T_{proc}$ – Concentration of N_2O in the liquid measured by the N_2O liquid microsensor without temperature compensation (mg $N\text{-}N_2O.m^{-3}$).

- $T_{process}$ – Temperature of water during the monitoring process (°C);
- $T_{calibration}$ – Temperature of the water when the calibration was performed (°C);

The dimensionless Henry's constant is temperature dependent as well. To perform the temperature correction of the Henry's constant, equation B9 was used. The Enthalpy of N_2O was then calculated using equation B10:

$$K_H = {K_H}^{\theta} \times e^{\left[\frac{-\Delta solnH}{R} \times \left(\frac{1}{T_{process}+273.15} - \frac{1}{T^{\theta}+273.15}\right)\right]} \quad \text{(B9)}$$

$$H_{N_2O,T_{process}} = \frac{1}{K_H \times R \times (T_{Process} + 273.15) \times 10^3} \quad \text{(B10)}$$

Where,

- K_H – Henry's constant at process temperature (mol.L^{-1}.bar^{-1})
- K_H^{θ} - Henry's constant at standard temperature (mol.L^{-1}.bar^{-1})
- $-\Delta_{soln}H$ – Enthalpy of the solution (K)
- R – Gas constant 8.314×10^{-5} (m^3.bar.mol^{-1}.K^{-1})
- T^{θ} - Standard temperature (25 °C)

N_2O gas emissions estimation through dissolved N_2O measurements:

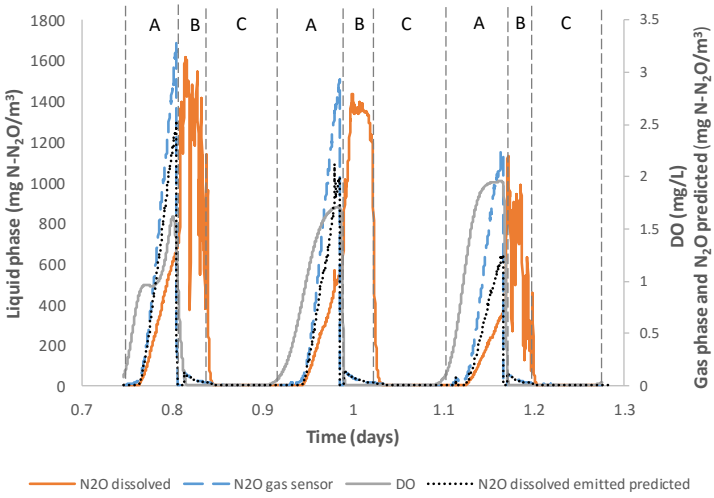

Figure B2 - Typical SBR profile at La Roca del Vallès WWTP of N_2O gas emissions (blue dashed line), liquid N_2O concentration (orange line), DO concentration (grey line) and N_2O dissolved emitted predicted (black dashed line) (Method 5 – period_a). A – aerobic phase, B – anoxic phase and C-settling and decant phase.

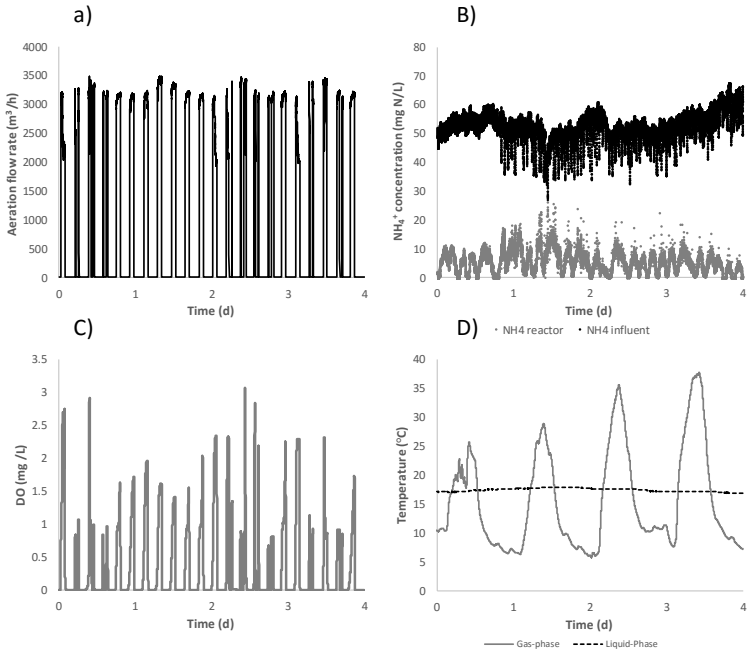

Figure B3 – Aeration flow rates (a), ammonia concentration in the influent and in the reactor (b), dissolved oxygen in the reactor (c) and temperature in the liquid and gas-phase (d).

APPENDIX C

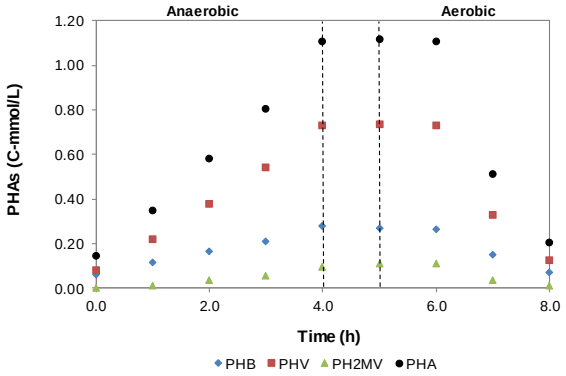

Figure C1 - PHB, PHV and PH2MV cycle during a typical SBR cycle study. Between the dashed lines, the settling and decant phases occur.

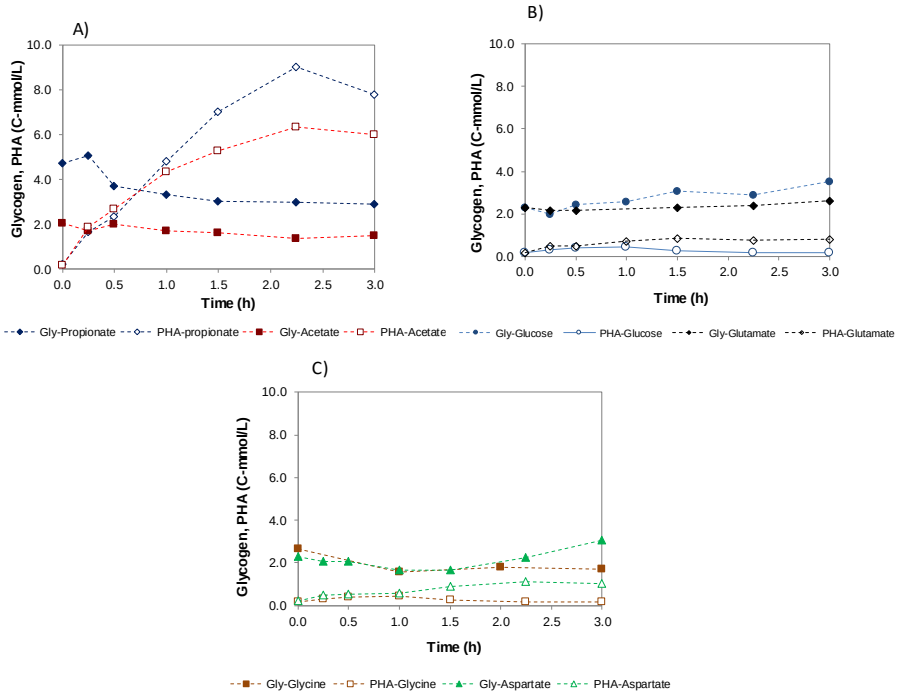

Figure C2 - Comparison of glycogen and PHAs profiles for the 1st batch experiments performed with different carbon sources: propionate and acetate (A), glucose and glutamate (B) and glycine and aspartate (C).

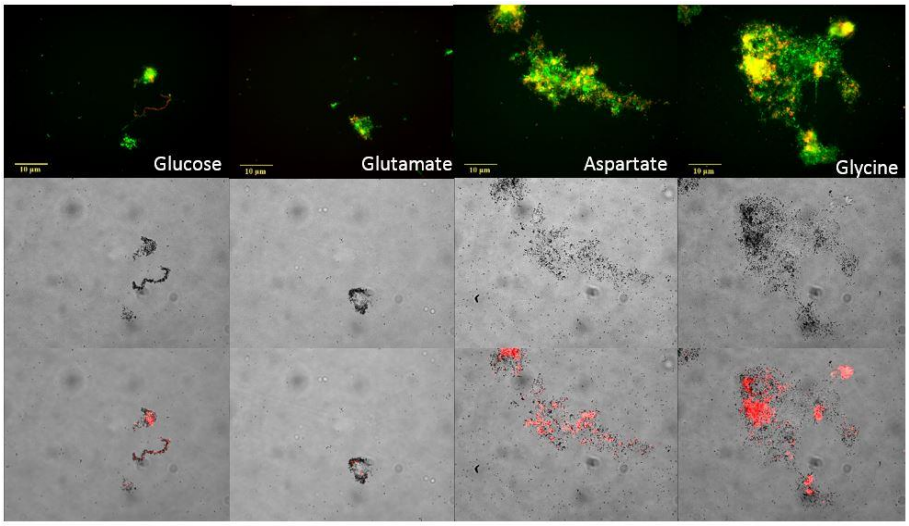

Figure C3 - MAR-FISH results performed for *Tetrasphaera* clade Tet1-266 with labelled carbon sources (glucose, glutamate, aspartate and glycine). EUBMIX is in green and Tet1-226 is in red, yellow microcolonies and cells are overlay of red and green in the FISH images (top row), while reddish dots account for positive uptake of the labelled carbon source in the MAR images (botton rows).

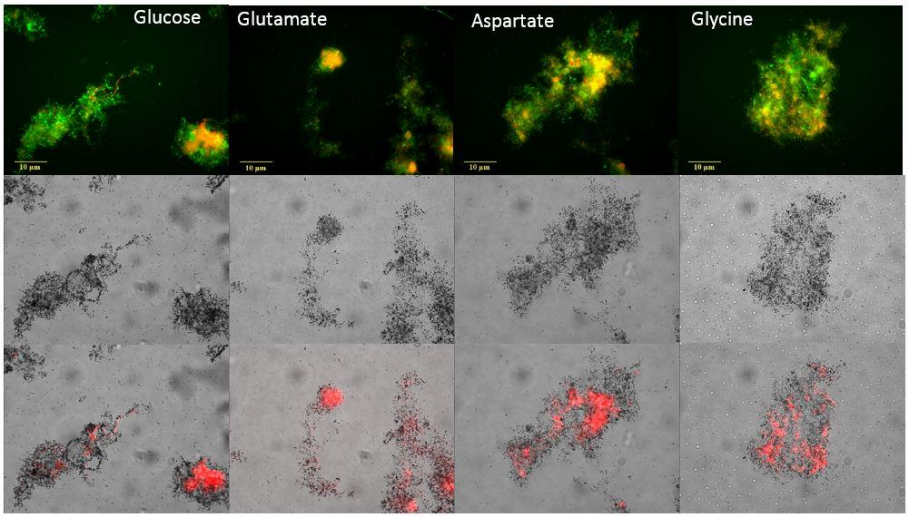

Figure C4 - MAR-FISH results performed for *Tetrasphaera* clade Tet2-174, with labelled carbon sources (glucose, glutamate, aspartate and glycine). EUBMIX is in green and Tet2-174 is in red, yellow microcolonies and cells are overlay of red and green, while reddish dots account for positive uptake of the labelled carbon source.

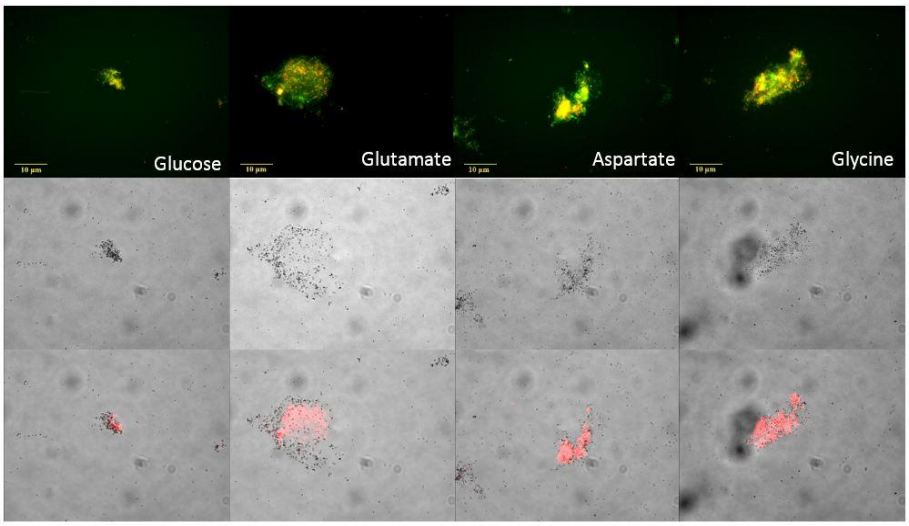

Figure C5 - MAR-FISH results performed for *Tetrasphaera* clade Tet1-892, with labelled carbon sources (glucose, glutamate, aspartate and glycine). EUBMIX is in green and Tet2-892 is in red, yellow microcolonies and cells are overlay of red and green,, while reddish dots account for positive uptake of the labelled carbon source.

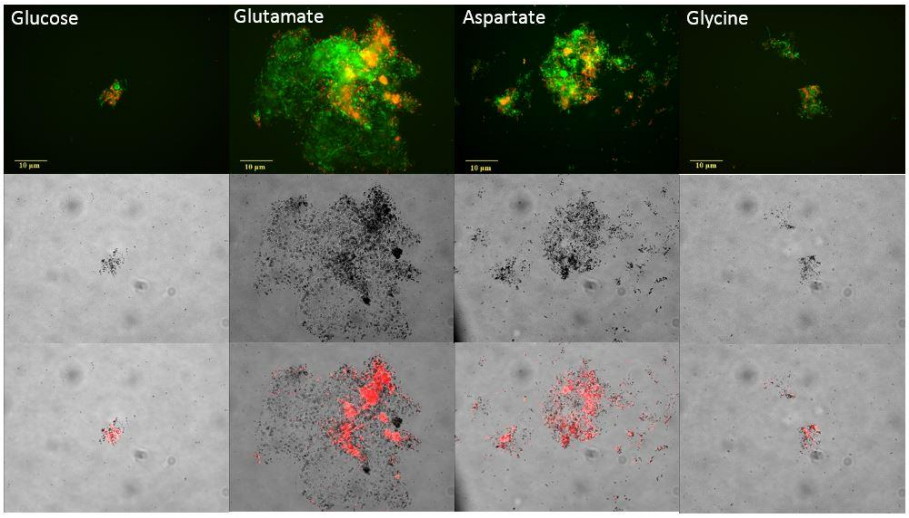

Figure C6 - MAR-FISH results performed for *Tetrasphaera* clade Tet3-654, with labelled carbon sources (glucose, glutamate, aspartate and glycine). EUBMIX is in green and Tet3-654 is in red, yellow microcolonies and cells are overlay of red and green, while reddish dots account for positive uptake of the labelled carbon source.

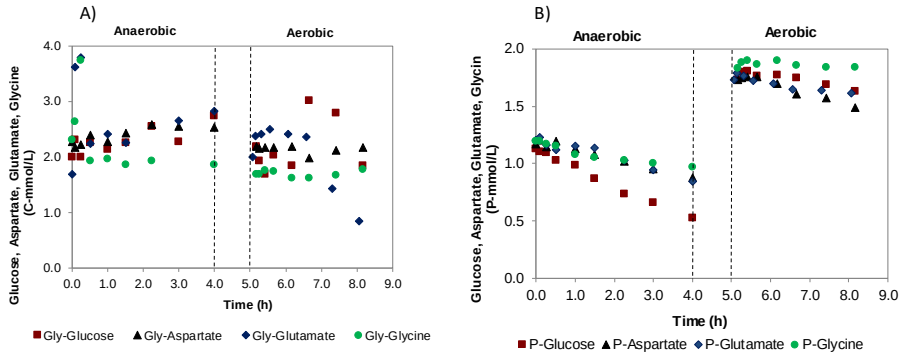

Figure C7 - Comparison of Glycogen (A) and PHAs (B) profiles for the 2nd batch experiments performed with different carbon sources (glucose, glutamate, aspartate and glycine).

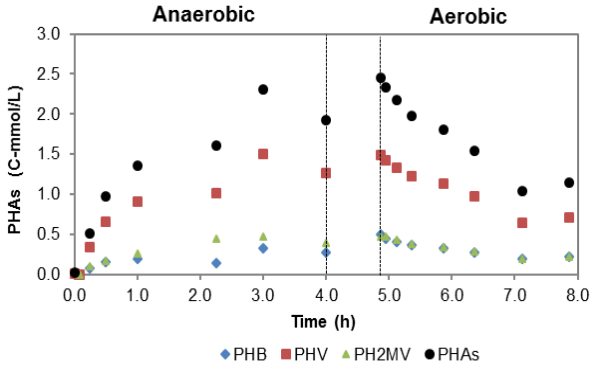

Figure C8 - PHB, PHV and PH2MV cycle during the 2nd batch test with a mixture of 3 carbon sources (acetate, propionate and Cas aa). Between the dashed lines, the settling and decant phases occur.

Table C1 - Oligonucleotide FISH probes employed in this study.

Probe	Sequence 5'-3'	Specifity	Formamide (%)	Reference
EUB338	GCTGCCTCCCGTAGGAGT	Most Bacteria	0-50	Amann et al., (1990)
EUB338-II	GCAGCCACCCGTAGGTGT	Planctomycetales and other Bacteria not detected by EUB338	0-50	Daims et al., (1999)
EUB338-III	GCTGCCACCCGTAGGTGT	Verrucomicrobiales and other Bacteria not detected by EUB338	0-50	Daims et al., (1999)
PAO462	CCGTCATCTACWCAGGGTATTAAC	Most Ca. Accumulibacter phosphatis	35	Crocetti et al., (2000)
PAO651	CCCTCTGCCAAACTCCAG	Most Ca. Accumulibacter phosphatis	35	Crocetti et al., (2000)
PAO846	GTTAGCTACGGCACTAAAAGG	Most Ca. Accumulibacter phosphatis	35	Crocetti et al., (2000)
GAOQ431	TCCCCGCCTAAAGGGCTT	Most Ca. Competibacter phosphatis	35	Crocetti et al., (2002)
GAOQ989	TTCCCCGGATGTCAAGGC	Most Ca. Competibacter phosphatis	35	Crocetti et al., (2002)
GB_G2	TTCCCCAGATGTCAAGGC	Most Ca. Competibacter phosphatis	35	Kong et al., (2002)
TFO_DF218	GAAGCCTTTGCCCCTCAG	Cluster 1 Defluviicoccus vanus-related organisms	35	Wong et al., (2004)
TFO_DF618	GCCTCACTTGTCTAACCG	Cluster 1 Defluviicoccus vanus-related organisms	35	Wong et al., (2004)
DF988	GATACGACGCCCATGTCAAGGG	Cluster 2 Defluviicoccus vanus-related organisms	35	Meyer et al., (2006)
DF1020	CCGGCCGAACCGACTCCC	Cluster 2 Defluviicoccus vanus-related organisms	35	Meyer et al., (2006)
DF1013	TAAGTTTCCTCAAGCCGC	Cluster 3 Defluviicoccus vanus-related organisms	35	Nittami et al., (2009)
DF1004	GAACTGAAGGCTCGAGTTTC	Cluster 3 Defluviicoccus vanus-related organisms	35-50	Nittami et al., (2009)
Tet1-266	CCCGTCGTCGCCTGTAGC	Uncultured T. elongata	25	Nguyen et al., (2011)
Tet2-892	TAGTTAGCCTTGCGGCCG	Clone ASM47	5	Nguyen et al., (2011)
Tet2-174	GCTCCGTCTCGTATCCGG	T. jenkinsii, T. australiensis, T. veronensis, and Candidatus N. limicola	20	Nguyen et al., (2011)
Tet3-654	GGTCTCCCCTACCATACT	Uncultured Tetrasphaera	35	Nguyen et al., (2011)

Table C2 - Aerobic parameters for *Accumulibacter*-PAO from literature and calculated in the current study.

Parameter	Value	Units	Description	Reference
a	0.262±0.016	C-mol/C-mol	PHB fraction in PHA	Current study
b	0.582±0.040	C-mol/C-mol	PHV fraction in PHA	Current study
c	0.156±0.035	C-mol/C-mol	PH2MV fraction in PHA	Current study
λ	0.495±0.016	C-mol/C-mol	Percentage of Acetyl-CoA* in PHA	Current study
β	0.505±0.016	C-mol/C-mol	Percentage of Propionyl-CoA* in PHA	Current study
K_1	1.7	ATP-mol/C-mol	ATP needed for biomass synthesis from Acetyl-CoA*	Smolders 1994
K_2	1.38	ATP-mol/C-mol	ATP needed for biomass synthesis from Propionyl-CoA*	Zeng 2003
δ (Y_{NADH_ATP})	1.85	ATP-mol/NADH-mol	ATP produced per NADH oxidized (Aerobic P/O ratio)	Smolders 1994
ε	7	P-mol/NADH-mol	Aerobic phosphate transport coefficient (PAO only)	Smolders 1994
Y_{PHA_PP}	3.94±0.01	P-mol Poly-P/C-mol PHA	Yield of Poly-P formation to PHA used	Current study

Table C3 - Anaerobic stoichiometric parameters for *Tetraphaera*-related organism.

	Parameter	Value	Units	Description	Source
Glucose	$Glucose_{AC}$	2/3	ATP mmol.C-mmol $Glucose^{-1}$	ATP mmol generated per glucose C-mmol fermented to Acetate	Kristiansen 2013
	P_{UPTAKE}	-1	ATP mmol.P-$mmol^{-1}$	ATP mmol consumed per P-mmol uptake	Smolders 1994
	$Glycogen_{FORMATION}$	-1/3	ATP mmol. C-mmol $Glucose^{-1}$	ATP consumed per C-mmol of glucose consumed	Smolders 1994
	$Maitenance_{ANO2}$	-1/2	ATP mmol. C-mmol $Glycogen^{-1}$	ATP consumed per C-mmol of glycogen consumed	Smolders 1994
Glutamate	$Glutamate_{AC}$	2/5	ATP mmol.C-mmol $Glutamate^{-1}$	ATP mmol generated per glutamate C-mmol fermented to Acetate	Ramsay 1997
	P_{UPTAKE}	-1	ATP mmol.P-$mmol^{-1}$	ATP mmol consumed per P-mmol uptake	Smolders 1994
	$Glycogen_{FORMATION}$	-1/5	ATP mmol. C-mmol $Glutamate^{-1}$	ATP consumed per C-mmol of glucose consumed	Ramsay 1997
	$Maitenance_{ANO2}$	-1/2	ATP mmol. C-mmol $Glycogen^{-1}$	ATP consumed per C-mmol of glycogen consumed	Smolders 1994
Aspartate	$Aspartate_{AC}$	2/5	ATP mmol.C-mmol $Aspartate^{-1}$	ATP mmol generated per aspartate C-mmol fermented to acetate	Ramsay 1997
	P_{UPTAKE}	-1	ATP mmol.P-$mmol^{-1}$	ATP mmol consumed per P-mmol uptake	Smolders 1994
	$Glycogen_{FORMATION}$	-2/4	ATP mmol. C-mmol $Aspartate^{-1}$	ATP consumed per C-mmol of aspartate consumed	Ramsay 1997
	$Maitenance_{ANO2}$	-1/2	ATP mmol. C-mmol $Glycogen^{-1}$	ATP consumed per C-mmol of glycogen consumed	Smolders 1994
Glycine	$Glycine_{AC}$	1/8	ATP mmol.C-mmol $Glycine^{-1}$	ATP mmol generated per glycine C-mmol fermented to acetate	Ramsay 1997
	P_{UPTAKE}	-1	ATP mmol.P-$mmol^{-1}$	ATP mmol consumed per P-mmol uptake	Smolders 1994
	$Glycogen_{Consumption}$	1/2	ATP mmol. C-mmol $Glycine^{-1}$	ATP generated per C-mmol of glycogen consumed	Smolders 1994
	$Maitenance_{ANO2}$	-1/2	ATP mmol. C-mmol $Glycogen^{-1}$	ATP consumed per C-mmol of glycogen consumed	Smolders 1994

APPENDIX D

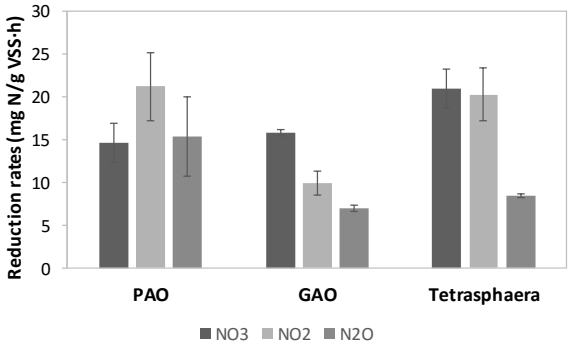

Figure D1 – Individual nitrogen oxide reduction rates obtained for NO_3^-, NO_2^- and N_2O for this culture (*Tetrasphaera*) and with PAOs and GAOs cultures from study of Ribera-Guardia et al., (2016).

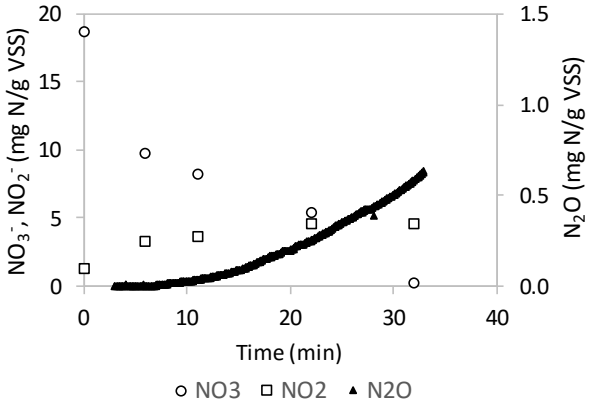

Figure D2 - Batch test profile performed with nitrate as electron acceptor and external carbon source as electron donor.

Table D1 - Aerobic parameters for GAOs from literature and those calculated in the current study.

Parameter	Value	Units	Description	Reference
a	0.363±0.032	C-mol/C-mol	PHB fraction in PHA	Current study
b	0.344±0.069	C-mol/C-mol	PHV fraction in PHA	Current study
c	0.293±0.042	C-mol/C-mol	PH2MV fraction in PHA	Current study
λ	0.500±0.013	C-mol/C-mol	Percentage of Acetyl-CoA* in PHA	Current study
β	0.500±0.013	C-mol/C-mol	Percentage of Propionyl-CoA* in PHA	Current study
K_1	1.7	ATP-mol/C-mol	ATP needed for biomass synthesis from Acetyl-CoA*	Smolders 1994
K_2	1.38	ATP-mol/C-mol	ATP needed for biomass synthesis from Propionyl-CoA*	Zeng (2003)
δ (Y_{NADH_ATP})	1.85	ATP-mol/NADH-mol	ATP produced per NADH oxidized (Aerobic P/O ratio)	Smolders (1994)
ε	7	P-mol/NADH-mol	Aerobic phosphate transport coefficient (PAO only)	Smolders (1994)

Table D2 – Nitrogen oxide reduction rates obtained with the different combinations of electron acceptors used in the batch tests.

Batch test type	NO_3^- (mg N/g VSS·h)	NO_2^- (mg N/g VSS·h)	N_2O (mg N/g VSS·h)
A	20.97 ± 2.31	15.24 ± 0.64	12.80± 0.76
B	-	20.30 ± 3.10	20.20 ± 0.19
C	-	-	8.53 ± 0.22
D	18.10 ± 5.62	14.82 ± 4.79	17.61 ± 5.00
E	-	19.85 ± 3.12	26.16 ± 1.45
F	14.67 ± 0.72	17.65 ± 1.43	14.58 ± 1.37
G	10.41 ± 0.33	15.09 ± 2.53	17.05 ± 1.76
Ext A	25.78	19.41	17.63